UNIVERSIDADE FEDERAL DE PERNAMBUCO

CENTRO DE BIOCIÊNCIAS

DEPARTAMENTO DE BOTÂNICA

PROGRAMA DE PÓS-GRADUAÇÃO EM BIOLOGIA VEGETAL

CLAUDIO CÉSAR MONTENEGRO JÚNIOR

Mapeamento citogenômico comparativo em representantes de Phaseoleae (Leguminosae), com ênfase no gênero *Macroptilium* (Benth.) Urb.

RECIFE

2023

Claudio César Montenegro Júnior

Mapeamento citogenômico comparativo em representantes de Phaseoleae (Leguminosae), com ênfase no gênero *Macroptilium* (Benth.) Urb

Tese de Doutorado apresentada ao Programa de Pós-graduação em Biologia Vegetal da Universidade Federal de Pernambuco, como requisito para obtenção do título de doutor em Biologia Vegetal

Orientadora: Profa. Dra. Andrea Pedrosa-Harand

Coorientadora: Profa. Dra. Ana Christina Brasileiro-Vidal

RECIFE

2023

Dados Internacionais de Catalogação na Publicação (CIP) de acordo com ISBD

Montenegro Júnior, Claudio César
Mapeamento citogenômico comparativo em representantes de Phaseoleae (Leguminosae), com ênfase no gênero Macroptilium (Benth.) Urb. / Claudio César Montenegro Júnior. – 2023.

138f. : il., col.

Orientadora: Andrea Pedrosa-Harand
Coorientadora: Ana Christina Brasileiro-Vidal
Tese (doutorado) – Universidade Federal de Pernambuco. Centro de Biociências. Programa de Pós-Graduação em Biologia Vegetal, Recife, 2023.
Inclui referências.

1. Genética vegetal 2. Cromossomos de plantas 3. Fabaceae 4. Phaseolus 5. Cariótipo 6. Oligonucleotídeos I. Pedrosa-Harand, Andrea (orient.) II. Brasileiro-Vidal, Ana Christina (coorient.) III. Título.

581.35 CDD (22.ed.) UFPE/CB – 2023 - 131

Elaborado por Marylu Souza - CRB-4/1564

CLAUDIO CÉSAR MONTENEGRO JÚNIOR

Mapeamento citogenômico comparativo em representantes de Phaseoleae (Leguminosae), com ênfase no gênero *Macroptilium* (Benth.) Urb.

Tese de doutorado apresentada ao Programa de Pós-graduação em Biologia Vegetal da Universidade Federal de Pernambuco, Centro de Biociências, como requisito para a obtenção do título de Doutor em Biologia Vegetal. Área de concentração: Sistemática e Evolução.

Aprovado em: 24/02/2023

BANCA EXAMINADORA

_____
Profª. Drª. Andrea Pedrosa-Harand (Orientadora)
Universidade Federal de Pernambuco - UFPE

_____
Prof. Dr. Marcelo Guerra (Examinador Interno)
Universidade Federal de Pernambuco – UFPE

_____
Profª. Drª. Giovana Augusta Torres (Examinador Externo)
Universidade Federal de Lavras - UFLA

_____
Prof. Dr. Lyderson Facio Viccini (Examinador Externo)
Universidade Federal de Juiz de Fora – UFJF

_____
Dr. Guilherme Tomaz Braz (Examinador Externo)
Universidade Estadual de Campinas – UNICAMP

_____
Prof. Dr. Luiz Gustavo Rodrigues Souza (Suplente interno)
Universidade Federal de Pernambuco – UFPE

_____
Dr. Lucas Alexandre de Souza Costa (Suplente externo)
Universidade Federal de Pernambuco – UFPE

Para todos os pesquisadores e alunos de pós-graduação do Brasil
que foram fortes e resilientes durante os últimos anos
Dedico.

AGRADECIMENTOS

Em primeiro lugar, gostaria a agradecer a minha mãe, por todo carinho, amor, dedicação e suporte durante toda minha jornada acadêmica. Muito obrigado por tudo, mãe.

Agradeço a minha orientadora, Andrea, por ter aceitado me orientar e ter me guiado durante os quatro anos de doutorado. Você não faz ideia o quanto me ajudou e me inspirou durante todos esses anos, muito obrigado por me dar credibilidade e confiança.

A minha coorientadora, Ana Christina, muito obrigado por toda a parceria durante esses anos. Você sempre foi muito gentil e prestativa comigo, jamais irei esquecer das suas palavras de carinho e incentivo.

A minha amiga e colega de trabalho Lívia do Vale, muito obrigado por toda a ajuda durante todo meu doutorado. Você foi fundamental para que eu chegasse até aqui.

Agradeço aos meus colegas do Laboratório de Citogenética e Evolução Vegetal que estiveram comigo nos últimos anos, em especial Lucas, Yhanndra, Brena, Natália, Jéssica, Erton, Paulo, Amália, Amanda, Gustavinho, Mariela, Yennifer, Pablo, Thiago, Mariana, Acalene, Ana, Bruna e Raíssa. Muito obrigado pelas conversas, risos, desabafos, cervejas e cafés. Jamais esquecerei esses anos com vocês.

Aos professores do laboratório, Gustavo e Marcelo, meu muito obrigado pelas conversas, dicas e orientações durante o meu doutorado.

Meus agradecimentos aos queridos amigos de longa data, Lucas Toscano, Luiz, Stephanne, Amanda, Amabile, Mateus, Ingrid e João Paulo. Vocês me acompanharam do ensino médio até aqui, me deram suporte emocional durante todos esses anos e jamais esquecerei de tudo o que vivemos.

Aos meus outros queridos amigos, Bruna, Sammara e Joelson, companheiros de graduação que seguiram na pós-graduação e me deram muita força sempre que precisei, meus sinceros agradecimentos. Eu tenho muito orgulho de ter seguido essa trilha ao lado de vocês.

Meu muito obrigado aos meus queridos amigos que tive prazer de conhecer/me aproximar enquanto esteva em Recife, Lucas Bernardo, Adalberto, Felipe, Bruno, Diego, João Hélio, Silas, Lucas Guedes e Gabriel.

Ao meu melhor amigo e companheiro, Evertton Lira, muito obrigado por esses três anos junto a mim. Tem sido uma honra compartilhar a experiência de fazer um doutorado junto a você.

Por fim, agradeço ao Programa de Pós-Graduação em Biologia Vegetal e a Fundação de Amparo a Ciência e Tecnologia de PE (FACEPE) por todo suporte técnico administrativo e financeiro durante meu doutorado.

RESUMO

Rearranjos cromossômicos são um dos principais mecanismos envolvidos no processo de especiação, podendo ser do tipo numérico ou estrutural. Embora comuns em plantas, em muitos grupos os números cromossômicos se mantem conservados, o que dificulta a detecção de possíveis rearranjos estruturais através técnicas citogenéticas convencionais. Com o avanço das técnicas de sequenciamento e montagem genômica, principalmente em grupos com espécies de interesse econômico, a genômica comparativa está auxiliando na detecção desses rearranjos. Os avanços da técnica de hibridização *in situ* florescente (FISH), por meio de sondas de oligonucleotídeos (oligos) únicos desenvolvidos a partir de sequências genômicas de plantas modelos, têm ampliado as análises comparativas para espécies relacionadas, através da detecção de cromossomos únicos ou segmentos deles. A tribo Phaseoleae (Papilionoideae; Leguminosae) é uma das principais dentro das leguminosas, pelo alto potencial de fixação de nitrogênio no solo e por representantes de grande interesse para a indústria alimentícia, como o feijão-comum (*Phaseolus vulgaris*), feijão-de-lima (*P. lunatus*) e feijão macassar (*Vigna unguiculata*), e por espécies forrageiras, como o siratro (*Macroptilium atropurpureum*). Apesar de $n = 11$ ser o número mais encontrado em representantes da tribo, análises de genômica comparativa dentro da família Leguminosae sugerem um cariótipo ancestral com $n = 16$, além de indicar que, apesar de quebras de sintenia e colinearidade, grandes blocos genômicos foram preservados. Análises citogenômicas entre *P. vulgaris* e *V. unguiculata* também confirmam quebras de sintenia e colinearidade, como demonstradas a partir da Oligo-FISH com sondas de pintura e *barcode* cromossômico. Tendo em vista a disponibilidade de espécies genoma montado na tribo Phaseoleae, o primeiro capítulo determinou criar um sistema de blocos genômicos a partir de genômica comparativa entre os representantes, reconstruindo o cariótipo ancestral de Phaseoleae (APK com $n = 11$), apontando os principais cromossomos e rearranjos cromossômicos que reduziram o número cromossômico tribo, além de evidenciar constantes reposicionamentos centroméricos. Já o segundo capítulo realizou um estudo citogenômico comparativo entre espécies do gênero *Macroptilium*, o qual é um gênero recente (~ 3 Ma) e não possui representante com genoma montado. No intuito de identificar possíveis rearranjos intergenéricos e interespecíficos, empregamos abordagens citogenômicas por meio da Oligo-FISH e análises *in silico* da fração repetitiva. Os resultados da Oligo-FISH para

pintura e *barcode* cromossômico apontaram rearranjos inter- e intragenéricos que permitem agrupar as espécies do gênero em três grupos citogenéticos, os quais não são suportados pela atual filogenia. No entanto, esses grupos citogenéticos são congruentes com a análise *in silico* da fração repetitiva. Alguns DNA satélites compartilhados entre diferentes grupos citogenéticos, foram amplificados de maneira independente. De maneira geral, os dois capítulos apontam para uma alta dinamicidade na evolução cromossômica dos representantes de Phaseoleae, mesmo com a manutenção do número cromossômico (n = 11) na maioria das espécies e em grupos com recente divergência evolutiva.

Palavras-chave: Evolução cromossômica; Rearranjos cromossômicos; Oligo-FISH; Cariótipo ancestral; *Macroptilium*

ABSTRACT

Chromosomal rearrangements are one of the main mechanisms involved in the speciation process and may be numerical or structural. Although common in plants, in many groups the chromosome numbers remain conserved, which makes it difficult to detect possible structural rearrangements through conventional cytogenetic techniques. With the advancement of sequencing techniques and genomic assembly, especially in groups with species of economic interest, comparative genomics is helping to detect these rearrangements. Advances in the fluorescent in situ hybridization (FISH) technique, using unique oligonucleotide (oligos) probes developed from genomic sequences of model plants, have expanded comparative analyzes for related species, through the detection of unique chromosomes or segments from them. The Phaseoleae tribe (Papilionoideae; Leguminosae) is one of the main ones among legumes, due to its high potential for nitrogen fixation in the soil and because of its representatives of great interest to the food industry, such as common bean (*Phaseolus vulgaris*), lima bean (*P. lunatus*) and cowpea (*Vigna unguiculata*), and forage species such as the siratro (*Macroptilium atropurpureum*). Although $n = 11$ is the most common number in representatives of the tribe, comparative genomic analyzes within the Leguminosae family suggest an ancestral karyotype with $n = 16$, also indicating that, despite breaks in synteny and collinearity, large genomic blocks were preserved. Cytogenomic analyzes between *P. vulgaris* and *V. unguiculata* also confirm breaks in synteny and collinearity, as demonstrated by Oligo-FISH with paint probes and chromosome barcode. In view of the availability of genome species assembled in the Phaseoleae tribe, the first chapter determined to create a system of genomic blocks from comparative genomics between representatives, reconstructing the ancestral karyotype of Phaseoleae (APK with $n = 11$), pointing out the main chromosomes and chromosomal rearrangements that reduced the tribe chromosome number, in addition to showing constant centromeric repositioning. The second chapter carried out a comparative cytogenomic study between species of the genus *Macroptilium*, which is a recent genus (~ 3 Ma) and does not have a representative with an assembled genome. To identify possible intergeneric and interspecific rearrangements, we used cytogenomic approaches through Oligo-FISH and *in silico* analyzes of the repetitive fraction. The results of Oligo-FISH for painting and chromosome barcode showed inter- and intrageneric rearrangements that allowed grouping the species of the genus into three

cytogenetic groups, which are not supported by the current phylogeny. However, these cytogenetic groups are congruent with the *in silico* analysis of the repeating fraction. Some satellite DNAs shared between different cytogenetic groups were independently amplified. In general, the two chapters point to a high dynamicity in the chromosomal evolution of Phaseoleae representatives, even with the maintenance of the chromosome number (n = 11) in most species and in groups with recent evolutionary divergence.

Keywords: Chromosomal evolution; Chromosomal rearrangements; Oligo-FISH; Ancestral karyotype; *Macroptilium*

SUMÁRIO

1 INTRODUÇÃO

À medida que mais genomas vegetais foram sequenciados e montados, ficou claro que as plantas superiores passaram por vários ciclos de poliplidização e diploidização durante seu processo evolutivo, levando a uma maior ou menor reorganização genômica (WANG et al., 2022). Apesar de grandes blocos genômicos serem conservados entre grupos próximos, rearranjos cromossômicos estruturais e numéricos fizeram parte desta reorganização (PONT et al., 2019). Estudos de genômica comparativa entre leguminosas da subfamília Papilionoideae (Leguminosae Juss. / Fabaceae Lindl) apontam um evento compartilhado de tetrapoliploidização (LCT – *Legume Common Tetraploidization*) na base da família (~ 60 milhões de anos), seguido de reorganização genômica por rearranjos cromossômicos (SCHMUTZ et al., 2010; WANG et al., 2017). Acredita-se que o cariótipo ancestral das leguminosas (ALK – *Ancestral Legume Karyotype*) possuía entre $n = 9$ (REN; HUANG; CANNON, 2019) e $n = 25$ (KREPLAK et al., 2019) cromossomos, contudo, $n = 16$ parece ser o mais consistente para o ALK (HUFNAGEL et al., 2020).

Dentro das leguminosas, Phaseoleae é a tribo com o maior número de representantes de interesse econômico, sejam eles de interesse da indústria alimentícia como o feijão-comum, o feijão-de-lima (*Phaseolus lunatus* L.), o feijão-caupi (*Vigna unguiculata* L. Walp.), o feijão mungu (*Vigna radiata* [L.] R.Wilczek) e a soja (*Glycine max* [L.] Merr.), ou para pastagem e fixação de nitrogênio no solo, como a grama de cavalo (*Macrotyloma uniflorum* [Lam.] Verdc.) e o siratro (*Macroptilium atropurpureum* [DC.] Urb.) (DONG et al., 2014; FERREIRA et al., 2018; RAMÍREZ-JIMÉNEZ et al., 2018; SHIRASAWA et al., 2021). Existem vários genomas sequenciados dentro da tribo, contudo, a maioria se restringe aos representantes de interesse para indústria alimentícia, como *Phaseolus, Vigna* e *Glycine*. Genômica comparativa entre esses grupos apontam alto grau de conservação de blocos genômicos, contudo, com quebras de sintenia e colinearidade entre os cromossomos, além de um evento independente de poliploidização em *Glycine* (LONARDI et al., 2019; SCHMUTZ et al., 2010; WANG et al., 2017). Análises citogenômicas por sondas de BAC (do inglês- *Bacterial Artificial Chromosomes*) e *oligos* para pintura e barcode cromossômico para FISH (do inglês- *Fluorescence in situ hybridization*) entre espécies do gênero *Phaseolus* e *Vigna* também apontam quebras de sintenia e colinearidade, além de reposicionamento centromérico (DE OLIVEIRA BUSTAMANTE et al., 2021; DO VALE MARTINS et al., 2021; VASCONCELOS et al., 2015). Sondas de BAC-FISH vindas do genoma de *P. vulgaris* também

foram usadas em um mapeamento citocomparativo entre *Phaseolus* e *Macroptilium* (gênero próximo, porém sem representantes com genoma montado), mostrando que houve quebras de sintenia em *Macroptilium* a partir de rearranjos independentes, sendo eles tanto interespecíficos como intergenéricos (BARROS FERREIRA, 2019).

Tendo em vista a disponibilidade de genomas montados para representantes da tribo Phaseoleae, além de dados prévios sobre o ALK, desenvolvemos, no primeiro capítulo, um sistema de blocos genômicos a partir de genômica comparativa, no intuito de propor um cariótipo ancestral para entender os principais eventos que moldaram a evolução cromossômica da tribo. No segundo capítulo, utilizamos sondas disponíveis de *oligos* para pintura e *barcode* cromossômico, provindas dos genomas de *P. vulgaris* e *V. unguiculata*, para investigar a evolução cromossômica *Macroptilium*, um gênero que não possui genomas montados. Revelamos rearranjos cromossômicos interespecíficos e intergenéricos dentro do grupo, que indicam relações distintas entre as espécies. Utilizamos sequenciamento de nova geração para analisar a fração repetitiva e propor novas relações filogenéticas para o gênero.

2 REVISÃO BIBLIOGRÁFICA

2.1 Evolução cromossômica

O surgimento de novas espécies vegetais depende dos processos de diferenciação genética e fenotípica de populações, podendo ser influenciado por processos de domesticação e interações com ecossistema (PURUGGANAN, 2019; WOLF; LINDELL; BACKSTRÖM, 2010). Mudanças nas sequências de DNA, desde mutações gênicas até alterações cromossômicas, podem contribuir com esses eventos populacionais, acelerando o processo de especiação (DE STORME; MASON, 2014). Os cromossomos são responsáveis pela transmissão hereditária do conteúdo genético nuclear (genoma) e o conjunto de cromossomos de uma espécie constitui o seu cariótipo, o qual é definido pelo número e morfologia cromossômicos. Os cariótipos costumam compartilhar similaridades entre espécies próximas, e diferenças entre espécies mais distantes, sendo um reflexo da evolução cromossômica e das relações filogenéticas (SCHUBERT; LYSAK, 2011). Dessa maneira, as variações na estrutura e número cromossômicos se mostram importantes para especiação (HESLOP-HARRISON; SCHWARZACHER, 2011).

A evolução cromossômica é mediada por dois tipos principais de alterações: numéricas e estruturais. Alterações numéricas afetam o número de cromossomos presentes em um cariótipo e podem ser do tipo aneuplodia, euplodia e displodia. As aneuploidias são perda ou ganho de um ou mais cromossomos, geralmente possuem efeito deletério, sendo um fator de seleção natural entre espécies (CHUNDURI; STORCHOVÁ, 2019; GEARHART et al., 1987; GORDON; RESIO; PELLMAN, 2012; STORCHOVA; KUFFER, 2008), As euploidias são mudanças que envolvem todo o conjunto de cromossomos de uma célula, sem mudança em relação ao número básico (*x*) ou ancestral daquela linhagem, podendo ser haploides ou monoploides (2*n*= *x*), diploides (2*n*= 2*x*), ou poliploides (2*n*= 3*x*, 4*x*, 6*x*, etc.). Já as disploidias são causadas por alterações estruturais envolvendo dois ou mais cromossomos dentro de um complemento cromossômico sem perda ou ganho de DNA, mas com alteração no número de cromossomos (DE STORME; MASON, 2014; SHAKOORI; AFTAB; SHAKOORI, 2017). Essas últimas foram e são fundamentais para evolução das plantas e outros organismos (BIRCHLER, 2013; JIAO et al., 2011; SINGHI et al., 2019). As alterações estruturais são caracterizadas por mudanças na ordem (colinearidade) e posição (sintenia) de blocos de sequências em um determinado genoma, podendo também estar combinadas com variações numéricas (disploidias) (WALDEN et al., 2020).

Sabe-se atualmente que o surgimento das plantas vasculares está relacionado a sucessivos eventos de duplicação do conjunto cromossômico (poliplodização), seguidos de eventos de reorganização genômica com redução do número de cromossômico (diploidização), por meio de inúmeros rearranjos estruturais e numéricos (BANIAGA et al., 2020; MANDÁKOVÁ; LYSAK, 2018; ZUO et al., 2022). Diante disso, é importante entender as implicações das alterações cromossômicas numéricas e estruturais em plantas vasculares, principalmente nas angiospermas.

2.1.1 Alterações Cromossômicas Numéricas

O número cromossômico é uma das variáveis cariotípicas que mais diferem entre grupos de plantas, indo de poucos cromossomos em *Brachyscome dichromosomatica* C. R. Carter (2*n* = 4) (WATANABE et al., 1999; CASTIGLIONE; CREMONINI, 2012) e *Rhynchospora tenuis* Link (2*n* = 4) (VANZELA; LUCEÑO; GUERRA, 2000), a mais de mil em *Ophioglossum reticulatum* L. (2*n* = 1.440) (KHANDELWAL, 1990; HESLOP-HARRISON; SCHWARZACHER, 2011). As origens dessas variações são atribuídas a eventos de euplodias

e disploidias. As euplodias são geralmente ocasionadas por erros na fase reducional da meiose, por não-disjunção cromossômica, gerando gametas não reduzidos e por ciclos endomitóticos, sendo a poliploidia o seu principal tipo (MOGHE; SHIU, 2014).

As poliplodias são as euplodias mais importantes na história evolutiva das plantas, uma vez que é atribuído a ocorrência de pelo menos um evento de duplicação completa do genoma durante o surgimento de todas as linhagens de plantas superiores (BANIAGA et al., 2020; JIAO et al., 2011). Os poliplóides podem ser originar por autopoliploidia e alopoliploidia. Os autopoliploides são classicamente conhecidos por espécies) que duplicam completamente o genoma, assim multiplicando o conjunto de cromossomos [ex: AA ($2n = 2$) → AAAA ($2n = 4$)] (PARISOD; HOLDEREGGER; BROCHMANN, 2010). Já os alopoliploides são gerados por eventos de duplicação completa do genoma por meio de hibridizações interespecíficas de dois ou mais genomas (AA × BB) resultando em espécies com subgenomas distintos [ex: AA ($2n = 2$) + BB ($2n = 2$) → AABB ($2n = 4$)] (DE STORME; MASON, 2014).

O significado evolutivo da poliploidia é discutido há décadas, entretanto, o sequenciamento completo do genoma da espécie modelo vegetal, *Arabidopsis thaliana* (L.) Heynh. (KAUL et al., 2000), foi o pontapé para a descoberta da importância evolutiva dos poliploides para as angiospermas. Análises genômicas apontaram ciclos de duplicação intermediados por rearranjos cromossômicos que reduziram o número cromossômico em *A. thaliana* (JIAO; SCHNEEBERGER, 2020; KAUL et al., 2000). O sequenciamento genômico foi impulsionado nos últimos anos principalmente com a era dos sequenciamentos de nova geração (NGS- do inglês *Next Generation Sequencing)*, possibilitando o barateamento dos custos e o aumento no número de plantas sequenciadas (PARK; KIM, 2016; REDDY et al., 2020), apontando para eventos de poliploidização na base da evolução das gimnospermas e angiospermas, além de diversos eventos posteriores e recorrentes em várias famílias (BANIAGA et al., 2020; ZUO et al., 2022 (AMBORELLA GENOME PROJECT et al., 2013; JIAO et al., 2011).

De acordo com o tempo e com nível de diploidização, os poliploides podem ser classificados em neopoliploides, mesopoliploides ou paleopoliploides (CARMAN, 1997; MANDÁKOVÁ et al., 2010; WU; HAN; JIAO, 2020; ZHANG; WANG; CHENG, 2019). Neopoliploides são os poliploides mais recentes, que ainda não passaram por eventos de diploidização, e, consequentemente, possuem tamanho do genoma e número cromossômico elevados, por exemplo *Arabidopsis suecica* (Fr.) Norrl. (BOMBLIES; MADLUNG, 2014). Espécies mesopoliploides possuem genomas completamente ou quase diploidizados, com

número cromossômicos reduzidos e meioses característica de diploides, como por exemplo, *Brassica rapa* L. (THE BRASSICA RAPA GENOME SEQUENCING PROJECT CONSORTIUM et al., 2011). Genomas paleopoliploides são caracterizados por serem completamente diploidizados, com ampla reorganização genômica e redução no número cromossômico (WU; HAN; JIAO, 2020; ZUO et al., 2022), a exemplo de *Vitis vinifera* L. (THE FRENCH–ITALIAN PUBLIC CONSORTIUM FOR GRAPEVINE GENOME CHARACTERIZATION, 2007).

A detecção de eventos antigos de poliploidia é feita a partir das análises de genes parálogos e detecção de blocos sintênicos (blocos gênicos que estão conservados) duplicados, que são consequências do processo de poliploidização (CHANDERBALI et al., 2022; SCHLUETER et al., 2007). Uma das principais técnicas para detecção de duplicação completas do genoma (WGD- do inglês *whole genome duplication*) é através das análises de picos taxa de substituição sinônimas por sítio (Ks) em genes parálogos (VANNESTE et al., 2014). Associado a técnica de Ks, detecção de blocos sintênicos compartilhados através comparações entre genomas sequenciados, também podem auxiliam na detecção de eventos de poliploidia através de blocos genômicos compartilhados que estão duplicados em um dos genomas, como é visto entre o poliploide *Brassica rapa e A. thaliana* (MUN et al., 2009), e entre genomas das leguminosas (HUFNAGEL et al., 2020).

Uma das consequências de eventos de poliploidia é a duplicação de genes, sendo um fator importante para o processo de especiação, uma vez que cópias do mesmo gene podem sofrer mutações que levam a sub funcionalidades ou neofuncionalização, significando novos fenótipos que podem aumentar o fitness ecológico, bem como a perpetuação desses indivíduos na natureza (BIRCHLER; YANG, 2022; HUGHES; LANGDALE; KELLY, 2014; TESHIMA; INNAN, 2008). Por outro lado, a duplicação de genes pode levar a um desbalanceamento genômico, causando efeitos de dose devido à interação desbalanceadas dos produtos gênicos. Dessa maneira, efeitos de dose podem contribuir na diminuição da expressão do gene duplicado (hipofuncionalização) ou para eventos de deleções e silenciamento epigenético (BIRCHLER; VEITIA, 2014; DE SMET et al., 2013; RODIN; RIGGS, 2003).

O processo de diploidização também é um fator importante para a estabilização e perpetuação dos poliploides (DODSWORTH; CHASE; LEITCH, 2016). A diploidização está relacionada a: i) redução do genoma (com redução do número cromossômico); ii) ao fracionamento de subgenomas nos alopoliploides; iii) modulação da expressão gênica; iv)

ativação de elementos transponíveis e v) reprogramação da maquinaria epigenética (MANDÁKOVÁ; LYSAK, 2018).

2.1.2 Alterações Cromossômicas Estruturais

Ao contrário das alterações numéricas, alterações estruturais não mudam o número cromossômico diretamente, exceto quando levam a disploidias. As disploidias são uma das principais chaves para a diplodização, sendo caracterizadas como uma alteração estrutural pode aumentar ou diminuir o número cromossômico. São divididas entre ascendentes e descendentes, sendo definidas pelo ganho e sem haver perdas de cromossomos inteiros ou alterações no tamanho do genoma, respectivamente. As disploidias descendentes são apontadas como peça fundamental para o processo de diplodização após eventos de poliploidia (LYSÁK; SCHUBERT, 2013; MANDÁKOVÁ; LYSAK, 2018), como visto em Asteraceae (HUANG et al., 2016; SENDEROWICZ et al., 2021), Brassicaceae (MANDÁKOVÁ et al., 2017), Melastomataceae ((ALMEDA; PENNEYS, 2022) e Poaceae (MURAT et al., 2010). Contudo, os impactos causados pelas alterações estruturais cromossômicas são dos mais diversos, mas, normalmente, afetam a morfologia cromossômica e a simetria cariotípica, podendo ser classificadas como inversões, inserções, transposições, translocações, duplicações e deleções (LYSÁK; SCHUBERT, 2013).

2.1.2.1 Inversões

As inversões são definidas como mudanças intracromossomais que invertem a ordem de segmentos cromossômicos ao longo da molécula de DNA, sendo classificadas em dois tipos: paracêntrica, quando não há envolvimento do centrômero, e pericêntrica, quando há envolvimento do centrômero (HOFFMANN; SGRO; WEEKS, 2004; PETTERSSON et al., 2020). As inversões mudam a colinearidade gênica, ou seja, a ordem de genes, ocasionando possíveis mudanças na expressão, podendo alterar o fitness ecológico, reduzir recombinações alélicas e, eventualmente, causar barreiras reprodutivas que podem levar a processos de especiação ((WELLENREUTHER; BERNATCHEZ, 2018). Ao contrário das inversões paracêntricas, inversões pericêntricas podem mudar a morfologia cromossômica, transformando, por exemplo, cromossomos metacêntricos em submetacêntricos, acrocêntricos ou até mesmo telocêntricos (GUERRA, 1988a).

Citogeneticamente, as inversões pericêntricas podem ser identificadas na meiose, caso haja formação de alça de inversão (*loop*) sem quiasmas no paquíteno-diplóteno (LIEHR et al., 2019), como observado no par cromossômico I em *Eleutherine bulbosa* (Mill.) Urb. (GUERRA, 1988b) ou por meio de análise citológicas mais detalhadas onde a mudança de posição de genes ou outras sequências ao longo do cromossomo possa ser observada. como é o caso dos genes de DNA ribossomal e por outras sequências repetitivas, visto também em *E. bulbosa* (BÁEZ et al., 2019; FEITOZA; GUERRA, 2011). O mapeamento citogenético comparativo através da FISH (Hibridização *in situ* Fluorescente) com sondas de BACs (Cromossomos Artificiais de Bactéria) também permitiu a detecção de inversões (para e pericêntricas) em representantes de *Solanum* L. e gêneros relacionados (SZINAY et al., 2012) e de membros da Brassicaceae (BAYAT; LYSAK; MANDÁKOVÁ, 2021; SCHRANZ; LYSAK; MITCHELLOLDS, 2006). Essas modificações estruturais são comumente encontradas ao analisar dados de sequenciamento genômico, revelando que as mesmas são mais frequentes do que se era imaginado, possibilitando um melhor entendimento da evolução cromossômica (MAYER et al., 2011; PETTERSSON et al., 2020).

Adicionalmente, inversões podem alterar o funcionamento do centrômero, principalmente se ocorrerem próximas às regiões centroméricas. A depender do ponto de quebra, inversões podem dar origem a cromossomos dicêntricos, geralmente seguido de silenciamento de um dos centrômeros e da perpetuação do outro (LYSÁK; SCHUBERT, 2013).

2.1.2.2 Transposições

Transposições acontecem quando segmentos de um cromossomo são transferidos de uma região para outra no mesmo cromossomo (GUERRA, 1988a). Este tipo de rearranjo é habitualmente causado por elementos transponíveis de classe II, denominados DNAs transposons (ou genes saltadores), sendo as mediada pela enzima da transposase, que também podem estar envolvidas em outros tipos de rearranjos (ALSEEKH; SCOSSA; FERNIE, 2020; HUANG; BURNS; BOEKE, 2012). Apesar de serem mais abundantes em animais, os transposons são responsáveis por quebras e transposições cromossômicas em algumas plantas, causando alterações genotípicas e fenotípicas, como visto no genoma do milho (*Zea mays* L) e do alopoliploide *Brassica napus* L. (ANDERSON et al., 2018; GRAY, 2000; HUANG; BURNS; BOEKE, 2012).

2.1.2.3 Translocações

A transferência de segmentos entre cromossomos não homólogos é definida como translocação, tendo dois tipos principais: translocações recíprocas e não recíprocas (GUERRA, 1988a; LYSÁK; SCHUBERT, 2013). As translocações recíprocas são aquelas em que há troca mútua de segmentos entre cromossomos não homólogos, comumente encontradas em diversos grupos de angiospermas, como nas leguminosas (DE OLIVEIRA BUSTAMANTE et al., 2021; DO VALE MARTINS et al., 2021; LONARDI et al., 2019a; TALUKDAR, 2010; VASCONCELOS et al., 2015; VERMA; PURBIYA; KHAH, 2019) e gramíneas (ALBERT et al., 2019; FRIEBE et al., 1996; LIU et al., 1992), entre outros. Já nas translocações não-recíprocas apenas um dos cromossomos é doador do segmento a ser t translocado de um cromossomo para outro. Parte das translocações não reciprocas são mediadas por elementos transponíveis ((ROBBERECHT et al., 2013). Um exemplo de translocação não-recíproca é visto entre DNA satélites específicos do cromossomo B (ou extranumerários) para cromossomos As (cromossomos do cariótipo normal) em uma população experimental de centeio (HASTEROK et al., 2002).

Transposons também podem mediar as translocações reciprocas, assim como visto em espécies de sojas selvagens (*Glycine* spp.), impactando na adaptação ambiental das mesmas (WANG et al., 2021). Um tipo mais específico de translocação recíproca são as translocações Robertsonianas, definidas pela transformação de dois cromossomos telocêntricos ou acrocêntricos em um cromossomo (sub)metacêntrico e vice-versa. Assim como as inversões, podem gerar cromossomos dicêntricos caso os dois centrômeros se mantenham funcionais. Contudo, é mais comum que apenas um dos centrômeros permaneça funcional (HOU et al., 2016; LYSÁK; SCHUBERT, 2013; MANDÁKOVÁ; LYSAK, 2018). Dados genômicos em Brassicaceae indicam que este tipo de translocação, junto com as inversões em cromossomos sub- e metacêntrico que geram cromossomos telo- ou acrocêntricos, são um dos principais caminhos para a disploidia descendente nas angiospermas, induzindo a redução no número cromossômico pós eventos de poliploidização e auxiliando na reorganização genômica (MANDÁKOVÁ et al., 2010, 2017). Outros casos de translocações Robertsonianas são encontradas em Poaceae, sejam elas atuando no surgimento de cromossomos monossômicos do trigo (FRIEBE et al., 2005), ou no melhoramento vegetal no híbrido interespecífico *Triticum aestivum* L. –*Dasypyrum villosum*(L.) Borbás (ZHAO et al., 2010). Atualmente, translocações Robertsonianas podem ser induzidas em linhagens hibridas, no intuito do melhoramento

genético, como visto recentemente no híbrido *Triticum aestivum-Agropyron cristatum* (QI et al., 2021).

2.1.2.4 Duplicações e Deleções

Duplicações e deleções são bastante comuns durante a evolução, estando sempre presentes em análises moleculares e genômicas das plantas, geralmente ocorrendo devido a erros de pareamento de cromossomos homólogos, recombinações homólogas desiguais ou ectópicas, e entre cromossomos heterozigotos para inversões (GABUR et al., 2019). Este tipo de alteração é frequentemente encontrado em regiões cromossômicas compostas por sequências de DNA repetitivo em tandem, como nos DNA ribossomais (DNAr). Exemplos disso podem ser evidenciados em genes de RNAr (RNA ribossomal) em gramíneas (Poaceae) da tribo Triticeae(SCOLES et al., 1988) e do gênero *Cynodon* Rich.(CHIAVEGATTO et al., 2019). Outros casos de eventos de deleções e duplicações do cistron de DNAr, inclusive envolvendo as cistrons expressos como RONs (Regiões Organizadoras do Nucléolo), são encontrados em representantes do gênero *Allium* L. (Liliaceae), adicionalmente envolvendo polimorfismos e inativações dessas regiões, como nas populações de *A. schoenoprasum*L. (GARRIDO et al., 1994), ou transposições (*jumping*) desses sítios em híbridos entre *A. cepa* e *A.fistulosum*L.(SCHUBERT; WOBUS, 1985). Diferente das duplicações, as deleções por alterações estruturais podem ocorrer de maneira independente, quando geradas por reparos de quebra da fita-dupla de DNA (ORDON et al., 2017; SCHUBERT et al., 1998).

2.1.3 Rearranjos Secundários

Rearranjos cromossômicos secundários ocorrem quando um cromossomo previamente rearranjado com outro participa de outro evento de rearranjo, devido ao pareamento entre regiões homólogas nos cromossomos. Por exemplo, pontos de quebra dos rearranjos primários podem levar a fusão de cromossomos acrocêntricos, diminuindo o número cromossômico e formando cromossomos dicêntricos (disploidia descendente via translocação Robertsoniana), que sofrem rearranjos secundários como duplicações, deleções e inversões em seguida (SCHUBERT, 2007). Um exemplo deste tipo de alteração foi encontrado em comparações genômicas e citogenéticas entre *Arabidopsis lyrata* (*n*= 8) e *A. thaliana* (*n* = 5), as quais apontaram eventos de inversões seguidas de translocações do tipo Robertsonianas que

fusionaram os cromossomos do cariótipo ancestral e resultaram na diminuição do número cromossômico em *A. thaliana* (KUITTINEN et al., 2004; YOGEESWARAN et al., 2005). Contudo, dados recentes de mapeamentos comparativos genômicos e citogenéticos mostram que eventos de reposicionamento centromérico (com inativação de um dos centrômeros) e surgimento de neocentrômeros são recorrentes na tribo Arabideae (Brassicaceae), explicando a essência monocêntrica do grupo, apesar dos eventos de fusão cêntrica (MANDÁKOVÁ et al., 2020).

Muitos dos rearranjos estruturais, principalmente os secundários, não são facilmente detectados e/ou visualizados, dependendo de vários fatores para que haja uma devida caracterização e comparação entre espécies. Além disso, muitos desses rearranjos se restringem a cromossomos específicos, e a caracterização de cromossomos únicos é um problema histórico nos estudos evolutivos de plantas, amplificado pela falta de resolução da maioria das técnicas citológicas disponíveis.

2.1.4 Eventos que causam rearranjos cromossômicos estruturais

Os eventos que acarretam alterações cromossômicas sempre são resultado de uma ou mais quebras da fita dupla de DNA, seguidas de mecanismos de reparo que podem eventualmente resultar em rearranjos cromossômicos. A quebra da fita dupla pode acontecer devido a uma série de fatores, sejam eles diretos, como exposição a raios X e gama, e/ou indiretos, por erros de replicação celular (KUMAR et al., 2011; SAX, 1941; SCOTT; FOX; FOX, 1974). A fita dupla que sofreu quebra pode ser reparada tanto por recombinações homólogas, aquelas que utilizam sequências de DNA homólogas; ou por recombinações ilegítimas, pelo processo de *Non-Homologous End-Joining* (*NHEJ*), através da utilização sequências não-homólogas, sejam elas alélicas ou não-alélicas. Quando não alélicas, resultam em recombinações ectópicas (LYSÁK; SCHUBERT, 2013).

Recombinações ectópicas podem levar a rearranjos estruturais, como inserções, deleções, duplicações e translocações (LYSÁK; SCHUBERT, 2013). Em plantas, muitos desses rearranjos acontecem devido a recombinações homólogas ou ilegítimas entre sequências de DNA repetitivo, dessa maneira, regiões como a heterocromatina, que são compostas por DNA satélites e elementos transponíveis, são constantemente alvos de rearranjos cromossômicos (GARRIDO-RAMOS, 2017). Registros de rearranjos cromossômicos causados

por recombinações ectópicas de sequências repetitivas são frequentemente encontradas em vários grupos, como a exemplo de translocações de regiões repetitivas dos cromossomos 4AL-7BS no alopoliploide *Triticum dicoccoides* (Körn.) Schweinf. (RASKINA; BELYAYEV; NEVO, 2002). Outro exemplo são as quebras cromossômicas encontradas nas regiões de DNAr 35S, consideradas regiões frangeis por serem envolvidas em eventos de quebras que levam a rearranjos cromossômicos, como translocações robertsonianas em espécies do gênero *Sideritis* L. (Lamiaceae) e no gênero da cidreira, *Cymbopogon* Spreng. (RASKINA et al., 2008).

Além do DNAr, muitas outras regiões cromossômicas com alta densidade de sequências repetitivas são *hot spots* para rearranjos cromossômicos, acreditando-se, inclusive, que eventos de reorganização genômica (e consequente especiação) pós-poliploidização são mediados por rearranjos promovidos por sequências repetitivas (DODSWORTH et al., 2020; GEORGE; ALANI, 2012; RASKINA et al., 2008).

2.1.5 Como detectar rearranjos estruturais?

Comparações de genomas sequenciados nos mostram que rearranjos estruturais são corriqueiros. Em análises entre blocos genômicos compartilhados entre *Brassica oleracea* e *Arabidopsis thaliana*, por exemplo, foi possível detectar várias alterações estruturais, como deleções, inserções e duplicações segmentares após a divergência dessas espécies (LIU et al., 2014; TOWN et al., 2006). O sistema de blocos genômicos foi previamente definido a partir de bibliotecas de cromossomos artificiais de bactérias (BAC- do inglês, *Bacterial Artificial Chromosome*) de *A. thaliana*, e desde então tem sido implementado *in situ* (BAC-FISH) e *in sílico* (genômica comparativa) em diversos representantes de Brassicaceae, apontando extensivas reorganizações genômicas durante a evolução cromossômica desse grupo (LYSAK; MANDÁKOVÁ; SCHRANZ, 2016; WALDEN et al., 2020). Entre legumes, dados de genômica comparativa apontam para a conservação de grandes blocos sintênicos (macrossintenia), com diversos rearranjos cromossômicos (HUFNAGEL et al., 2020; LONARDI et al., 2019; MCCLEAN et al., 2010; REN; HUANG; CANNON, 2019; SHIRASAWA et al., 2013). Entretanto, a maioria das análises genômicas é restrita a grupo de plantas modelos e/ou cultivadas, uma vez que há maior interesse econômico para o sequenciamento e conhecimento da informação genômica dessas espécies.

Em outros casos, técnicas citomoleculares menos dispendiosas e mais simples podem ser aplicadas para visualização dos rearranjos estruturais. Em geral, é possível a detecção de

segmentos cromossômicos mais extensos e rearranjos menos complexos, devido a resolução da maioria das técnicas disponíveis. A associação da genômica comparativa com a citogenética é uma abordagem utilizada para contornar essa limitação, porém, essas análises carecem de sondas específicas para identificação de cromossomos individuais que carregam esses rearranjos (JIANG, 2019). Sendo assim, ferramentas que possibilitem a identificação de cromossomos individuais são essenciais.

2.1.6 Pintura cromossômica: as principais técnicas e novas perspectivas

A pintura cromossômica consiste na identificação de cromossomos específicos por meio da utilização de sondas que hibridizem o cromossomo por inteiro ou segmentos específicos do mesmo (como o braço curto, por exemplo), sendo uma das principais estratégias para a detecção de rearranjos cromossômicos (SCHUBERT et al., 2001). Técnicas de pintura cromossômica desenvolvidas para animais, como microdissecção por citometria de fluxo (AUVINET et al., 2021), apresentam dificuldades em serem reproduzidas na maioria das plantas o que está relacionada à natureza e complexidade dos genomas vegetais (JIANG, 2019; SHENG et al., 2020). Em ambos os grupos as sequências repetitivas geralmente representam uma fração significativa desses genomas. Em plantas, no entanto, além da alta abundância de DNA repetitivo (podendo chegar até 80% do genoma [(SCHNABLE et al., 2009). As sequências repetitivas são em grande parte constituídas de elementos transponíveis (TE), conhecidos como elementos saltadores, pois tem a habilidade de mudar de localização e se proliferarem pelo genoma, muitas vezes flanqueando genes em regiões eucromáticas do cromossomo (ALSEEKH; SCOSSA; FERNIE, 2020). Esses elementos tendem a serem mais dispersos na plantas, enquanto em animais, tendem a ser mais compartimentalizadas, ou seja, localizadas em regiões específicas dos cromossomos, o torna o bloqueio dessas sequências repetitivas mais viável (HESLOP-HARRISON; SCHWARZACHER, 2011; LÓPEZ-FLORES; GARRIDO-RAMOS, 2012).

Bibliotecas de BACs são frequentemente empregadas na identificação de cromossomos individuais em espécies de genoma pequeno (JIANG, 2019a). Os BACs são vetores que carregam grandes insertos de DNA genômico (~ 100kb). Quando selecionados a partir de regiões de cópia única do genoma e utilizados como sonda na FISH (BAC-FISH), sinais em cromossomos específicos (correspondendo a sua região de origem no genoma) geralmente são

produzidos, servindo para estudos de sintenia e evolução cromossômica e, principalmente, para mapeamentos citogenéticos comparativos entre espécies relacionadas (JIANG, 2019a).

Em Brassicaceae, a pintura cromossômica foi baseada em bibliotecas de BACs de *A. thaliana*, utilizadas como sondas na FISH (LYSAK et al. 2001), e juntamente com um sistema de blocos genômicos (SCHRANZ et al. 2006), foi usado para elucidar o cariótipo evolução dentro da família. Esses estudos permitiram a inferência do Cariótipo Ancestral das Cruciferas (ACK), revelando rearranjos cromossômicos relacionados a disploidia decrescente observada em *A. thaliana* (LYSAK et al. 2006), rearranjo cromossômico após todo o genoma triplicação (WGT) como visto em espécies de *Brassica* (CHENG; WU; WANG, 2014), e reposicionamento do centrômero (ou seja, a posição do centrômero muda sem colinearidade pausas) em toda a família (WILLING et al. 2015; LYSAK et al. 2016; MANDAKOVÁ et al. 2020). Contudo, pintura cromossômica por meio de bibliotecas de BACs são restringidas a poucos grupos fora de Brassicaceae, como em *Brachypodium* (Poaceae) (BETEKHTIN; JENKINS; HASTEROK, 2014). Apesar disso, mapeamentos comparativos por BAC-FISH foram realizados em outros grupos de plantas com genoma pequeno, como por exemplo em *Phaseolus* L. (FERRAZ; FONSÊCA; PEDROSA-HARAND, 2020b; FONSÊCA et al., 2010; FONSÊCA; FERRAZ; PEDROSA-HARAND, 2016a) e *Citrus* L. (SILVA et al., 2015, 2019), revelando a capacidade de detecção de quebras de sintenia e colinearidade em *Phaseolus* e conservação em *Citrus*.

Ainda que a utilização de bibliotecas de BACs permita a identificação e caracterização de cromossomos individuais, essa abordagem é trabalhosa e demorada, uma vez que depende da identificação de muitos marcadores individuais, seleção dos BACs e sucessivas rodadas de FISH, tornando este tipo de análise limitada a um pequeno grupo de plantas (JIANG, 2019a).

Uma abordagem mais atual, baseada em sondas de oligonucleotídeos (oligos), foi desenvolvida para identificação cromossômica como sonda para FISH (Oligo-FISH). Esses oligos são construídos a partir de dados de genomas sequenciados e montados, caracterizam-se como sequências curtas oriundas de regiões cópia única de um ou mais cromossomos selecionados pelo software *Chorus*2 (ZHANG et al., 2021). Essas sequências são sintetizados em massa, marcadas em conjunto e então utilizadas como sondas (HAN et al., 2015a). Duas abordagens principais são possíveis na utilização de Oligos em FISH: pintura cromossômica (*Oligopaint*) e barcode (*Oligobarcode*). *Oligopaint* foi inicialmente desenvolvida através do genoma de pepino (*Cucumis sativus* L.), utilizando dois conjuntos de sondas marcados de cores diferentes, foi possível a identificação de cromossomos individuais na espécie, bem como em

grupos relacionados sem genoma montado (HAN et al., 2015a). *Oligopaint* vem sendo aplicado com eficácia em vários grupos de plantas e animais (ALBERT et al., 2019; BRAZ et al., 2018b; FILIAULT et al., 2018; HE et al., 2018, 2020; HOU et al., 2018; QU et al., 2017a; ROSIN et al., 2021; SHI et al., 2022) permitindo, por exemplo, comparações intraespecíficas que relevam rearranjos cromossômicos complexos, como em linhagens do milho (ALBERT et al., 2019), e comparações interespecíficas, como nos representantes de *Citrus*, a qual apontou extrema conservação de sintenia cromossômica dentro do gênero (HE et al., 2020).

Os preceitos iniciais do *Oligobarcode* são semelhantes aos do *Oligopaint*, contudo, os *oligos* são derivados de regiões menores (em torno de 1 Mpb) de todos os cromossomos do cariótipo e selecionados de modo a criar um padrão específico de sinais para identificação de cromossomos específicos. O uso simultâneo de um conjunto de sequências cromossomo-específicas em duas cores (verde e vermelho) gera um código de barras cariotípico para uma determinada espécie (BRAZ et al., 2018b; JIANG, 2019a). A primeira aplicação desse método em plantas utilizou o genoma de *Solanum tuberosum* L. (THE POTATO GENOME SEQUENCING CONSORTIUM, 2011), criando um sistema de identificação cariotípica útil não só para batata, mas também para tomate (*S. lycopersicum* L.) e outras espécies do gênero *Solanum*. Mudança nos padrões de bandas entre espécies analisadas apontou para as possíveis alterações cromossômicas envolvidas na evolução das mesmas (BRAZ et al., 2018b).

Deste modo, o uso da Oligo-FISH para pintura cromossômica e caracterização cariotípica é bastante promissor, já que a técnica mostrou ser reproduzível e eficaz em várias plantas, além de permitir comparações intra e interespecíficas em espécies não-modelos, desde que um genoma montado de qualidade esteja disponível no gênero (JIANG, 2019).

2.2 Elementos repetitivos e sua importância para evolução do genoma

2.2.2 Elementos repetitivos e a composição do genoma

O DNA repetitivo constitui a maior parte dos genomas de eucariotos, podendo representar mais de 85%, como por exemplo no milho (SCHNABLE et al., 2009). A porção repetitiva está diretamente ligada ao tamanho do genoma e é o principal componente das bandas heterocromáticas visualizadas nos cromossomos nas regiões subterminais, intersticiais e pericentroméricas (GARRIDO-RAMOS, 2017; PLOHL; MEŠTROVIC; MRAVINAC, 2012; VAN-LUME et al., 2019). Denominada no passado de “DNA lixo” ou “egoísta” (GREGORY,

2005), inúmeros trabalhos hoje mostram a fração repetitiva como um dos protagonistas responsáveis por aspectos importantes da evolução do genoma. Além de sua importância na geração de rearranjos cromossômicos numéricos e estruturais (LI et al., 2017), essa fração está diretamente ligada a: 1) aumento e diminuição do tamanho do genoma (KELLY et al., 2015; PELLICER et al., 2018); 2) mecanismos de silenciamento e ativação epigenética, podendo gerar mutações de interesse econômico (LISCH; BENNETZEN, 2011); 3) amplificação de sequências gênicas em tandem (CANNON et al., 2004), dentre muitas outras. Além disso, as sequências repetitivas são comumente utilizadas como marcadores genéticos para estudos de evolução e organização cromossômica (CHALUP et al., 2015; KIROV et al., 2017) e análises filogenéticas (VITALES; GARCIA; DODSWORTH, 2020).

O DNA repetitivo pode ser separado em dois grupos principais de acordo com sua organização e distribuição no genoma: sequências repetidas em tandem e sequências dispersas. As sequências em tandem são organizadas em uma conformação "*head-to-tail*", ou seja, com as cópias da unidade básica de repetição (monômero) encontradas sempre na mesma direção. Podem ser representados por genes codificantes (genes de RNAr) ou por regiões não-codificantes como micro-, mini- e DNA satélites (GARRIDO-RAMOS, 2017). Já as sequências dispersas são elementos que podem se mover dentro do genoma (elementos transponíveis) de forma autônoma ou não-autônoma, a partir de diversos mecanismos como os de "copiar e colar" (retrotransposons) ou de "cortar e colar" (transposons) (WICKER et al., 2007).

2.2.3 Sequências gênicas em tandem

A duplicação em tandem é fruto de *crossing-over* desigual e por replicação *slippage*, gerando múltiplas cópias repetitivas proximamente localizadas (YU et al., 2015). Muitos genes que sofreram duplicação em tandem estão relacionados a funções importantes, como tolerância a estresse e funções celulares em *Arabidoposis* e em arroz (RIZZON et al., 2006; HANADA et al., 2008).

Os genes de RNAr 5S e 18S-5.8S-28S (35S) são os principais exemplos de DNA codificante repetido em tandem. Esses genes são altamente conservados nos eucariontes, principalmente o 35S, o qual geralmente está localizado nas regiões terminais, pericentroméricas e nas constrições secundárias (RONs - região organizadora do nucléolo). Apesar de serem conservados em sequência, os sítios DNAr são bastante polimórficos em tamanho, número e localização em plantas, devido à alta frequência de recombinação ectópica, crossing-over desigual e slippage tornando-os um dos principais marcadores citogenéticos

identificados por FISH (GARCIA et al., 2017) . Embora ambos os DNAr sejam variáveis, muitos grupos apresentam variação principalmente em um ou outro tipo, seja no 5S, como em Orchidaceae (LAN; ALBERT, 2011) ou no 35S, caso de Cactaceae (HARPKE; PETERSON, 2006).

Outras sequências repetitivas podem estar envolvidas na proliferação do DNAr no genoma. Estudos em uma espécie selvagem próxima ao trigo (*Aegilops speltoides* Tausch) indicam que elementos transponíveis se inseriram em regiões espaçadoras intergênicas (IGS) e proliferam cópias de DNAr pelo o genoma (BELYAYEV et al., 2010). Em um exemplo contrário, mas também envolvendo o IGS, foram encontradas evidências que uma família de DNA satélite de tomate se formou a partir da sequência IGS do DNAr, tendo se proliferado pelo genoma por mediação de elementos transponíveis (JO et al., 2009).

2.2.4 DNA satélites

DNAs satélites (DNAsat) constituem uma importante fração do genoma, podendo chegar a 36% em plantas (EMADZADE et al., 2014; GARRIDO-RAMOS, 2015a). Os DNAs satélites podem sofrer amplificação e mutações, acarretando surgimento de diferentes famílias de DNAsat, presente em diferentes proporções em uma espécie, como visto nas 15 famílias de DNAsat presentes no genoma de *Pisum sativum* L. (MACAS; NEUMANN; NAVRÁTILOVÁ, 2007). Além disso, mutações ocorrentes em um monômero podem se espalhar para os demais da mesma família pelo processo de homogeneização, levando a evolução em concerto dessa sequência e a uma divergência da mesma quando comparada com espécies próximas (GARRIDO-RAMOS, 2017; LOUZADA et al., 2020).

O conjunto de famílias de DNAsat de um genoma pode ser referido como satelitoma (RUIZ-RUANO et al., 2016). As famílias componentes do satelitoma podem seguir diferentes caminhos, podendo se manterem em uma única espécie ou se conservar no gênero, a depender dos mecanismos e eventos de especiação. Por exemplo, um DNAsat pode estar presente em uma única espécie, como a variante do satélite ZpS1 em *Zamia paucijuga* Wieland (Zamiaceae) (CAFASSO; CHINALI, 2014) ou ser um componente genômico em várias espécies de um gênero e de gruposrelacionados, como a CsSat181 em *Citrus* e gêneros próximos (BARROS E SILVA et al., 2010). Em animais, podemos encontrar satélites ainda mais conservados,

presentes em diferentes representantes de uma família ou até mesmo entre diferentes famílias (GARRIDO-RAMOS, 2017).

A eliminação ou fixação de famílias de DNAsat em diferentes táxons pode estar relacionada a possíveis funcionalidades dessas sequências. A disposição dos satélites em regiões heterocromáticas centroméricas e pericentroméricas, por exemplo, sugere o envolvimento dos DNAsat na segregação dos cromossomos, com potencial participação na formação e organização do cinetócoro, regulação da segregação cromossômica durante a mitose e meiose, suporte a estrutura cromossômica e regulação epigenética dos centrômeros (BISCOTTI; OLMO; HESLOP-HARRISON, 2015; PEZER et al., 2012; PLOHL et al., 2008). Por essa razão, podemos encontrar diversos casos de satélites abundantes localizados na próximos/flanqueando a região centromérica, juntamente a proteínas específicas do centrômero (histona H3 e variantes). Contudo, satélites centroméricos tendem a ser restrito a espécies proximamente relacionadas devido a rápida evolução (PLOHL; MEŠTROVIĆ; MRAVINAC, 2014), como no caso do feijão comum, que possui dois satélites centroméricos: CentPv1 (Nazca) e CentPv2 (IWATA et al., 2013). Por outro lado, o satélite centromérico "*Tyba*", originalmente encontrado na espécie holocêntrica *Rhynchospora pubera* (Vahl) Boeckeler (MARQUES et al., 2015), foi também localizado em diferentes espécies de *Rhynchospora* Vahl, indicando que, apesar da rápida evolução dos satélites centroméricos, alguns deles podem se manter conservados entre espécies (RIBEIRO et al., 2017a).

Os DNAsat também são poderosos marcadores cromossômicos e podem ser usados para descrições cariotípicas, como visto em *Allium fistulosum* (2*n* = 16), na qual dois satélites (HAT58 e CAT36) estão presentes nos cromossomos 5, 6, 7 e 8 nas regiões heterocromáticas pericentroméricas e intersticiais (KIROV et al., 2017).

2.2.5 Elementos Móveis

Apesar de sua descoberta por Barbara McClintock (1956), os elementos transponíveis foram por muito tempo negligenciados, até que, nas últimas décadas, tenham sido reconhecidos como importantes para a composição e evolução dos genomas (BOURQUE et al., 2018; WICKER et al., 2007). Hoje sabemos que esses elementos estão envolvidos no aumento e diminuição do tamanhos do genoma (Lee& Kim, 2014), rearranjos cromossômicos

(CARVALHO; LUPSKI, 2016), regulação transcricional (CHUONG; ELDE; FESCHOTTE, 2017) e entre vários outros eventos.

Conceitualmente, os elementos transponíveis consistem em sequências de DNA com habilidade de locomoção, mudando de posição e proliferando-se de maneira dispersa pelo genoma. Entretanto, apesar de dispersas, essas sequências não são distribuídas aleatoriamente, havendo preferências por determinadas sequências ou domínios genômicos para inserções (BOURQUE et al., 2018). Os elementos transponíveis podem ser divididos de acordo com seu mecanismo de transposição em duas grandes classes: Classe I, denominada de retrotransposons, e Classe II, denominada de transposons. Cada uma dessas classes pode ser subdividida em subclasses, e cada subclasse em superfamílias e famílias de acordo com características compartilhada entre esses elementos, como por exemplo a ordem dos domínios gênicos (WICKER et al., 2007).

Elementos de Classe I se transpõem por mecanismo de "copia-e-cola", utilizando a enzima trasncriptase reversa. Já os elementos de Classe II, ou transposons, se locomovem no genoma por mecanismos diversos, sendo o mais conhecido o mecanismo de "corta–e-cola". Esse processo consiste na clivagem da fita dupla de DNA mediante a enzima transposase, fazendo com que o DNA seja retirado e reinserido em outro local do genoma gerando *repeats* terminais invertidos de tamanhos variados, denominados de TIRs (subclasse I) (WICKER et al., 2007). Devido ao mecanismo e preferência de inserção, os elementos da classe II estão envolvidos em processos de regulação epigenética, mutagênese, rearranjos, dentre outros (LISCH, 2013). No genoma de plantas, entretanto, os transposons são os elementos móveis menos abundantes, representando, em geral, uma pequena fração dos elementos repetitivos (KRASILEVA, 2019; WICKER et al., 2007)

Os elementos de Classe I são divididos em duas subclasses: LTR e não-LTR. A diferença entre as duas é a presença ou ausência da Repetição Terminal Longa (*Long Terminal Repeat*-LTR). Os elementos LTR se subdividem ainda em Ty1/*Copia* e Ty3/*Gypsy*, enquanto dentre os não-LTR podemos citar os LINEs e SINEs. No geral, a estrutura básica do LTR é conservada, consistindo na presença de *repeats* nas extremidades 5' e 3', sítios de iniciação e finalização de transcrição, domínios proteicos do tipo GAG, protease (PROT), transcriptase reversa (RT), ribocluase H (RH) e integrase (INT), dentre outras características (NEUMANN et al., 2019). As características dos domínios proteicos, como a ordem da INT e RT,são responsáveis pela diferenciação de Ty1/*copia* e Ty3/*gypsy* (WICKER et al., 2007), e auxiliam na identificação de diferentes linhagens dessas superfamílias (NEUMANN et al., 2019).

Embora a sua natureza seja dispersa, algumas linhagens de retrotransposons do tipo LTR apresentam localização preferencial no genoma, exibindo padrões específicos no cariótipo de algumas plantas. O mapeamento de elementos LTR por FISH em trigo, por exemplo, permitiu identificar diferentes subgenomas do alopoliploide (AABBDD), mostrando que diferentes linhagens são predominantes em cada subgenoma, como a linhagem Ty3/*gypsy-Fatima* no subgenoma B (SALINA et al., 2011; ZHANG et al., 2004). Já uma investigação sobre estrutura e localização de linhagens de LTR em cana-de-açúcar (*Saccharum* spp.), mostrou que os elementos Ty1/*copia* são preferencialmente encontrados nas regiões eucromáticas, enquanto os elementos Ty3/*gypsy* estão mais presentes em regiões heterocromáticas (DOMINGUES et al., 2012). Por outro lado, análises em gramíneas forrageiras (*Brachiaria*) mostraram linhagens derivadas de Ty3/*gypsy* que apresentam diferentes padrões de distribuição nos cromossomos, podendo ser dispersas *(Del/Tekay* e *Tat)* ou se concentrarem nas regiões proximais dos cromossomos (*CRM* e *Athila*) (SANTOS et al., 2015). Outra característica interessante dos LTR é a constante relação com famílias de DNAsat, muitas vezes compartilhando sequências homogeneizadas, como no caso das linhagens Ty3/*gypsyOgre* e *Tat* com o satélite PisTR-A em ervilha (*Pisum sativum*), sugerindo o envolvimento desses elementos no surgimento, amplificação e proliferação desse satélite no genoma dessa espécie (MACAS et al., 2009).

Os impactos dos elementos repetitivos, principalmente dos retroelementos, sobre o genoma das plantas ficam cada vez mais evidentes à medida em que mais dados genômicos vão sendo disponibilizados. Esses dados mostram o papel fundamental da fração repetitiva na evolução do genoma de plantas, além de fornecer apontamentos sobre a dinâmica da evolução cromossômica dentro de populações, gêneros, tribos e até mesmo famílias.

2.3 A tribo Phaseoleae: Perspectivas filogenéticas, citogenéticas e genômicas

2.3.1 Relações filogenéticas

As leguminosas (Leguminosae Juss.) constituem uma família monofilética e cosmopolita, com cerca de 750 gêneros e 19.500 espécies (CHRISTENHUSZ; BYNG, 2016). Muitos representantes desta família são cultivares de grande importância econômica, sendo essenciais para a nutrição humana e animal em regiões mais carentes do mundo, significando uma fonte rica em proteínas e em vitaminas para a população (ANDERSON et al., 1984; GEIL; ANDERSON, 1994; MAPHOSA; JIDEANI, 2017). A maior parte das leguminosas em cultivo fazem parte do grupo phaseoloide, que possui cerca de 114 gêneros e aproximadamente 2.000

espécies, distribuídas nas tribos Phaseoleae, Psoraleeae e Desmodieae (LEWIS et al., 2005(STEFANOVIĆ et al., 2009)). Análises filogenéticas utilizando os marcadores cloroplastidiais *rbcL*, *trnL-F* e *trnK/matK* estimam que o grupo sofreu diversificação há 39.5 milhões de anos (Ma), tendo os principais clados sido formados após dois eventos de diversificação, um de 28.6 Ma (R1) e outro de 21.9 Ma (R2) (LI et al., 2013a). Na tribo Phaseoleae, considerada polifilética, há quatro subtribos específicas que pertencem ao grupo phaseoloide: Phaseolinae, Glycininae, Cajaninae e Kennediinae (DOYLE; DOYLE, 1993a; LI et al., 2013a; STEFANOVIĆ et al., 2009). Dentre os principais representantes de Phaseoleae podemos destacar a soja [*Glycine Max* (L.) Merr.], o feijão comum (*Phaseolus vulgaris*), o feijão-caupi (*Vigna unguiculata* (L.) Walp.), o feijão-guandu (*Cajanus cajan* (L.) Millsp.) e o siratro (*Macroptilium atropurpureum* (DC.) Urb.) (LEWIS et al., 2005; LI et al., 2013).

A subtribo Phaseolinae é composta por cerca de 30 gêneros e 315 espécies, tendo se diversificado há cerca de 14.3 Ma (Figura 1) (SCHRIRE, 2005(LI et al., 2013a). A subtribo inclui gêneros como *Phaseolus*, *Vigna* Savi e *Macroptilium* (Benth.) Urb., os quais divergiram há ~ 10 Ma (LI et al., 2013).

Esses três gêneros representavam um complexo taxonômico, no qual, inicialmente, todos eram considerados como *Phaseolus*, até que estudos, como o de VERDCOURT (1970), os classificassem como gêneros distintos (SNAK; MIOTTO; GOLDENBERG, 2011). *Macroptilium* apresenta 21 espécies atualmente aceitas (POWO, 2022; THE PLANT LIST, 2013) distribuídas do sudoeste dos Estados Unidos ao norte da Argentina (ESPERT; DREWES; BURGHARDT, 2007b). Análises filogenéticas (com marcadores nucleares ITS-1 e ITS-2) e biogeográficas indicam que *Macroptilium* surgiu há cerca de 2-4 Ma, constituindo um grupo monofilético subdividido em dois clados: *Macroptilium* (sessão A) e *Microcochle* (sessão B); que podem ser distinguidos de acordo com sua inflorescência (ESPERT; BURGHARDT, 2010a).

Figura 1 - Filogenia da subtribo Phaseolinae retirada e modificada de Li et al. (2013)

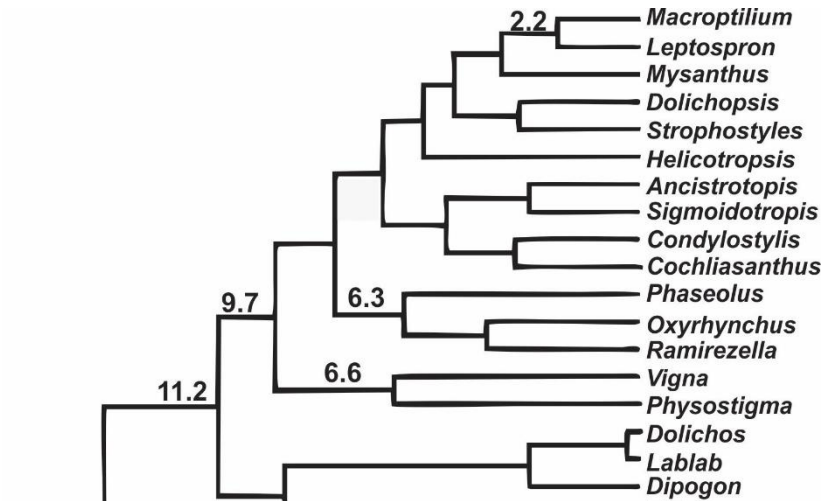

][

Fonte: LI et al., 2013

Apesar das relações filogenéticas serem bem resolvidas, existe uma lacuna em análises sobre a diversidade molecular e cariotípica em *Macroptilium*, assim como em gêneros próximos. Apenas *Phaseolus* e *Vigna* possuem genomas sequenciados (LONARDI et al., 2019a; SCHMUTZ et al., 2014a) e vários estudos citogenéticos moleculares e mapeamentos comparativos (DE OLIVEIRA BUSTAMANTE et al., 2021; DO VALE MARTINS et al., 2021; FONSÊCA et al., 2010; OLIVEIRA et al., 2020; RIBEIRO et al., 2020; VASCONCELOS et al., 2015).

2.3.2 Genomas sequenciados e comparações de sintenia e colinearidade

Devido ao grande apelo socioeconômico, algumas espécies da tribo Phaseoleae possuem genomas sequenciados. Existem 39 acessos com genomas sequenciados e montados a nível cromossômico disponíveis na plataforma do NCBI (do inglês- *National Center for Biotechnology Information* - https://www.ncbi.nlm.nih.gov/assembly/?term=phaseoleae), sendo o gênero Glycine com a maior representação entre eles (Tabela 1). A comparação desses genomas mostra conservação de blocos sintênicos, porém com vários rearranjos resultando em quebras de macrossintenia (LONARDI et al., 2019a; QIN et al., 2019; SCHMUTZ et al., 2010a, 2014a; VARSHNEY et al., 2012; YANG et al., 2015).

A comparação de *V. unguiculata*, *V. radiata* e *V. angularis* mostrou alta conservação de blocos sintênicos, com poucos rearranjos envolvidos. Além disso, foi proposto que o elemento Ty3/*gypsy* é um dos principais responsáveis pela diferença entre os tamanhos dos genomas dessas espécies (LONARDI et al., 2019a). Já a comparação de *V. unguciulata* com *P. vulgaris*, mostrou que seis cromossomos de *V. unguiculata* (*Vu*04, *Vu*06, *Vu*07, *Vu*09, *Vu*10 e *Vu*11) possuem extensa macrossintenia em relação a *P. vulgaris*, enquanto cinco cromossomos (*Vu*01, *Vu*02, *Vu*03, *Vu*05 e *Vu*08) estão envolvidos em quebras de macrossintenia por rearranjos cromossômicos, (Figura 2) (LONARDI et al., 2019a). Entre *P. vulgaris* e *G. Max* foram

detectados extensos blocos sintênicos, com os blocos em *G. max* duplicados, uma vez que o mesmo passou por um evento de poliplodia recente (~ 10 Ma) (Figura 3) (SCHMUTZ et al., 2014a).

Figura 2 - Comparação entre blocos sintênicos dos genomas de *P. vulgaris* e *V. unguiculata* (figura adaptada de LONARDI et al., 2019). As linhas de diferentes cores conectando as pseudomoléculas das duas espécies demonstram os segmentos conservados entre elas.

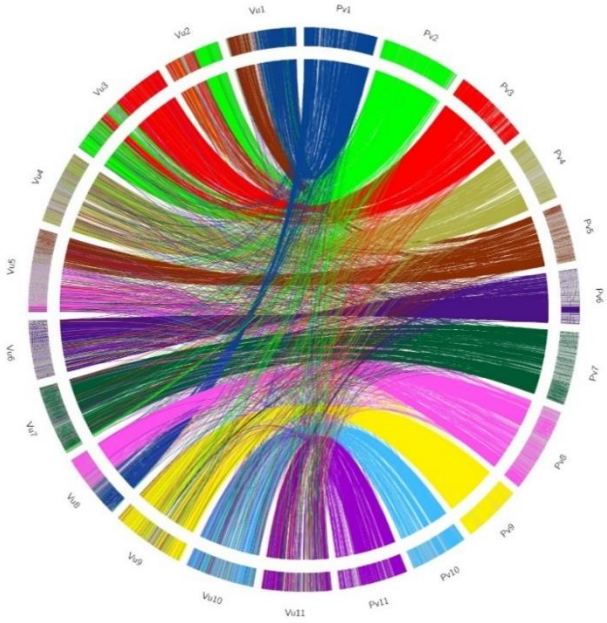

Fonte: LONARDI et al., 2019

As frequências de recombinação ao longo dos cromossômicos também foram avaliadas nesses genomas, mostrando alta densidade nas regiões subterminais e baixa nas regiões pericentroméricas e centroméricas (LONARDI et al., 2019a; SCHMUTZ et al., 2010a, 2014a). O baixo índice de recombinação nas regiões pericentroméricas é explicado pela predominância dos elementos repetitivos nessas regiões, representando geralmente as regiões heterocromáticas (SCHMUTZ et al., 2010).

Análises de bioinformática e mapeamentos cromossômicos de elementos repetitivos mostram a alta dinâmica evolutiva dessas sequências neste grupo, apesar da distribuição geral da heterocromatina ocorrer nas regiões peri- e centromerérica e subterminais (RIBEIRO et al., 2020a; SCHMUTZ et al., 2010a, 2014a). Esse é o caso do DNA satélite subtelomérico *khipu* em *Phaseolus*, que está presente em todos os representantes investigados do gênero, mas apresenta diferentes níveis de amplificação entre as espécies (RIBEIRO et al., 2017b). Além disso, análises em *Phaseolus*, *Vigna* e *Cajanus* sugerem que elementos transponíveis LTR do tipo Ty3/*gypsy* e DNAsat são os principais elementos repetitivos nos genomas desse grupo. Um conjuntoconjunto de *repeats* específico para cada espécie pode ser observado, porém se

acumulando preferencialmente nas regiões centroméricas e pericentroméricas (RIBEIRO et al., 2020a). Isso mostra que a porção repetitiva dos genomas da tribo Phaseoleae são partes interessantes para serem analisadas, uma vez que elas podem contribuir no entendimento da composição e estrutura cromossômica.

Figura 3 - Comparação entre blocos sintênicos dos genomas de *P. vulgaris* e *G. max*

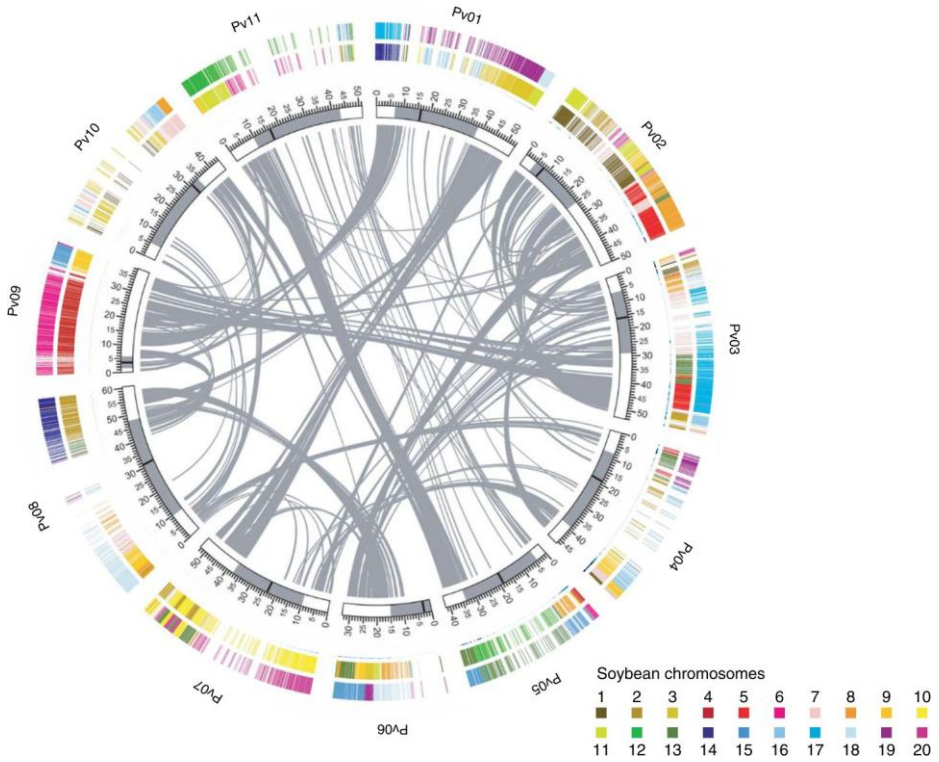

Fonte: SCHMUTZ et al., 2014.

Tabela 1 - Genomas de representantes da tribo Phaseoleae que estão sequenciados e montados a nível cromossômico no NCBI.

Acessos com genoma montado da tribo Phaseoleae (NCBI)							
Gênero	**Espécie**	**Nome infraespecifico**	**Nº cromossômico (*n*)**	**Tamanho total da sequência (em pb)**	**Tamanho do genoma (valor 2C)**	**Acesso GenBank**	**Referência**
Amphicarpaea	*A. edgeworthii*	Ecotype: Qianfo Mountain	11	299059313	0,612	JACEGY000000000.1	LIU et al. 2021
Cajanus	*C. cajan*	-	11	590523786	1,208	AGCT00000000.1	VARSHNEY et al. 2011
Glycine	*G. latifolia*	-	20	939492075	1,921	QARZ00000000.1	LIU et al., 2018
Glycine	*G. max*	Cultivar: Williams 82	20	978941695	2,002	ACUP00000000.4	SCHMUTZ et al. 2010
Glycine	*G. max*	Cultivar: Jidou 17	20	995269373	2,035	JACKXA000000000.1	YI et al. 2020
Glycine	*G. max*	Cultivar: Zhonghuang 13	20	1011378317	2,068	QKRT00000000.2	SHEN et al. 2020
Glycine	*G. max*	Cultivar: Hwangkeum	20	933123489	1,908	JAGRRG000000000.1	KIM et al. 2021
Glycine	*G. max*	Cultivar: PI594527	20	992121078	2,029	JAGMTN000000000.1	WANG et al. 2021
Glycine	*G. max*	Cultivar: Huaxia 3	20	985988379	2,016	WIXC00000000.1	CHU et al. 2021
Glycine	*G. max*	Cultivar: EMBRAPA BRS 537	20	1000033753	2,045	JAAFZW000000000.2	Dados não publicados
Glycine	*G. max*	Cultivar: Jinyuan	20	995708058	2,036	WIXB00000000.1	CHU et al. 2021
Glycine	*G. max*	Cultivar: Tianlong1	20	1020982885	2,088	JACDZO000000000.1	JIA et al., 2020
Glycine	*G. max*	Cultivar: Hefeng 25	20	987260260	2,019	WIWX00000000.1	CHU et al. 2021
Glycine	*G. max*	Cultivar: ZN6	20	1011398009	2,068	JAHKKD000000000.1	LIU et al. 2022
Glycine	*G. max*	Cultivar: Williams 82	20	993001975	2,031	WIWW00000000.1	Dados não publicados
Glycine	*G. max*	Cultivar: Wenfeng 7	20	996720390	2,038	WIWY00000000.1	Dados não publicados
Glycine	*G. max*	Cultivar: Zhonghuang 35	20	1001328948	2,048	WIWZ00000000.1	Dados não publicados
Glycine	*G. max*	Cultivar: Lee	20	1016275704	2,078	PELE00000000.1	Dados não publicados
Glycine	*G. soja*	Cultivar: W05	20	1013766566	2,073	QZWG00000000.1	XIE et al., 2019
Glycine	*G. soja*	Cultivar: F	20	975918537	1,996	WIXD00000000.1	CHU et al. 2021
Glycine	*G. soja*	Cultivar: PI 483463	20	985259865	2,015	PGFP00000000.1	VALLIYODAN et al., 2019
Mucuna	*M. pruriens* var. utilis	-	11	479662982	0,981	JANPWY000000000.1	HAO et al. 2022
Phaseolus	*P. lunatus*	Cultivar: G27455	11	546419622	1,117	JAAFYQ000000000.1	GARCIA et al., 2021
Phaseolus	*P. vulgaris*	Cultivar: G19833	11	521076696	1,066	ANNZ00000000.1	SCHMUTZ et al. 2014

Phaseolus	*P. vulgaris*	Cultivar: OAC Rex	11	423735710	0,867	JADFUL000000000.1	COX et al., 2021
Phaseolus	*P. vulgaris*	Cultivar: BAT93	11	549748340	1,124	LPQZ00000000.1	VLASOVA et al., 2016
Pueraria	*P. montana*	-	11	978589990	2,001	JANIXD000000000.1	MO et al. 2022
Vigna	*V. radiata* var. radiata	Cultivar: VC1973A	11	463637892	0,948	JJMO00000000.1	KANG et al. 2015
Vigna	*V. angularis*	Cultivar: LongXiaoDou No.4	11	447806493	0,916	JABFOF000000000.1	Dados não publicados
Vigna	*V. angularis* var. angularis	Cultivar: Shumari	11	522761097	1,069	PRJDB3778	SAKAI et al., 2015
Vigna	*V. angularis* var. angularis	Cultivar: Kyungwonpat	11	444438822	0,909	JRFV00000000.1	KANG et al. 2015
Vigna	*V. mungo*	Cultivar: IPU-94-1	11	454426400	0,929	JAMTDO000000000.1	AMBREEN et al., 2022
Vigna	*V. mungo*	-	11	498912072	1,020	JABCND000000000.1	Dados não publicados
Vigna	*V. unguiculata*	Cultivar: IT97K-499-35	11	518747877	1,061	NBOW00000000.1	LONARDI et al., 2019
Vigna	*V. unguiculata*	Cultivar: Xiabao 2	11	597519742	1,222	PRJNA454850	Dados não publicados
Vigna	*V. umbellata*	Cultivar: FF25	11	475513050	0,972	JALEER000000000.1	Dados não publicados
Vigna	*V. reflexopilosa*	Cultivar: glabra	22	985987933			

2.3.3 Caracterização cariotípica e mapeamento citogenético comparativo

O número cromossômico básico da tribo Phaseoleae é *x* = 11 (ESPERT et al., 2008; LEE et al., 2017). Entretanto, é possível encontrar variação entre as subtribos, tanto no conteúdo de DNA (2C), quanto no número cromossômico (2*n*), como visto na Tabela 1. As subtribos Phaseolinae, Cajaninae e Kennediinae, por exemplo, exibem o padrão geral de 2*n* = 22, com conteúdo 2C variando entre 0.70 (*Lablab purpureus* (L.) Sweet) a 2.57 picogramas (pg) (*Cajanus albicans* (Wight & Arn.) Maesen), enquanto Glycininae exibe variação de 2*n* = 22 (*Amphicarpaea bracteata* (L.) Fernald) a 2*n* = 44 (*Teyleria koordersii* (Backer) Backer), com conteúdo 2C variando entre 0.70 a 2.26pg (PELLICER; LEITCH, 2020; RICE et al., 2015a). Grupos incertos da tribo, como *Erytrina+Psophorcapus* (proposto por (STEFANOVIĆ et al., 2009), apresentam variações ainda maiores, com espécies de 2*n* = 18 (*Psophocarpus tetragonolobus* (L.) DC.)e 2*n*= 84 (*Erythrina acanthocarpa* E. Mey), e com conteúdo de 2C de 1.55 (*P. tetragonolobus*)a 3.53 pg (*Erythrina caffra* Thunb.)(PELLICER; LEITCH, 2020; RICE et al., 2015a).

Há também variabilidade no número de sítios de DNAr 5S e 35S (Tabela 1).Representantes da subtribo Phaseolinae demonstram variação interpopulacional, como visto em *P. vulgaris* e *V. unguiculata* (PEDROSA-HARAND et al., 2006; VITALES et al., 2017); variação interespecífica, como, em *V. unguiculata* e *V. angularis* (CHOI et al., 2013; VITALES et al., 2017); e variação intergenérica, como entre *M. atropurpureum, P. vulgaris* e *V. unguiculata* (BARROS FERREIRA, 2019; VITALES et al., 2017). As espécies listadas das subtribos Cajaninae e Glycininae mostram números menores de sítios de DNAr 5S e 35S em relação a Phaseolinae, mesmo em casos de número cromossômico maior, como em *G. max*, que apresenta apenas um par de DNAr 5S e 35S (VITALES et al., 2017). Já o grupo *Erytrina+Psophorcapus* apresenta um par de sítios de DNAr 5S e de seis a 10 de DNAr 35S (CHAOWEN et al., 2004; VITALES et al., 2017).

Mapeamentos citogenéticos permitiram identificar diversos eventos de rearranjos cromossômicos em Phaseolinae, como a exemplo dos representantes do gênero *Phaseolus*. A maioria das espécies do gênero possui 2*n* = 22 (*x* = 11), exceto pelas espécies do grupo Leptostachyus (*P. leptostachyus* Benth., *P. macvaughii* A. Delgado e

P. micranthus Hook. & Arn.), as quais passaram por um evento de disploidia descendente, que reduziu o número cromossômico para 2*n* = 20, além de uma extensa reorganização genômica, como foi elucidado por trabalhos de BAC-FISH (FERRAZ; FONSÊCA; PEDROSA-HARAND, 2020b; FONSÊCA; FERRAZ; PEDROSA-HARAND, 2016a; FONSÊCA; PEDROSA-HARAND, 2017a) e por meio de Oligo-FISH (NASCIMENTO, 2022).

As espécies com 2*n* = 22 se diferenciam por inversões e transposições, encontradas, por exemplo, na comparação entre *P. vulgaris* e *P. lunatus* L. (ALMEIDA; PEDROSA-HARAND, 2011; BONIFÁCIO et al., 2012). Já mapeamentos comparativos por BAC-FISH e Oligo-FISH entre *P. vulgaris, V. unguiculata, V. angularis* e *V. aconitifolia* (Jacq.) Marechal, também mostraram quebra de macrossintenia e colinearidade, envolvendo rearranjos por translocações, inversões e duplicações, principalmente entre os cromossomos 1, 2, 3 e 5, além de reposicionamentos centroméricos (OLIVEIRA et al., 2020a; VASCONCELOS et al., 2015).

Tabela 2 - Número cromossômico, conteúdo de DNA e número de sítios de DNAr de representantes das principais subtribos de Phaseoleae [a].

Subtribo	*2n* [b]	2C (pg) [c]	DNAr 5S [d]	DNAr 35S [d]
Phaseolinae				
Lablab purpureus (L.) Sweet	22	0.70	2	16
Phaseolus leptostachyus Benth.	20	1.00	2	2
Phaseolus vulgaris L.	22	1.20	2 - 4	4 -18
Vigna angularis (Willd.) Ohwi & Ohashi	22	1.10	4	6
Vigna unguiculata (L.) Walp.	22	1.20	4	8 - 10
Macroptilium atropurpureum (DC.) Urb *.	22	-	2	4
Glycininae				
Glycine canescens F.J.Herm	40	1.90	2	2
Glycine max (L.) Merr.	40	2.26	2	2
Amphicarpaea bracteata (L.) Fernald	22	0.70	-	-
Pueraria montana var. lobata (Willd.) Sanjappa & Pradeep	22	2.20	-	-
Teyleria koordersii (Backer) Backer	44	-	-	-
Cajaninae				
Cajanus albicans (Wight & Arn.) Maesen	22	2.57	-	-
Cajanus cajan (L.) Millsp.*	22	1.70	2	4
Rhynchosia minima (L.) DC.	22	2.51	-	-
Kennediinae				
Hardenbergia comptoniana (Andrews) Benth.	22	-	-	-

Kennedia coccinea Vent.	22	-	-	-
Vandasina retusa (Benth.) Rauschert	22	-	-	-
Grupo *Erytrina+Psophorcapus* [e]				
Psophocarpus tetragonolobus (L.) DC. *	18	1.55	2	6
Erythrina acanthocarpa E. Mey.	84	-	-	-
Erythrina falcata Benth.	42	-	2	10
Erythrina caffra Thunb.	42	3.53	-	-

[a] Classificação de acordo com LI et al., 2013 e STEFANOVIĆ et al., 2009;

[b] Números cromossômicos provenientes do CCDB (RICE et al., 2015);

[c] Plant DNA C-values database (PELLICER; LEITCH, 2020);

[d] Plant rDNA database (VITALES et al., 2017);

[e] Grupo *Erytrina+ Psophorcapus* proposto por STEFANOVIĆ et al., 2009;

*Macroptilium atropurpureum** : Número de sítios de DNAr 5S e 35S de BARROS FERREIRA, 2019;

*C. cajan** : DNAr 5S e 35S retirados de IWATA; GREENLAND; JACKSON, 2013;

*P. tetragonolobus** : 2C e DNAr 5S e 35S retidos de MARIE; BROWN, 1993 e CHAOWEN et al., 2004, respectivamente.

Para *Macroptilium*, os dados prévios de mapeamento utilizando DNAr e BACs de *Phaseolus* em espécies do gênero mostraram conservação de sintenia dos sítios de DNAr 35S e 5S nos cromossomos *Pv*6 e *Pv*10 na maioria das espécies analisadas. Por outro lado, translocações e inversões foram detectadas por mapeamento de BACs do *Pv*3 em *M. lathyroides* (L.) Urb., mostrando quebras de macrossintenia e colinearidade entre essas espécies, apesar da estabilidade cromossômica numérica (BARROS FERREIRA, 2019). Nesse contexto, a aplicação da Oligo-FISH (pintura e *barcode*) em outros representantes de Phaseoleae, sejam os com genomas sequenciados (*G. max* e *C. cajan*, por exemplo) ou não (*Macroptilium* e outros), se mostra extremamente plausível e pode permitir uma melhor visão sobre os rearranjos que delinearam a evolução cariotípica do grupo assim como visto nos estudos em *Solanum* utilizando a mesma estratégia (BRAZ et al., 2018b).

3 ARTIGO 1:

Comparative oligo- FISH mapping reveals structural chromosome variation supporting phylogenomic relationships in *Macroptilium* (Benth.) Urb. legume beans

* To be submitted to New Phytologist (https://nph.onlinelibrary.wiley.com/)

Claudio Montenegro[1], Amália Ibiapino[1], Thiago Nascimento[1], Antônio Félix da Costa[3], Ana Christina Brasileiro-Vidal[2], Andrea Pedrosa-Harand[1]✉

[1]Laboratory of Plant Cytogenetics and Evolution, Department of Botany, Federal University of Pernambuco, Recife, PE, Brazil.

[2]Laboratory of Plant Genetics and Biotechnology, Department of Genetics, Federal University of Pernambuco, Recife, PE, Brazil.

[3] Agronomic Institute of Pernambuco, Recife, PE, Brazil

Claudio Montenegro - ORCID: 0000-0003-2089-1608

Amália Ibiapino - ORCID: 0000-0002-2613-5259

Thiago Nascimento - ORCID: 0000-0002-7742-0260

Antônio Félix da Costa - ORCID: 0000-0001-9866-3504

Ana Christina Brasileiro-Vidal - ORCID: 0000-0002-9704-5509

Andrea Pedrosa-Harand - ORCID: 0000-0001-5213-4770

✉ For correspondence (e-mail: andrea.harand@ufpe.br)

SUMMARY

Macroptilium is an American legume genus from the Phaseolinae subtribe (Leguminosae; Papilionoideae; Phaseoleae) mainly used as forage. It is closely related to *Phaseolus* and *Vigna* crop beans, sharing the same chromosome number (2*n* = 22). Previous cytogenetic data, however, revealed intra- and interspecific chromosome variation for the genus, despite its recent diversification. In this study, we aimed to investigate chromosomal evolution within *Macroptilium* species, as well as to compare it to *Phaseolus* and *Vigna*. For this, we characterized nine *Macroptilium* species with a cytogenomic comparative approach, using oligo probes previously designed for *P. vulgaris* and *V. unguiculata*, and 5S and 35S rDNA markers.

Moreover, we investigated the *in silico* dynamics of its repetitive fraction by genome skimming sequencing for six species and compared these approaches to phylogenomic relationships established using plastome and rDNA cistron sequences.

The oligo-FISH pattern for each *Macroptilium* chromosome showed high conserved synteny to the Ancestral Phaseolinae Karyotype (APnK), sharing some rearrangements with *P. vulgaris* and *V. unguiculata*. Although some species showed translocations on chromosomes 2, 3, 6 and 11, these rearrangements were not in agreement with the current phylogenetic hypothesis and taxonomic treatment for the genus.

Three karyotypes were observed among species: I – standard pattern; II – translocation between chromosomes 2 and 6; III – translocation between chromosomes 3 and 11. The repetitive comparative *in silico* analysis and the phylogenetic reconstruction using plastome + ITS sequences for six representatives from groups I, II and III corroborates the cytogenetic groups. Altogether, we demonstrate the efficiency of different cytogenomic approaches to investigate genomic evolution in *Macroptilium*, and indicate the need of a systematic re-evaluation of its infrageneric classification.

KEYWORDS: Chromosome painting; FISH; Oligo probes; 5S and 35S rDNA; Phaseoleae beans.

DECLARATIONS

Funding

This work was supported by CAPES (Coordenação de Pessoal de Nível Superior, Finance Code 001), CNPq (Conselho Nacional de Desenvolvimento Científico e Tecnológico, grants no. 407522/2021-2, 312694/2021-0 and no. 313944/2020-2), and FACEPE (Fundação de Amparo à Ciência e Tecnologia do Estado de Pernambuco, grants no. IBPG-1520-2.03/18).

Conflicts of interest/Competing interest

The authors declare no conflicts of interest.

Availability of data and material

All data generated or analyzed during this study are included as supplementary materials.

Code Availability

Not applicable

Author's contributions

C.M.: extracted genomic DNA, performed FISH experiments, elaborated figures, and drafted the manuscript. A.I: performed the bioinformatic analyses on RepeatExplorer, analysed the results and helped to write the manuscript. T.N: performed plastome and rDNA assemblies and annotation and phylogenetic reconstruction, analysed the data and helped to write the manuscript. A.F.C: propagated the plant material. A.C.B.V: co-supervised the experiments and contributed to the data analyses and discussion. A.P.H: conceptualized and supervised the experiments, discussed the data and provided resources for this research. All authors reviewed the manuscript.

Ethical approval

Not applicable

Consent to participate

Not applicable

Consented for publication

Not applicable

Key message

A comparative cytogenomic analyses in *Macroptilium* revealed interspecific and intergeneric structural chromosome rearrangements, as well as variation in rDNA sites and satDNA abundance. Chromosomal rearrangements, repeatome composition and phylogenomic analyses do not support current phylogenetic hypothesis, but are congruent with one another, suggesting that species relationship should be re-evaluated.

Acknowledgments

We thank CIAT (International Center for Tropical Agriculture), Desert Legume Program (DELEP), Prof. Marcelo Guerra (UFPE), Prof. Leonardo Pessoa Félix and Erton Almeida for providing *Macroptilium* seeds. We also thank CAPES (Coordenação de Pessoal de Nível

Superior, Finance Code 001), CNPq (Conselho Nacional de Desenvolvimento Científico e Tecnológico), and FACEPE (Fundação de Amparo à Ciência e Tecnologia do Estado de Pernambuco) for their financial support.

Abbreviations:

8HQ: 8-hydroxyquinoline

APK: Ancestral Phaseoleae Karyotype

APnK: Ancestral Phaseolinae Karyotype

BAC: Bacterial Artificial Chromosome

DAPI: 4,6-Diamidino-2-phenylindole

FISH: Fluorescence *in situ* Hybridization

GB: Genomic Block

LTR: Long Terminal Repeat

Mya: Million Years Ago

Oligo: Oligonucleotide

satDNA: Satellite DNA

INTRODUCTION

Leguminosae Juss. (Fabaceae Lindl.) is the third largest angiosperm family and the second in social economic importance, with most species belonging to the Papilionoideae subfamily (LGWP, 2017). Beans, for instance, are target for the food industry, mainly because of their rich source of proteins, especially those from Phaseoleae tribe, such as common bean (*Phaseolus vulgaris* L.), cowpea (*Vigna unguiculata* [L.] Walp.), and soybean (*Glycine max* [L.] Merr.) (Dong *et al*., 2014; Ramírez-Jiménez *et al*., 2018; Lonardi *et al*., 2019). Additionally, within the tribe, horse gram (*Macrotyloma uniflorum* [Lam.] Verdc.) and siratro (*Macroptilium atropurpureum* [DC.] Urb.) are used as pasture and for nitrogen fixation (Angus *et al.*, 2013; Ferreira *et al.*, 2018; Shirasawa *et al.*, 2021). Thus, different Phaseoleae species have been investigated, aiming to improve the understanding of legume evolution and to provide additional tools for their breeding (Mousavi-Derazmahalleh *et al*., 2019).

Cytogenetics and whole genome sequencing (WGS) approaches indicate that these beans share high conserved synteny and preserved large genomic blocks (GBs) during their evolutionary

history (Schmutz *et al*., 2010; Wang *et al*., 2017; Kreplak *et al*., 2019; Hufnagel *et al*., 2020; Montenegro *et al*., 2022). Fluorescent *in situ* hybridization (FISH) using Bacterial Artificial Chromosomes (BAC) probes (BAC-FISH) and oligonucleotide based probes (Oligo-FISH) between *Phaseolus* and *Vigna* unraveled chromosomal rearrangements that shaped the karyotype evolution within and between genera (do Vale Martins *et al*., 2021; de Oliveira Bustamante *et al*., 2021). Recently, GB system using comparative genomics from *P. vulgaris* and related species was used for reconstructing the ancestral karyotype for Phaseoleae (APK), indicating $n = 11$ as the ancestral state within the tribe. The main chromosomal rearrangements that shaped the evolution of this tribe involved APK1, 6 and 9, followed by extensive centromere repositioning within the group (Montenegro *et al*., 2022). Additionally, chromosome painting for *P. vulgaris* chromosomes 2 and 3 were hybridized *in situ* to *M. atropurpureum* chromosomes, showing similar painting pattern with *V. unguiculata* and APK ortholog chromosomes (Montenegro *et al*., 2022). Despite the phylogenetic proximity to *Phaseolus* and *Vigna*, there is no species with sequenced genome in *Macroptilium* (Benth.) Urb.

Macroptilium (Phaseolinae subtribe) comprises a small genus with ~20 species, mainly distributed in tropical and subtropical regions of North, Central, and South America, with recent diversification [~3 million years ago (Mya)] (Espert & Burghardt 2010; Li *et al*., 2013; POWO 2022). Besides siratro, there are other socioeconomic important species, such as *M. lathyroides* (L.) Urb (Reis *et al*., 2021). and *M. martii* (Benth.) Maréchal & Baudet (Souza *et al*., 2020). Morphological variation is observed within species, as seen in *M. gracile* (Poepp. ex Benth.) Urb., which is considered a species complex (Berlingeri *et al.,* 2020). Additionally, phylogenetic studies using plastid and ITS regions, morphological and biogeographical evidences corroborate the existence of two main sections for the genus: *Macroptilium* (section A) and *Microchocle* (section B) (Espert *et al.*, 2007; Espert & Burghardt, 2010). However, the current phylogeny does not offer good support for the branches. The six cytogenetically analyzed species showed the same chromosome number $2n = 22$, similar to observed for most *Phaseolus*, *Vigna* and other Phaseoleae species (Rice *et al.*, 2015). However, variation in number and location of 5S and 35S rDNA sites were observed within and between *Macroptillium* sections, including an intraspecific variation in 5S rDNA sites among *M. gracile* individuals (Barros Ferreira, 2019). This suggests that *Macroptilium* may have more inter- and intrageneric genomic variation when compared to other groups. In this sense, additional cytogenomic analyses could improve the understanding of the chromosomal evolution inside Phaseoleae, as well as in the two *Macroptillium* sections.

Therefore, we aimed to investigate intergeneric and interspecific cytogenetic differences among species from sections A and B from *Macroptilium*, and between *Macroptilium*, *Phaseolus* and *Vigna*. For this purpose, we develop chromosome painting probes for two additional *P. vulgaris* chromosomes (chr1 and 5), and performed chromosome painting (chr1, 2, 3 and 5) and

dual-color barcode Oligo-FISH, together with 5S and 35S rDNA probes. Our results showed intergeneric and interspecific chromosome rearrangements involving four chromosomes, in addition to variation in rDNA sites numbers. These results support three distinct cytogenetic groups, which does not corroborate the current phylogeny topology. To test if these cytogenetics groups are monophyletic, we sequenced in low coverage the genome of two species representing each cytogenetic group, to assemble the plastome and reconstruct a simplified phylogeny of this genera. Furthermore, we evaluated *in silico* the differences in the repetitive nuclear DNA fraction of these groups. Altogether, our cytogenetic, phylogenomic and repeatome analyses supported the three different groups for *Macroptilium*. When compared to *Phaseolus* and *Vigna*, we found similarities and differences, suggesting that *Macroptilium* is well preserved in relation to APK. Our findings demonstrate the importance of combine cytogenomic data and sequences analysis to establish intrageneric relationships in *Macroptilium*. Moreover, it highlights the usefulness of integrating available genomic data and intergeneric probes for investigating species without genome assemblies available.

MATERIAL AND METHODS

Plant material

For our cytogenetics analyses, we used *Macroptilium* species from section A - Macroptilium: *M. atropurpureum* (International Center for Tropical Agriculture, CIAT 4413; UFP 87.697), *M. bracteatum* (Nees & Mart.) Maréchal & Baudet (EAN 22643), *M. erythroloma* (Mart. ex Benth.) Urb. (UFP 87.695), *M. gracile* (Poepp. ex Benth.) Urb. (UFP 87.696), *M. lathyroides* (UFP 85.456) and *M. panduratum* (Mart. ex Benth.) Maréchal & Baudet (Desert Legume Program - 10DLEG, 890243); and from section B - Microchole: *M. fraternum* (Piper) Juárez (Desert Legume Program - 8DLEG 900226), *M. martii* (Benth.) Maréchal & Baudet (UFP 81.830) and *M. supinum* (Wiggins & Rollins) A.Delgado & L.Torres (Desert Legume Program - 4DLEG 900549). We used *P. vulgaris* 'BAT 93' (Embrapa Recursos Genéticos e Biotecnologia - Cenargen, Brasília, Distrito Federal, Brazil) as outgroup.

Chromosome preparation

Root tips from germinated seeds were pre-treated with 2 mM 8-hydroxyquinoline (8-HQ) for 5 h at 18 ºC, fixed in methanol or ethanol: acetic acid (3:1 v/v) for 2-24 h at room temperature, and stored at -20 ºC until use. The root tips were washed twice with distilled water, digested with an enzymatic solution containing 2% pectolyase (Sigma-Aldrich), 4% cellulase (Onozuka), and 20% pectinase (Sigma-Aldrich) for 1 h at 37 ºC (in a humid chamber). The slides were prepared

following the air dry protocol (De Carvalho & Saraiva 1993; Ribeiro *et al.*, 2017), with minor modifications.

Oligo and rDNA FISH, image acquisition, and data processing

For chromosome painting, we used oligo probes from *P. vulgaris* chromosomes 2 and 3 (*Pv*2 and *Pv*3; do Vale Martins *et al.*, 2021). In addition, we developed new probes for chromosomes 1 and 5 of *P. vulgaris* (*Pv*1 and *Pv*5), as described by do Vale Martins *et al.* (2021). The oligo-FISH barcode probes designed for *V. unguiculata* and *P. vulgaris* were used according to de Oliveira Bustamante *et al.*, (2021). Oligo-FISH procedure was carried out according to the protocol proposed by Braz *et al.*, (2020). The hybridization mixture consisted of 50% formamide, 10% dextran sulphate, 2× saline sodium citrate (SSC), 350 ng of indirect biotin-labelled probe (green), and 300 ng of the indirect digoxigenin-labelled probe (red). Oligo probes were detected with anti-biotin fluorescein (Vector Laboratories) and anti-digoxigenin rhodamine (Roche), respectively, both diluted (1:100) in 1× TNB (1M Tris HCl pH 7.5, 3 M NaCl and blocking reagent, Sigma-Aldrich), followed by incubation for 1 h at 37 ºC.

Additionally, we used a 500-bp fragment of the 5S rDNA from *Lotus japonicus* (Regel) K.Larsen (D2, Pedrosa *et al.*, 2002) and the 18S-5.8S-25S repeat unit of *Triticum aestivum* L. (p*Ta*71, Gerlach & Bedbrook 1979) to identify the 5S and 35S rDNA sites, respectively. Plasmid DNA was amplified by miniprep (Qiagen). rDNA probes were directly labelled with Cy5-dUTP (GE) by nick translation. The final volume for the rDNA and Oligo hybridization mixtureapplied to the slides was 15 µL. Slides were denatured for 5 min at 75 °C and hybridized for 1 to 3 days at 37 °C. The chromosomes were counterstained with 2 µg/mL DAPI in Vectashield antifade solution (Vector Laboratories).

FISH images were captured using a Leica DM5500B fluorescence microscope using the LEICA LAS-X software. The chromosomes images were adjusted for brightness and contrast using Adobe Photoshop® CC (2020).

DNA extraction and *in silico* repetitive DNA analysis

Genomic DNA from *M. atropurpureum*, *M. erythroloma*, *M. panduratum*, *M. bracteatum* (section A), *M. martii* and *M. fraternum* (section B) were extracted according to Doyle & Doyle (1993). Samples of the genomic DNA were sequenced in low coverage (just over 1Gb of data for each species), generating 250-bp paired-end reads in an Illumina HiSeq 2500 platform for *M. atropurpureum* and 150-bp paired-end reads in an Illumina DNBseq platform for *M. bracteatum*, *M. erythroloma*, *M. fraternum*, *M. martii* and *M. panduratum* (BGI, Hong Kong, China). To standardize our reads data, we trimmed *M. atropurpureum* reads to 150-bp. The repetitive fraction

comparative analysis of the genomes of these species was carried using the RepeatExplorer pipeline (https:// galaxy- elixir. cerit- sc. cz/; Novák *et al.*, 2013; Novák *et al.*, 2020). First, a read sampling was performed on the dataset of each species, where 500,000 were randomly selected. All datasets were renamed using six-character prefixes corresponding to the abbreviation of the species name, eg "Mfrate" for *M. fraternum*. After that, each dataset was concatenated and used to run the analysis, where reads showing at least 95% similarity in at least 55% of its length were clustered together. All contigs with tandem repeats were identified by Tandem Repeat Analyzer (TAREAN; Novák *et al.*, 2017). Other satellites not identified by this tool but which presented typical satellite graph layouts after clustering were confirmed with dot-plot (DOTTER software; Sonnhammer & Durbin, 1995). In addition, a comparative dotplot of the described satellites and the consensus monomers that showed similarity in dotplot were aligned using Muscle in Geneious. Different satellite families were considered as part of the same superfamily when monomer sequences showed identity between 50 and 80%. Sequences with 80–95% similarity were considered subfamilies of the same family and similarity greater than 95% were considered variants of the same family (Ruiz-Ruano *et al.*, 2016). Satellites were named as follows: three letters referring to the species name with the higher abundance (for example, *Mfr* for *M. fraternum*), followed by "SAT", a number referring to the abundance order in this analysis and the size of the consensus monomer in base pairs.

Plastome assembling and phylogeny analysis

The plastome assemblies and annotation were conducted using the plastomes of *P. vulgaris* (DQ886273) and *V. unguiculata* (NC_018051) as references. The raw sequence data for each species was aligned to the *P. vulgaris* plastomes using Bowtie2 v 2.4 (Langmead & Salzberg, 2012) with default parameters, then a consensus sequence was generated using SAMtools and BCFtools (Danecek *et al.*, 2021). Each consensus was annotated using the GeSeq tool from CLOROBOX platform (https://chlorobox.mpimp-golm.mpg.de/index.html), using *P. vulgaris* and *V. unguiculata* as references. For the phylogenetic analysis, the ITS sequence and the plastomes were aligned using MAFFT v 7.0 (Katoh *et al.*, 2019), then a Neighbor-Joining tree with 100,000 replicates and bootstrap was generated in the Geneious® software v 7.0, and another tree with Bayesian inference was generated using MrBayes v 3.2.6 (Ronquist *et al.*, 2012), using the GTR-G model with 10,000,000 MCMC, both of them considering *V. unguiculata* and *P. vulgaris* as external groups.

RESULTS

High conserved synteny and independently rearrangements in *Macroptilium* revealed by oligo-FISH

All *Macroptilium* accessions shared the same chromosome number of 2*n* = 22. Oligo painting and barcode probes showed clear FISH signals, enabling the identification of all the chromosome pairs and the orthology among the analysed *Macroptilium* species (Supplementary Figure 1a-r). To facilitate the comparison among the genera, we chose *M. atropurpureum* (*Mat*) as a reference for paint and barcode patterns for the genus (Supplementary Figure 1a-b), since this species demonstrated similarity with *V. unguiculata* and with *P. vulgaris*, respectively, and it showed the most common pattern inside the genus.

The painting results confirmed the reciprocal translocation between chromosomes 2 and 3 comparing *Macroptilium* (Figure 1 and Supplementary Figure 1a-r) and *P. vulgaris* (Figure 1 and Supplementary Figure 1s-t) chromosomes. Additional independent translocations involving these two chromosomes within *Macroptilium* were detected: chr2 / chr6 for *M. erythroloma*, and *M. fraternum* (Figure 1 and Supplementary Figure 1i and k), and chr3 / chr11 for *M. supinum*, *M. bracteatum* and *M. panduratum* (Figure 1 and Supplementary Figure 1g, m and o). For the barcode results, *Mat* chromosomes showed similar patterns to their respective *Pv* or *Vu* orthologs. *Ma*4, 5, 6, 7, 8 and 9 chromosomes were identical their *Pv* orthologs, while *Ma*2, 3, 10 and 11 were to *Vu* ones (Supplementary Figure 2). The barcode results confirmed the paint results for the two exclusive translocations in the genus above referred (chr3 / chr11; chr2 / chr6). We hypothesized a non-reciprocal translocation between part of the short arm of chr3 with the short arm of chr11 (Supplementary Figure 2D), and a reciprocal translocation between the short arms of chr2 and chr6 (Supplementary Figure 2E).

Our oligo-FISH results enable us to cluster the *Macroptillium* species in three different cytogenetic groups: I) the main pattern, resembling *V. unguiculata* and *P. vulgaris*: *M. atropurpureum*, *M. gracile*, *M. lathyroides* and *M. martii*; II) species with translocation between chr 2 and chr 6: *M. erythroloma* and *M. fraternum*; and III) species with translocation between chr 3 and chr 11: *M. bracteatum*, *M. panduratum* and *M. supinum* (Figure 1). However, the available phylogeny does not support our cytogenetics groups, suggesting that are some incongruences in the phylogeny or the occurrence of independent rearrangements involving these chromosomes in different species.

Chromosome painting of chr1 and 5 from *P. vulgaris* in *Macroptilium* cytogenetic groups evidenced ancestral condition of *Macroptilium* group I karyotype

To investigate if additional chromosome translocations were present among *Macroptilium* species but remained undetected by the barcode analysis, we generated additional oligo-based probes for chr1 and 5 painting. These chromosomes were selected because they were

involved in rearrangements between and within *Vigna* and *Phaseolus* species (Lonardi *et al.*, 2019; de Oliveira Bustamante *et al.*, 2021; Montenegro *et al.*, 2022). Oligo-FISH and *in silico* results showed that the select oligos covered almost the entire chr1 and 5 from *P. vulgaris*, except for a small terminal region of chr1 and the pericentromeric region of chr5 (Figure 2a). We choose four *Macroptilium* species, representing two species of each group I (*M. atropurpureum* and *M. lathyroides*) one of group II (*M. erythroloma*) and one of group III (*M. bracteatum*) to investigate possible translocations involving these two chromosomes. All species shared the same painting pattern, with the *Pv*5 probe conserved in a single chromosome, while *Pv*1 was involved in a reciprocal translocation with another chromosome (Figure 2c-h). Sequential Oligo-FISH of chr1 and 5 probes to metaphases of *M. erythroloma* and *M. bracteatum* previously hybridized with chr2 and 3, as well as barcode probes, identified this translocated chromosome as chr8 (Figure 3d and f), differing from the *Phaseolus* painting pattern and suggesting an ancestral karyotype (Figure 2b). Unfortunately, we couldn't get the sequential Oligo-FISH probes for group I species.

Correlation of the Oligo-FISH patterns with APK helps to suggest GBs for *M. atropurpureum*

We plotted the barcode signals into the genomic blocks of APK proposed by Montenegro *et al.*, (2022) and compared the barcode and painting results of *Macroptilium* with those of *Phaseolus*, *Vigna* and the putative positions in the APK and APnK (Figure 3A and B). Based on these results, we hypothesized that the GB pattern of *M. atropurpureum* (Figure 3C) are basically the same of APnK, differing from *V. unguiculata* due to the lack of a translocation between chr1 and 5 (Figure 3D), and from *P. vulgaris* due to the lack of translocations involving chr1 and 8, as well as 2 and 3. When compared to APK, we identified a conservation for eight of the 11 chromosomes (chr2, 3, 4, 5, 7, 8, 10 and 11, Figure 3A), only diverging due to translocations that resulted in chr 1, 6 and 9 from APnK. The similarity and differences with both *Phaseolus* and *Vigna* karyotypes suggest an ancestral Phaseolinae pattern for *Macroptilium* group I.

The oligo-FISH results also enabled the identification of the chromosomes that carry the rDNA sites in each species. We observed a variation in the number and positions for 35S rDNA sites, either two (*M. atropurpureum*, *M. bracteatum*, *M. erythroloma*, *M. fraternum*, *M. gracile* and *M. martii*), three (*M. lathyroides* and *M. supinum*) or five sites (*M. panduratum*) (Figure 1 and Supplementary Figure 1). The 35S was usually located on chr2 and 6, but in different chromosomes of *M. bracteatum* (chr 4 and 8), *M. lathyroides* and *M. supinum* (minor or major extra site in chr 8, respectively) and *M. panduratum* (sites on chr 4, 5, 6, 8 and 10). A single 5S rDNA site was usually placed on the chromosomes 10. However, 5S rDNA sites were also found in chr 1, 2, 4, 10 and 11 in *M. martii*, with a duplicated 5S rDNA site in chr10. The rDNA conservation in *Phaseolus*, *Vigna* and *Macroptilium* suggests two main GBs associated with

rDNA sites: K (35S) and R (5S). This result corroborates ancestral rDNA sites probably localized in APK6 and 10.

Repetitive fraction comparative analysis support *Macroptilium* cytogenetic groups

Because the cytogenetic groups defined by structural rearrangements revealed by Oligo-FISH mapping were not monophyletic in the current phylogenetic hypothesis (Espert et al., 2010), we searched for additional evidence of genomic similarity within each cytogenetic group. For that, we characterized the composition of the repetitive fraction of two representatives of each of the three groups. For the comparative analysis, an input with 6,000,000 reads from the six species in total was used, from which 1,000,000 were randomly selected by RepeatExplorer. A total of 560,687 reads grouped into 93,752 clusters, with 330 clusters containing at least 0.01% of genome abundance. These were grouped into 212 superclusters and annotated.

The repetitive fraction corresponded, in average, to 16.17% of the total genomes, and 16.17% of *M. atropurpureum* genome, which was annotated in detail (Supplmentary Table 1). Satellite DNAs represented 2.79% of its genome, whereas for 5S and 35S ribosomal DNAs the abundances were 0.21% and 1.88%, respectively. LTR-retrotransposons from the Ty1/copia superfamily comprised 3.34% of the genome, while Ty3/gypsy elements were less abundant corresponding to 2.56%. Within Ty1/copia, the SIRE lineage was the most abundant (1.91%), while Tekay was the most represented among Ty3/gypsy with 1.22%. The comparative analysis showed high similarity among the repetitive fractions of all species, with most of the cluster shared among species, especially the transposable elements, which showed similar abundances. However, satellite DNA abundances were more variable among species and revealed higher genomic similarities within species from groups II and III (Figure 4).

A total of 26 satellites were identified (Table 1). The most abundant, MbrSAT1-155, was enriched in almost all species, except for *M. fraternum*. Some of these satellites turned out to be shared by all six species (MmaSAT2-174, MmaSAT4-1948, MpaSAT5-59, MbrSAT7-110, MatSAT8-415, MpaSAT9-168, MmaSAT9-249, MpaSAT10-201, MmaSAT12-304, MatSAT15-48, MatSAT18-16 and MbrSAT23-123), while others were exclusively amplified in a single species from group I (MmaSAT16-59, MatSAT20-21, MmaSAT22-28 and MatSAT26-26). Two satellites (MpaSAT21-263 and MmaSAT25-353) showed similarity in the dotplot analysis and had their consensus sequences aligned, presenting 57.1% identity, and being grouped in the same superfamily.

Plastome assembling and phylogenetic reconstruction

The same short reads used for repeat comparative analysis were employed for plastome assembly, representing two species of each cytogenetic group, were generated using *P. vulgaris* and *V. unguiculata* as reference. Plastomes were conserved in structure and varied from 150,283 to 150,285 pb (Supplementary Figure 3). Neighbour-Joining and Bayesian trees were reconstructed using concatenated sequences alignment of plastomes and compared to ITS1 and 2 aligments obtained from the same dataset. Both were congruent with our cytogenetic groups, with good support values (Supplementary Figure 4 and 5). Representantives of groups II (*M. fraternum* and *M. erythroloma*) and III (*M. bracteatum* and *M. panduratum*) formed independent clades, while *M. martii* were in a more basal position, and *M. atropurpureum* sister to group II (Supplementary Figure 4 and 5). This corroborates group I as paraphyletic and ancestral. Based on the phylogenetic reconstruction, we placed the *Macroptilium* karyotypes accordingly with our topology and compared with the current phylogeny (Figure 2). Sessions A and B are not natural groups.

DISCUSSION

Oligo-FISH probes for chromosome painting and barcode have been applied for karyotype comparisons in many groups of plants (eg. Han *et al.*, 2015; Qu *et al.*, 2017; Braz *et al.*, 2018; Jiang 2019; Song *et al.*, 2020; Li *et al.*, 2021). For *P. vulgaris* and *V. unguiculata*, these approaches have been useful for unrevealing translocations, collinearity breaks and centromere repositioning between these species (do Vale Martins *et al.*, 2021; de Oliveira Bustamante *et al.*, 2021). Here we performed the first cytogenomic study with chromosomal paint and dual color-barcode in nine representatives of *Macroptillium*, which is closely related to *Phaseolus* and *Vigna*. Our results showed intergeneric and interspecific chromosome rearrangements, enabling us to divide the genus into three distinct cytogenetic groups (group I, II and III), which did not corroborate with the current phylogenetic hypothesis (Espert *et al.*, 2007, 2010). Nevertheless, these results were supported by our phylogenetic reconstruction using plastome and ITS sequences from six *Macroptilium* species, and by repetitive comparative analysis, demonstrating the usefulness of an integrative cytogenetic approach for assisting systematics in plants (Vitales *et al.*, 2020; Walden *et al.*, 2020).

Chromosomal painting also helped to resolve phylogeny inconsistency, in *Lophostoma* bats. Probes from related genera to species from this group suggested the paraphyletic status for the genus (da Silva *et al.*, 2022). Comparative cytogenomics are constantly helping the resolution of phylogenetic incongruences, as seen in *Ipomoea* L, in which oligo- and rDNA-FISH results

suggested a different topology (Chen *et al.*, 2020). In the bird family Rhynchocyclidae, chromosome mapping using BACs in different genera also helped clarifying phylogenetic incongruences (Kretschmer *et al.*, 2021).

Macroptilium followed the general Phaseoleae trend of karyotype evolution, showing limited genome reshuffling with maintenance of chromosome number, as evidenced in *Phaseolus* (Schmutz et *al.*, 2014; Garcia *et al.*, 2021; Montenegro *et al.*, 2022) and *Vigna* (Lonardi *et al.*, 2019; Oliveira *et al.*, 2020; do Vale Martins *et al.*, 2021), but contrasting with *Amphicarpaea edgeworthii* Benth, which showed massive reshuffling (Liu *et al.*, 2020; Montenegro *et al.*, 2022). Using *Pv* and *Vu* oligo probes, we were able to reveal shared patterns with *Phaseolus* and/or *Vigna*, as well as independent rearrangements within this genus. Similar outcome for chromosomal rearrangements was evidenced in sugarcane *Saccharum spontaneum* L. using combined oligo-FISH barcode probes designed for *Sorghum bicolor* (L.), which helped to clarify the karyotype evolution within *Saccharum*, with two major chromosomal rearrangements, and among closely related genera (Meng *et al.*, 2022). Another similar example was evidenced in Triticeae. Combined oligo-FISH painting probes designed for barley (*Hordeum vulgare* L.) and wheat (*Triticum aestivum* L.) genomes and *in situ* hybridized in related genera from the family elucidated interspecific and intergeneric chromosomal rearrangements (Li *et al.*, 2021).

Association of the APK (Montenegro *et al.*, 2022) with the barcode and painting patterns allowed us to suggest a hypothetical GBs pattern for *M. atropurpureum*, showing high synteny with APK, APnK, *Phaseolus* and *Vigna*. Genomic blocks for *Macroptilium* supports the independent translocations events for *Phaseolus* (*Pv*2 and *Pv*3; *Pv*1 and *Pv*8) and *Vigna* (*Vu*1 and *Vu*5) previously suggested by Montenegro *et al.*, (2022) and indicates that the translocation between theses chromosomes have occurred after *Macroptilium* divergence (Li *et al.*, 2013). Although the genus conserved the ancestral karyotype in different lineages and despite its recent diversification (~ 3 Mya, Li *et al.*, 2013), species from group II and III showed lineage-specific translocation events involving four chromosomes (2/6 and 3/11, respectively). The involvement of chromosomes 2 and 3 corroborates the hypothesis of these two chromosomes being hotspot for chromosome rearrangements within Phaseolinae (do Vale Martins *et al.*, 2021), whereas chromosomes 6 and 11 were involved in rearrangements in representatives of Glycininae (Montenegro *et al.*, 2022).

Interspecific rearrangements are commonly seen in other Phaseoleae beans, such as in *Phaseolus* (Fonsêca & Pedrosa-Harand, 2017; Ferraz *et al.*, 2020), *Vigna* (Oliveira *et al.*, 2020; do Vale Martins *et al.*, 2021), *Glycine* (Liu *et al.*, 2018), and now in *Macroptilium*. In contrast, oligo-FISH barcode in other crops groups shows karyotype conservation during genus evolution. For example, *Oryza sativa* L. and *O. australiensis* Domin, with ~7 Mya divergence, showed the

same barcode pattern (Tang *et al.*, 2010; Liu *et al.*, 2020a). Moreover, karyotype stability was also evidenced by oligo-FISH barcode in *Solanum* L. species, which have diverged 15 Mya (Braz *et al.*, 2018). This may suggest that Phaseoleae representants are more prone to genome reorganization, reflecting directly in the intergeneric and interspecific chromosomal rearrangements.

Our *in silico* repeat analyses using *M. atropurpureum* and *M. martii* (group I), *M. erythroloma* and *M. fraternum* (group II) and *M. bracteatum* and *M. panduratum* (group III), demonstrated high conservation of their repeatome, except for the abundance of satDNAs clusters. This indicates that genomic divergence is mainly related to different amplification and contraction of the same satDNA repeats, supporting the library hypothesis of satDNA evolution (López-Flores and Garrido-Ramos 2012; Garrido-Ramos 2015; Garrido-Ramos, 2017). Similar results were previously described in other Phaseoleae members. For example, the subtelomeric satDNA *khipu* in *Phaseolus* is observed in all analyzed species of the genus, but with different amplification levels and distribution between the species (Ribeiro *et al.*, 2017). In addition, comparative repetitive analysis from *Phaseolus*, *Vigna* and *Cajanus* L. suggests that retrotransponsons and satDNAs were the main repetitive elements responsible for Phaseoleae repetitive landscape, with satDNAs being very diverse between the analyzed genera. Our results in *Macroptilum* corroborate the fast diversification of the satDNA families within Phaseoleae genomes (Ribeiro *et al.*, 2020).

Additionally, we found a high variation in the number of 35S rDNA sites in *Macroptilium*, which was also seen in *Phaseolus* (Pedrosa *et al.*, 2003; Pedrosa-Harand *et al.*, 2006; Almeida & Pedrosa-Harand, 2011; Fonsêca *et al.*, 2016; Ferraz *et al.*, 2020) and *Vigna* (de A. Bortoleti *et al.*, 2012; She *et al.*, 2020; Oliveira *et al.*, 2020; do Vale Martins *et al.*, 2021). The 35S rDNA sites on chromosomes 6, 9 and 10 were suggested to be the ancestral state for *Phaseolus* (Almeida & Pedrosa-Harand, 2011; Fonsêca *et al.*, 2016), whereas the chromosome 6 site was also conserved among *Vigna* species (Oliveira *et al.*, 2020). Interestingly, all analyzed *Macroptilium* species presented the 35S rDNA site on chromosome 6, except for *M. bracteatum*, supporting that rDNA 35S on chromosome 6 is the ancestral state for the tribe. The variation in number of 5S rDNA sites in *M. martii* and 35S in *M. panduratum* differs from *P. vulgaris* because the new sites in these species are proximal, not terminal, and thus should not be as susceptible to ectopic recombination between chromosomes (Pedrosa-Harand *et al.*, 2006). These new sites were not associated to translocations, except for the new site on *Mb*2 and *Mf*2, shared by the group II species, which showed a translocation between chromosomes 2 and 6. It is suggested that rDNA sites are constantly involved into structural chromosome rearrangements (Raskina *et al.*, 2008; Gross *et al.*, 2010; Roa & Guerra, 2015), but, in this case, a rearrangement may explain the origin of a new rDNA site.

Here, we split the genus into three cytogenetic groups. Two are derived and monophyletic, while group I represents the ancestral karyotype. This hypothesis was corroborated by repeatome similarities and plastome and ITS phylogenomic analyses, indicating the need of general re-evaluating phylogenetic and taxonomic relationships in *Macroptilium.* We also highlight the effectiveness of the oligo-based probes in the chromosome evolutionary studies in groups/species with no assembled genome.

REFERENCES

de A. Bortoleti KC, Benko-Iseppon AM, de Melo NF, Brasileiro-Vidal AC. **2012**. Chromatin differentiation between Vigna radiata (L.) R. Wilczek and V. unguiculata (L.) Walp. (Fabaceae). *Plant Systematics and Evolution* **298**: 689–693.

Almeida C, Pedrosa-Harand A. **2011**. Contrasting rDNA Evolution in Lima Bean (Phaseolus lunatus L.) and Common Bean (P. vulgaris L., Fabaceae). *Cytogenetic and Genome Research* **132**: 212–217.

Angus AA, Lee A, Lum MR, Shehayeb M, Hessabi R, Fujishige NA, Yerrapragada S, Kano S, Song N, Yang P, *et al.* 2013. Nodulation and effective nitrogen fixation of Macroptilium atropurpureum (siratro) by Burkholderia tuberum, a nodulating and plant growth promoting beta-proteobacterium, are influenced by environmental factors. *Plant and Soil* **369**: 543–562.

Azani N, Babineau M, Bailey CD, Banks H, Barbosa AR, Pinto RB, Boatwright JS, Borges LM, Brown GK, Bruneau A, *et al.* 2017. A new subfamily classification of the Leguminosae based on a taxonomically comprehensive phylogeny: The Legume Phylogeny Working Group (LPWG). *TAXON* **66**: 44–77.

Braz GT, He L, Zhao H, Zhang T, Semrau K, Rouillard J-M, Torres GA, Jiang J. **2018**. Comparative Oligo-FISH Mapping: An Efficient and Powerful Methodology To Reveal Karyotypic and Chromosomal Evolution. : 11.

Braz GT, do Vale Martins L, Zhang T, Albert PS, Birchler JA, Jiang J. **2020**. A universal chromosome identification system for maize and wild Zea species. *Chromosome Research* **28**: 183–194.

Carvalho CR, Saraiva LS. **1993**. An Air Drying Technique for Maize Chromosomes without Enzymatic Maceration. *Biotechnic & Histochemistry* **68**: 142–145.

Chen L, Su D, Sun J, Li Z, Han Y. **2020**. Development of a set of chromosome-specific oligonucleotide markers and karyotype analysis in the Japanese morning glory Ipomoea nil. *Scientia Horticulturae* **273**: 109633.

Danecek P, Bonfield JK, Liddle J, Marshall J, Ohan V, Pollard MO, Whitwham A, Keane T, McCarthy SA, Davies RM, *et al.* 2021. Twelve years of SAMtools and BCFtools. *GigaScience* **10**: giab008.

Dong D, Fu X, Yuan F, Chen P, Zhu S, Li B, Yang Q, Yu X, Zhu D. **2014**. Genetic diversity and population structure of vegetable soybean (Glycine max (L.) Merr.) in China as revealed by SSR markers. *Genetic Resources and Crop Evolution* **61**: 173–183.

Doyle JJ, Doyle JL. **1993**. Chloroplast DNA Phylogeny of the Papilionoid Legume Tribe Phaseoleae. *Systematic Botany* **18**: 309.

Espert SM, Burghardt AD. **2010**. Biogeography and divergence times of genus Macroptilium (Leguminosae). *AoB PLANTS* **2010**.

Espert SM, Drewes SI, Burghardt AD. **2007**. Phylogeny of Macroptilium (Leguminosae): morphological, biochemical and molecular evidence. *Phylogeny of Macroptilium (Leguminosae): morphological,biochemical and molecular evidence* **23**: 11.

Ferraz ME, Fonsêca A, Pedrosa-Harand A. **2020**. Multiple and independent rearrangements revealed by comparative cytogenetic mapping in the dysploid Leptostachyus group (Phaseolus L., Leguminosae). *Chromosome Research* **28**: 395–405.

Ferreira PAA, Dahmer S de FB, Backes T, Silveira A de O, Jacques RJS, Zafar M, Pauletto EA, Santos MAO dos, Silva K da, Giachini AJ, *et al.* 2018. Isolation, Characterization and Symbiotic Efficiency of Nitrogen-Fixing and Heavy Metal-Tolerant Bacteria from a Coalmine Wasteland. *Revista Brasileira de Ciência do Solo* **42**.

Fonsêca A, Ferraz ME, Pedrosa-Harand A. **2016**. Speeding up chromosome evolution in Phaseolus: multiple rearrangements associated with a one-step descending dysploidy. *Chromosoma* **125**: 413–421.

Fonsêca A, Pedrosa-Harand A. **2017**. Cytogenetics and Comparative Analysis of Phaseolus Species. In: Pérez de la Vega M, Santalla M, Marsolais F, eds. Compendium of Plant Genomes. The Common Bean Genome. Cham: Springer International Publishing, 57–68.

Garcia T, Duitama J, Zullo SS, Gil J, Ariani A, Dohle S, Palkovic A, Skeen P, Bermudez-Santana CI, Debouck DG, *et al.* 2021. Comprehensive genomic resources related to domestication and crop improvement traits in Lima bean. *Nature Communications* **12**: 702.

Garrido-Ramos MA. **2015**. Satellite DNA in Plants: More than Just Rubbish. *Cytogenetic and Genome Research* **146**: 153–170.

Gerlach WL, Bedbrook JR. **1979**. Cloning and characterization of ribosomal RNA genes from wheat and barley. *Nucleic Acids Research* **7**: 1869–1885.

Gross MC, Schneider CH, Valente GT, Martins C, Feldberg E. **2010**. Variability of 18S rDNA locus among Symphysodon fishes: chromosomal rearrangements. *Journal of Fish Biology* **76**: 1117–1127.

Han Y, Zhang T, Thammapichai P, Weng Y, Jiang J. **2015**. Chromosome-Specific Painting in *Cucumis* Species Using Bulked Oligonucleotides. *Genetics* **200**: 771–779.

Hufnagel B, Marques A, Soriano A, Marquès L, Divol F, Doumas P, Sallet E, Mancinotti D, Carrere S, Marande W, *et al.* 2020. High-quality genome sequence of white lupin provides insight into soil exploration and seed quality. *Nature Communications* **11**: 492.

Jiang J. **2019**. Fluorescence in situ hybridization in plants: recent developments and future applications. *Chromosome Research* **27**: 153–165.

Katoh K, Rozewicki J, Yamada KD. **2019**. MAFFT online service: multiple sequence alignment, interactive sequence choice and visualization. *Briefings in Bioinformatics* **20**: 1160–1166.

Kreplak J, Madoui M-A, Cápal P, Novák P, Labadie K, Aubert G, Bayer PE, Gali KK, Syme RA, Main D, *et al.* 2019. A reference genome for pea provides insight into legume genome evolution. *Nature Genetics* **51**: 1411–1422.

Kretschmer R, Franz I, de Souza MS, Garnero ADV, Gunski RJ, de Oliveira EHC, O'Connor RE, Griffin DK, de Freitas TRO. **2021**. Cytogenetic Evidence Clarifies the Phylogeny of the Family Rhynchocyclidae (Aves: Passeriformes). *Cells* **10**: 2650.

Li H, Wang W, Lin L, Zhu X, Li J, Zhu X, Chen Z. **2013**. Diversification of the phaseoloid legumes: effects of climate change, range expansion and habit shift. *Frontiers in Plant Science*: 9.

Li G, Zhang T, Yu Z, Wang H, Yang E, Yang Z. **2021**. An efficient Oligo-FISH painting system for revealing chromosome rearrangements and polyploidization in Triticeae. *The Plant Journal* **105**: 978–993.

Liu Q, Chang S, Hartman GL, Domier LL. **2018**. Assembly and annotation of a draft genome sequence for Glycine latifolia, a perennial wild relative of soybean. *The Plant Journal* **95**: 71–85.

Liu X, Sun S, Wu Y, Zhou Y, Gu S, Yu H, Yi C, Gu M, Jiang J, Liu B, *et al.* 2020a. Dual-color oligo-FISH can reveal chromosomal variations and evolution in *Oryza* species. *The Plant Journal* **101**: 112–121.

Liu Y, Zhang X, Han K, Li R, Xu G, Han Y, Cui F, Fan S, Seim I, Fan G, *et al.* 2020b. Insights into amphicarpy from the compact genome of the legume *Amphicarpaea edgeworthii*. *Plant Biotechnology Journal*: pbi.13520.

Lonardi S, Muñoz-Amatriaín M, Liang Q, Shu S, Wanamaker SI, Lo S, Tanskanen J, Schulman AH, Zhu T, Luo M, *et al.* 2019. The genome of cowpea (*Vigna unguiculata* [L.] Walp.). *The Plant Journal* **98**: 767–782.

López-Flores I, Garrido-Ramos MA. **2012**. The Repetitive DNA Content of Eukaryotic Genomes. In: Garrido-Ramos MA, ed. Genome Dynamics. Basel: S. KARGER AG, 1–28.

Martins L do V, de Oliveira Bustamante F, da Silva Oliveira AR, da Costa AF, de Lima Feitoza L, Liang Q, Zhao H, Benko-Iseppon AM, Muñoz-Amatriaín M, Pedrosa-Harand A, *et al.* 2021. BAC- and oligo-FISH mapping reveals chromosome evolution among Vigna angularis, V. unguiculata, and Phaseolus vulgaris. *Chromosoma*.

Meng Z, Wang F, Xie Q, Li R, Shen H, Li H. **2022**. Reconstruction of karyotypic evolution in Saccharum spontaneum species by comparative oligo-FISH mapping. *BMC Plant Biology* **22**: 599.

Montenegro C, do Vale Martins L, Bustamante F de O, Brasileiro-Vidal AC, Pedrosa-Harand A. **2022**. Comparative cytogenomics reveals genome reshuffling and centromere repositioning in the legume tribe Phaseoleae. *Chromosome Research* **30**: 477–492.

Mousavi-Derazmahalleh M, Bayer PE, Hane JK, Valliyodan B, Nguyen HT, Nelson MN, Erskine W, Varshney RK, Papa R, Edwards D. **2019**. Adapting legume crops to climate change using genomic approaches. *Plant, Cell & Environment* **42**: 6–19.

Novák P, Ávila Robledillo L, Koblížková A, Vrbová I, Neumann P, Macas J. **2017**. TAREAN: a computational tool for identification and characterization of satellite DNA from unassembled short reads. *Nucleic Acids Research* **45**: e111–e111.

Novák P, Neumann P, Macas J. **2020**. Global analysis of repetitive DNA from unassembled sequence reads using RepeatExplorer2. *Nature Protocols* **15**: 3745–3776.

Novak P, Neumann P, Pech J, Steinhaisl J, Macas J. **2013**. RepeatExplorer: a Galaxy-based web server for genome-wide characterization of eukaryotic repetitive elements from next-generation sequence reads. *Bioinformatics* **29**: 792–793.

de Oliveira Bustamante F, do Nascimento TH, Montenegro C, Dias S, do Vale Martins L, Braz GT, Benko-Iseppon AM, Jiang J, Pedrosa-Harand A, Brasileiro-Vidal AC. **2021**. Oligo-FISH barcode in beans: a new chromosome identification system. *TAG. Theoretical and applied genetics. Theoretische und angewandte Genetik* **134**: 3675–3686.

Oliveira AR da S, Martins L do V, Bustamante F de O, Muñoz-Amatriaín M, Close T, da Costa AF, Benko-Iseppon AM, Pedrosa-Harand A, Brasileiro-Vidal AC. **2020**. Breaks of macrosynteny and collinearity among moth bean (Vigna aconitifolia), cowpea (V. unguiculata), and common bean (Phaseolus vulgaris). *Chromosome Research*.

Pedrosa A, Sandal N, Stougaard J, Schweizer D, Bachmair A. **2002**. Chromosomal map of the model legume Lotus japonicus. *Genetics* **161**: 1661–1672.

Pedrosa A, Vallejos C, Bachmair A, Schweizer D. **2003**. Integration of common bean (Phaseolus vulgaris L.) linkage and chromosomal maps. *Theoretical and Applied Genetics* **106**: 205–212.

Pedrosa-Harand A, de Almeida CCS, Mosiolek M, Blair MW, Schweizer D, Guerra M. **2006**. Extensive ribosomal DNA amplification during Andean common bean (Phaseolus vulgaris L.) evolution. *Theoretical and Applied Genetics* **112**: 924–933.

Qu M, Li K, Han Y, Chen L, Li Z, Han Y. **2017**. Integrated Karyotyping of Woodland Strawberry (Fragaria vesca) with Oligopaint FISH Probes. *Cytogenetic and Genome Research* **153**: 158–164.

Ramírez-Jiménez AK, Gaytán-Martínez M, Morales-Sánchez E, Loarca-Piña G. **2018**. Functional properties and sensory value of snack bars added with common bean flour as a source of bioactive compounds. *LWT* **89**: 674–680.

Raskina O, Barber JC, Nevo E, Belyayev A. **2008**. Repetitive DNA and chromosomal rearrangements: speciation-related events in plant genomes. *Cytogenetic and Genome Research* **120**: 351–357.

Reis LK, Fonseca DR da, Roghanian S, Barros BC de, Sigrist MR. **2021**. Reproductive strategies of the Macroptilium lathyroides (Papilionoideae: Phaseoleae) explain the success of ruderal species in anthropized environments. *Rodriguésia* **72**: e01782020.

Ribeiro T, Dos Santos KGB, Richard MMS, Sévignac M, Thareau V, Geffroy V, Pedrosa-Harand A. **2017**. Evolutionary dynamics of satellite DNA repeats from Phaseolus beans. *Protoplasma* **254**: 791–801.

Ribeiro T, Vasconcelos E, dos Santos KGB, Vaio M, Brasileiro-Vidal AC, Pedrosa-Harand A. **2020**. Diversity of repetitive sequences within compact genomes of Phaseolus L. beans and allied genera Cajanus L. and Vigna Savi. *Chromosome Research* **28**: 139–153.

Rice A, Glick L, Abadi S, Einhorn M, Kopelman NM, Salman-Minkov A, Mayzel J, Chay O, Mayrose I. **2015**. The Chromosome Counts Database (CCDB) – a community resource of plant chromosome numbers. *New Phytologist* **206**: 19–26.

Roa F, Guerra M. **2015**. Non-Random Distribution of 5S rDNA Sites and Its Association with 45S rDNA in Plant Chromosomes. *Cytogenetic and Genome Research* **146**: 243–249.

Ronquist F, Teslenko M, van der Mark P, Ayres DL, Darling A, Höhna S, Larget B, Liu L, Suchard MA, Huelsenbeck JP. **2012**. MrBayes 3.2: Efficient Bayesian Phylogenetic Inference and Model Choice Across a Large Model Space. *Systematic Biology* **61**: 539–542.

Schmutz J, Cannon SB, Schlueter J, Ma J, Mitros T, Nelson W, Hyten DL, Song Q, Thelen JJ, Cheng J, *et al.* 2010. Genome sequence of the palaeopolyploid soybean. *Nature* **463**: 178–183.

Schmutz J, McClean PE, Mamidi S, Wu GA, Cannon SB, Grimwood J, Jenkins J, Shu S, Song Q, Chavarro C, *et al.* 2014. A reference genome for common bean and genome-wide analysis of dual domestications. *Nature Genetics* **46**: 707–713.

She C-W, Mao Y, Jiang X-H, He C-P. **2020**. Comparative molecular cytogenetic characterization of five wild Vigna species (Fabaceae). *Comparative Cytogenetics* **14**: 243–264.

Shirasawa K, Chahota R, Hirakawa H, Nagano S, Nagasaki H, Sharma T, Isobe S, Chahota R, Hirakawa H, Nagano S, *et al.* 2021. A chromosome-scale draft genome sequence of horsegram (Macrotyloma uniflorum). *Gigabyte* **2021**: 1–23.

da Silva NKN, Nagamachi CY, Rodrigues LRR, O'Brien PCM, Yang F, Ferguson-Smith MA, Pieczarka JC. **2022**. Chromosome painting and phylogenetic analysis suggest that the genus Lophostoma (Chiroptera, Phyllostomidae) is paraphyletic. *Scientific Reports* **12**: 19514.

Song X, Song R, Zhou J, Yan W, Zhang T, Sun H, Xiao J, Wu Y, Xi M, Lou Q, *et al.* 2020. Development and application of oligonucleotide-based chromosome painting for chromosome 4D of Triticum aestivum L. *Chromosome Research* **28**: 171–182.

Sonnhammer ELL, Durbin R. **1995**. A dot-matrix program with dynamic threshold control suited for genomic DNA and protein sequence analysis. *Gene* **167**: GC1–GC10.

Souza RB de L, do Nascimento YM, Gouveia RG, Souto AL, Sobral MV, Costa VCO, de Melo JIM, Silva MS, Tavares JF. **2020**. Dereplication-guided isolation of a new flavonoid triglycoside from Macroptilium martii and its cytotoxicity evaluation. *Phytochemistry Letters* **39**: 144–150.

Tang L, Zou X, Achoundong G, Potgieter C, Second G, Zhang D, Ge S. **2010**. Phylogeny and biogeography of the rice tribe (Oryzeae): evidence from combined analysis of 20 chloroplast fragments. *Molecular Phylogenetics and Evolution* **54**: 266–277.

do Vale Martins L, de Oliveira Bustamante F, da Silva Oliveira AR, da Costa AF, de Lima Feitoza L, Liang Q, Zhao H, Benko-Iseppon AM, Muñoz-Amatriaín M, Pedrosa-Harand A, *et al.* 2021. BAC- and oligo-FISH mapping reveals chromosome evolution among Vigna angularis, V. unguiculata, and Phaseolus vulgaris. *Chromosoma* **130**: 133–147.

Vitales D, Garcia S, Dodsworth S. **2020**. Reconstructing phylogenetic relationships based on repeat sequence similarities. *Molecular Phylogenetics and Evolution* **147**: 106766.

Walden N, Nguyen T-P, Mandáková T, Lysak MA, Schranz ME. **2020**. Genomic Blocks in Aethionema arabicum Support Arabideae as Next Diverging Clade in Brassicaceae. *Frontiers in Plant Science* **11**: 719.

Wang J, Sun P, Li Y, Liu Y, Yu J, Ma X, Sun S, Yang N, Xia R, Lei T, *et al.* 2017. Hierarchically Aligning 10 Legume Genomes Establishes a Family-Level Genomics Platform. *Plant Physiology* **174**: 284–300.

TABLES

Table 1. Shared satellites among the sequenced *Macroptilium* species

SatDNA	*Mat*	*Mfr*	*Mer*	*Mbr*	*Mma*	*Mpa*	CL	Total abundance %
MbrSAT1-155	0,01	-	0,001	**3,573**	0,349	2,004	1 e 135	5,938
MmaSAT2-174	0,516	0,693	0,766	0,963	**1,599**	0,754	18, 31 e 108	5,29
MmaSAT3-170	-	0,001	0,004	-	**5,167**	-	2	5,173
MmaSAT4-1948	0,321	0,71	0,615	0,389	**0,839**	0,323	7	3,197
MpaSAT5-59	0,002	0,004	0,001	1,023	0,002	**1,375**	22	2,407
MerSAT6-500	-	0,782	**0,854**	-	-	-	56	1,636
MbrSAT7-110	0,027	0,043	0,023	**0,783**	0,012	0,726	53	1,616
MatSAT8-415	**0,771**	0,155	0,134	0,142	0,201	0,156	92 e 96	1,56
MpaSAT9-168	0,042	0,019	0,017	0,666	0,006	**0,686**	64	1,437
MmaSAT9-249	0,252	0,223	0,188	0,171	**0,279**	0,204	72	1,317
MpaSAT10-201	0,01	0,016	0,024	0,413	0,001	**0,719**	76	1,184
MbrSAT11-59	-	-	-	**0,705**	-	0,422	79	1,128
MmaSAT12-304	0,001	0,054	0,06	0,001	**0,863**	0,001	91 e 149	0,981
MpaSAT13-213	0,001	0,001	-	0,261	0,002	**0,342**	100	0,606
MatSAT14-15	**0,475**	-	-	-	-	-	106	0,475
MatSAT15-48	**0,117**	0,099	0,101	0,036	0,045	0,057	110	0,454
MmaSAT16-59	-	-	-	-	**0,405**	-	116	0,405
MbrSAT17-117	-	-	-	**0,295**	-	0,06	120	0,355
MatSAT18-16	**0,297**	0,016	0,005	0,001	0,001	0,013	122	0,334
MmaSAT19-445	-	0,004	0,002	-	**0,319**	-	125	0,325
MatSAT20-21	**0,317**	-	-	-	-	-	123	0,317

SF1 (MpaSAT21-263 and MmaSAT25-353)	0,004	-	-	0,012	**0,131**	**0,147**	155 e 163	0,294
MmaSAT22-28	-	-	-	-	**0,234**	-	137	0,234
MbrSAT23-123	0,012	0,008	0,003	**0,103**	0,018	0,056	143	0,199
MerSAT24-488	-	0,088	**0,092**	-	-	-	151	0,18
MatSAT26-26	**0,094**	-	-	-	-	-	180	0,094

Supplementary Table 1. Individual annotation of the repeat type and genome proportion (%) of *Macroptilium atropurpureum*

Repeat type	%
Unclassifield	3.71
5S	0.21
35S	1.88
Satellite	2.79
LTR elements	
LTR non-classified	-
Ty1/*Copia*	
Ale	0.67
Ikeros	0.34
Ivana	0.02
SIRE	1.91
TAR	0.1
Tork	0.39
Ty3/*Gypsy*	
Athila	0.61
Ogre	0.47
CRM	0.4
Tekay	1.22
Pararetrovirus	0.26
Class II	
CACTA	0.57
hAT	0.15
Mutator	0.1
Total	16.17

FIGURE LEGENDS

Figure 1. Chromosome bacorde, painting and rDNA FISH in *Macroptilium* species. *Phaseolus vulgaris* was used as outgroup. The first line of each rectangle corresponds to the oligo-FISH barcode (dual color); the second line corresponds to the oligo painting (probes from *Pv*2 in green; probes from *Pv*3 in red) with the rDNA sites (5S in yellow and 35S in magenta). Left-side topology corresponding of the cytogenetics groups that were supported by repetitive fraction and plastome + ITS phylogeny. The right-side topology corresponds to the current phylogeny from Espert et al., (2007, 2010), with the respective sections A and B. Arrowheads indicate exclusive translocations within group II (chr2 to chr6) and III (chr3 to chr11). Bar = 5 µm.

Figure 2. Oligo-FISH painting results for *Pv*1 (blue), *Pv*2 (green), *Pv*3 (red) and *Pv*5 (light brown) in *P. vulgaris* (**a-b**), *M. erythroloma* (**c-d**), *M. bracteatum* (**e-f**), *M. atropurpureum* (**g**) and *M. lathyroides* (**h**). Sequential barcode hybridizations were applicated in the species (**b**, **d** and **f**), with the exception of group I species (**g** and **h)**. Bar = 5 µm.

Figure 3. Correlation between genomic blocks proposed by Montenegro et al. (2022) and the oligo-FISH barcode and rDNA positions in APK (A), APnK (B), *M. atropurpureum* (C), *P. vulgaris* (D) and *V. unguiculata* (E). Colors for GBs from APK as proposed by Montenegro et al. (2022): dark blue, APK1; light green, APK2; red, APK3; brass, APK4; brown, APK5; purple, APK6; dark green, APK7; pink, APK8; yellow, APK9; light blue, APK10; orange, APK11.

Figure 4. Automatic annotation from RepeatExplorer comparative analyses between *M. erythroloma*, *M. fraternum* (group II), *M. atropurpureum*, *M. martii* (group I), *M. panduratum* and *M. bracteatum* (group III). Each repeat element corresponds to a specific cluster, and it is represented by a specific color. Bars indicate the abundance of the elements in each genome.

Supplementary Figure 1. Oligo and rDNA-FISH results in metaphase cells from *M. atropurpureum* (**a-b**), *M. gracile* (**c-d**), *M. martii* (**e-f**), *M. lathyroides* (**g-h**), *M. fraternum* (**i-j**), *M. erythroloma* (**k-l**), *M. bracteatum* (**m-n**), *M. panduratum* (**o-p**), *M. supinum* (**q-r**) and *P. vulgaris* BAT'93 (**s-t**). FISH results images were merged in two parts: 1) painting of *Pv*2 (green)

and *Pv*3 (red) with rDNA 5S (yellow) and 35S (magenta) [**a, c, e, g, i, k, m, o, q** and **s**]; 2) barcode results in green and red (**b, d, f, h, j, l, n, p, r** and **t**). Bar = 5 µm.

Supplementary Figure 2. Oligo-FISH pattern derived from chromosomes 2 (green color) and 3 (red color) of *P. vulgaris*. A) *P. vulgaris*, B) *V. unguiculata*, C) *M. atropurpureum* (section A, group I), *M. bracteatum* (section A, group II) and *M. fraternum* (section B, group III).

Supplementary Figure 3. Plastome assembly and annotation from *M. atropurpureum* (**a**), *M. martii* (**b**), *M. erythroloma* (**c**), *M. fraternum* (**d**), *M. bracteatum* (**e**) and *M. panduratum* (**f**).

Supplementary Figure 4. Neighbor-Joining tree with ITS and plastomes concatenated alignment with 100,000 replicates bootstrap. *V. unguiculata* and *P. vulgaris* were used as outgroup. Red highlighted represents the outgroup, light green represents *Macroptilium* genus, yellow represents group I, dark green represents group II and blue represents group III.

Supplementary Figure 5. Bayesian tree made with MrBayes, using *V. unguiculata* and *P. vulgaris* as outgroup. Model GTR+G for 10000000 of generations sampling at each 1000. Red highlighted represents the outgroup, light green represents *Macroptilium* genus, yellow represents group I, dark green represents group II and blue represents group III.

FIGURES

Figure 1

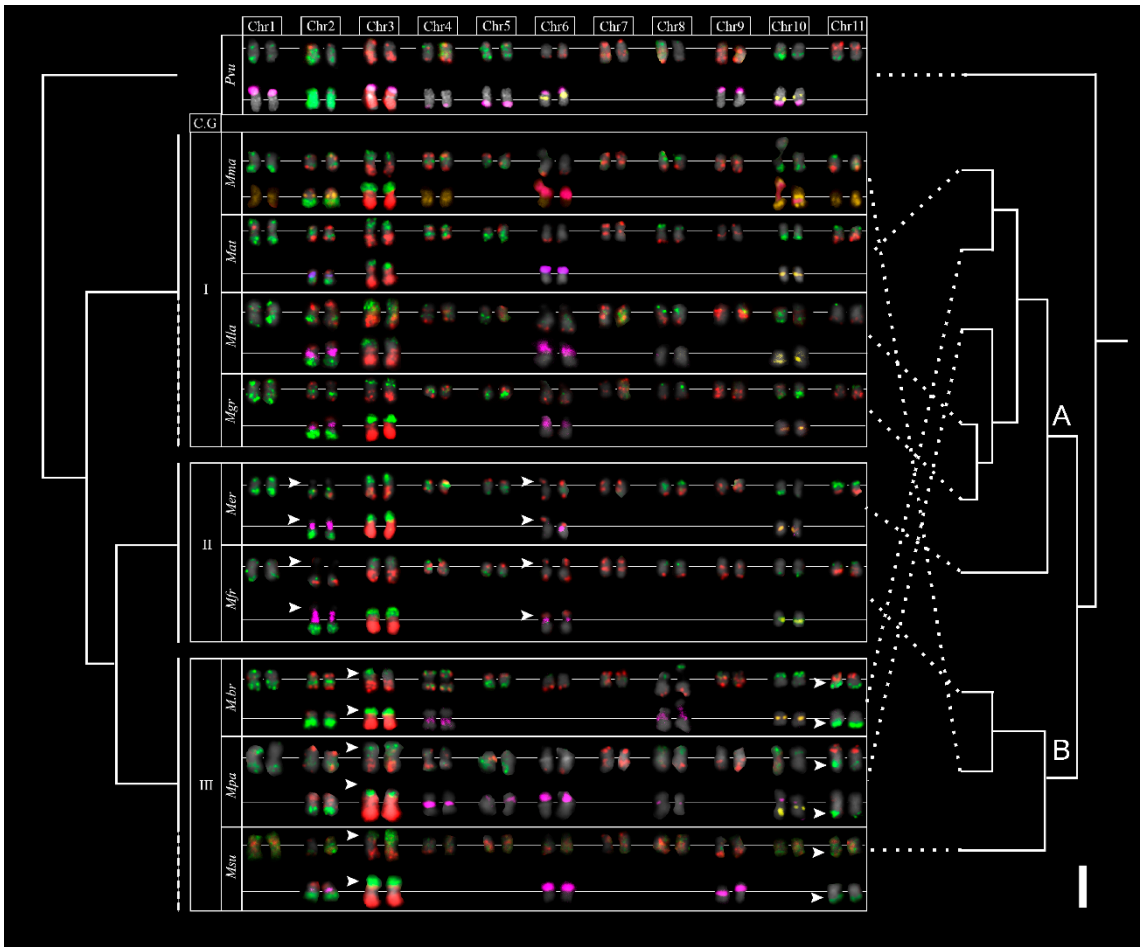

Figure 2

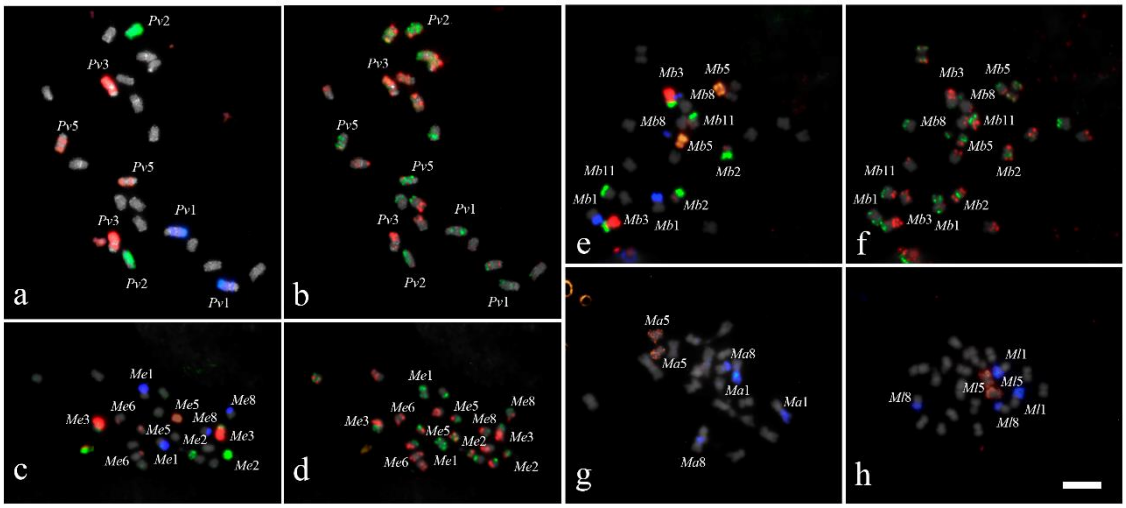

Figure 3

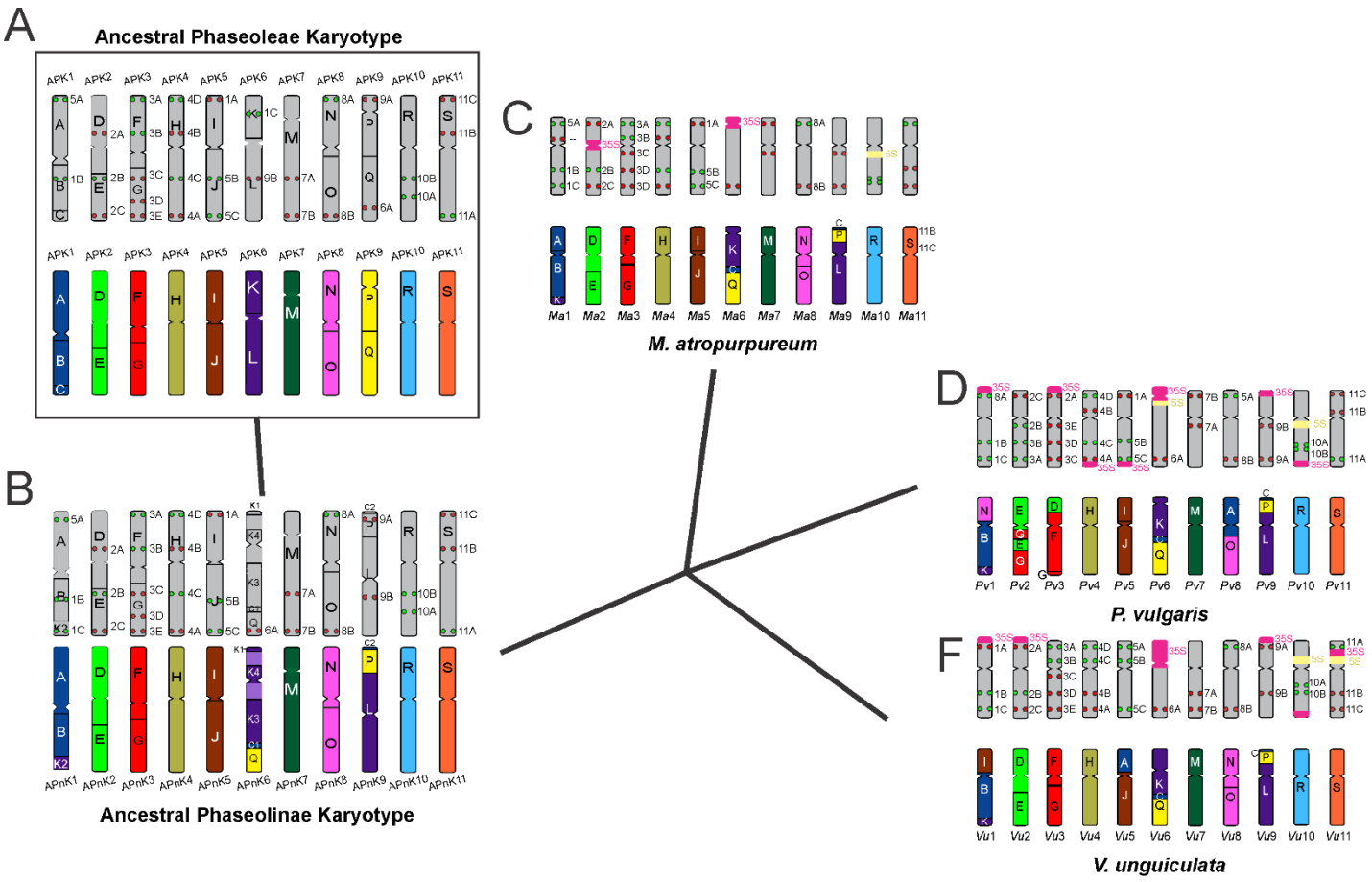

Figure 4


Automatic annotation
Cluster size
repeat
satellite
SIRE
45S_rDNA
Tekay
Ale
Athila
EnSpm_CACTA
Ogre
CRM
Other
M. erythroloma
M. fraternum
M. atropurpureum
M. martii
M. panduratum
M. bracteatum
GROUP II
GROUP I
GROUP III
Cluster Id

Supplementary Figure 1

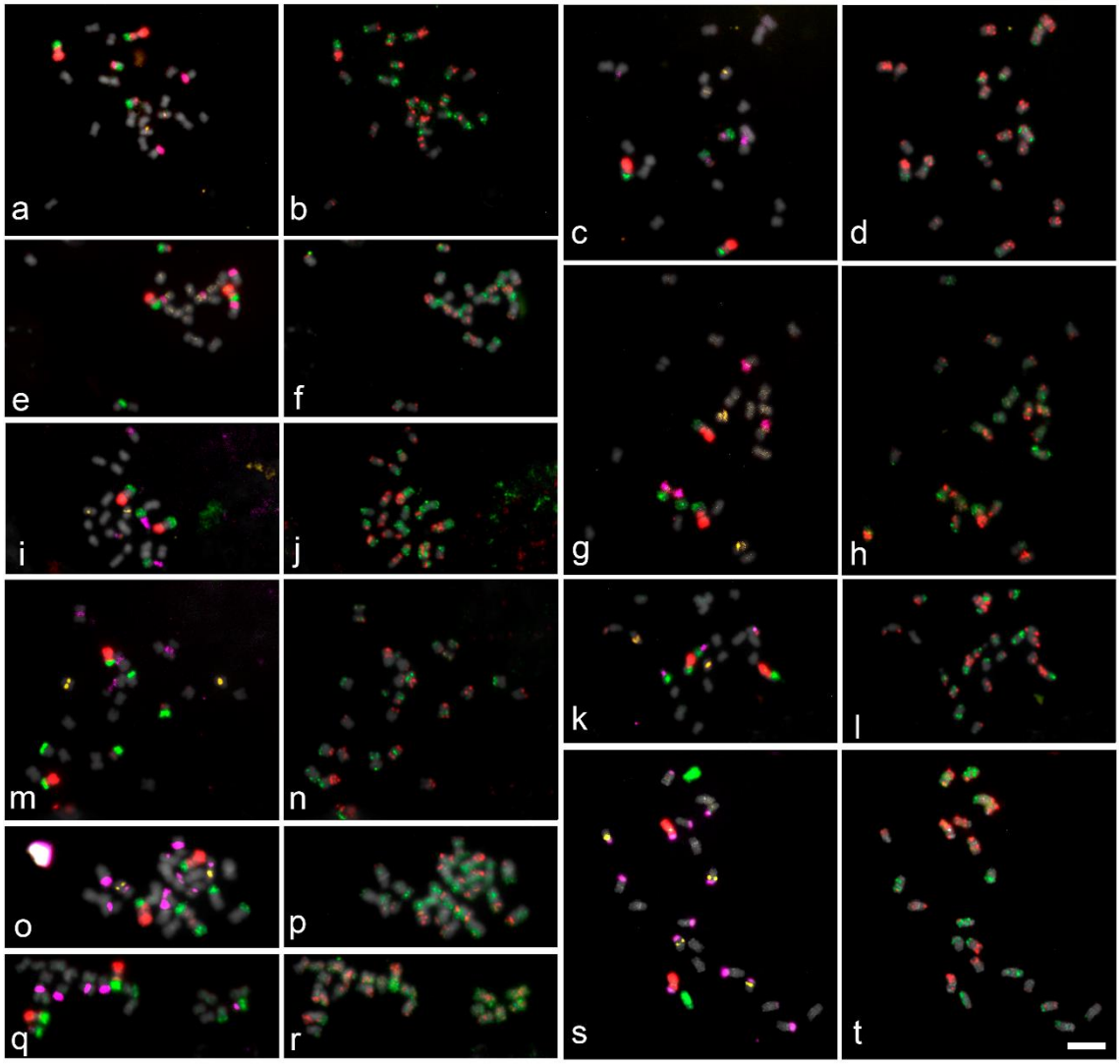

Supplementary Figure 2

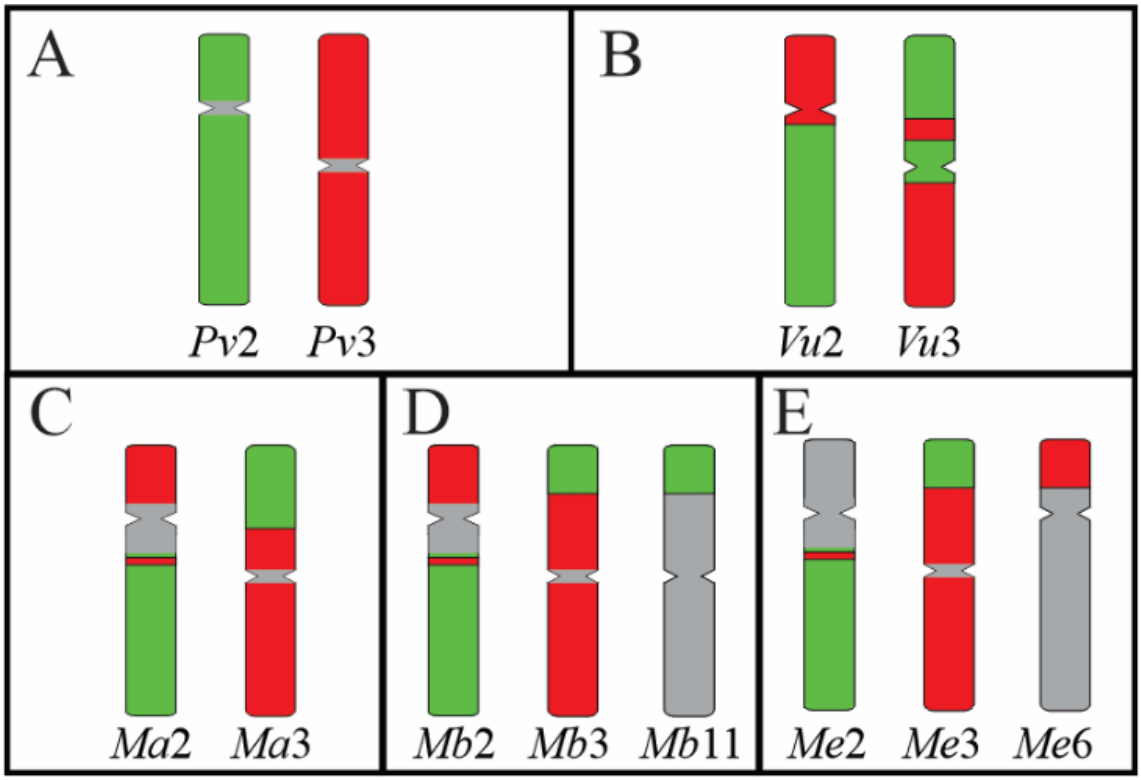

Supplementary Figure 3

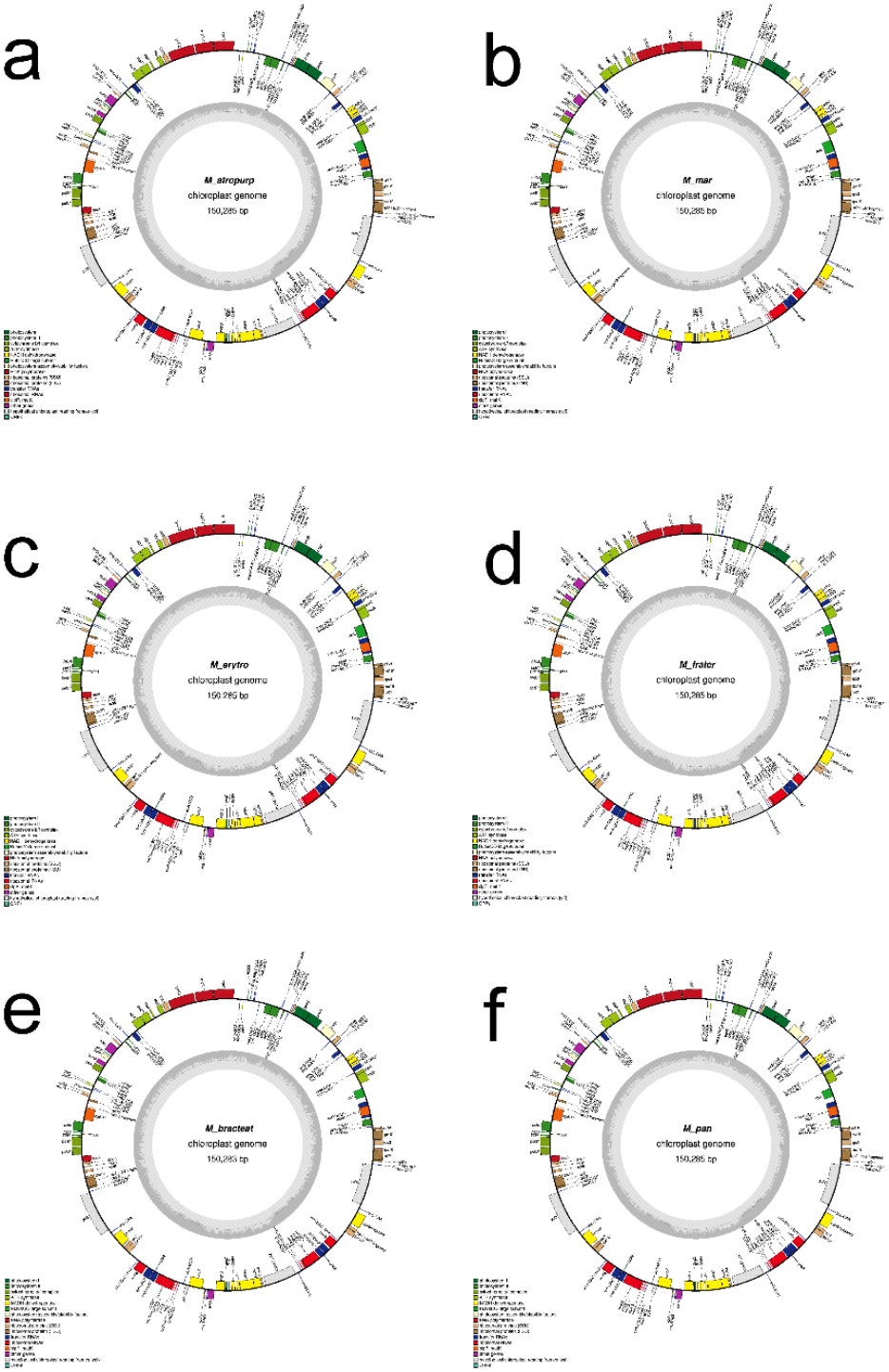

Supplementary Figure 4

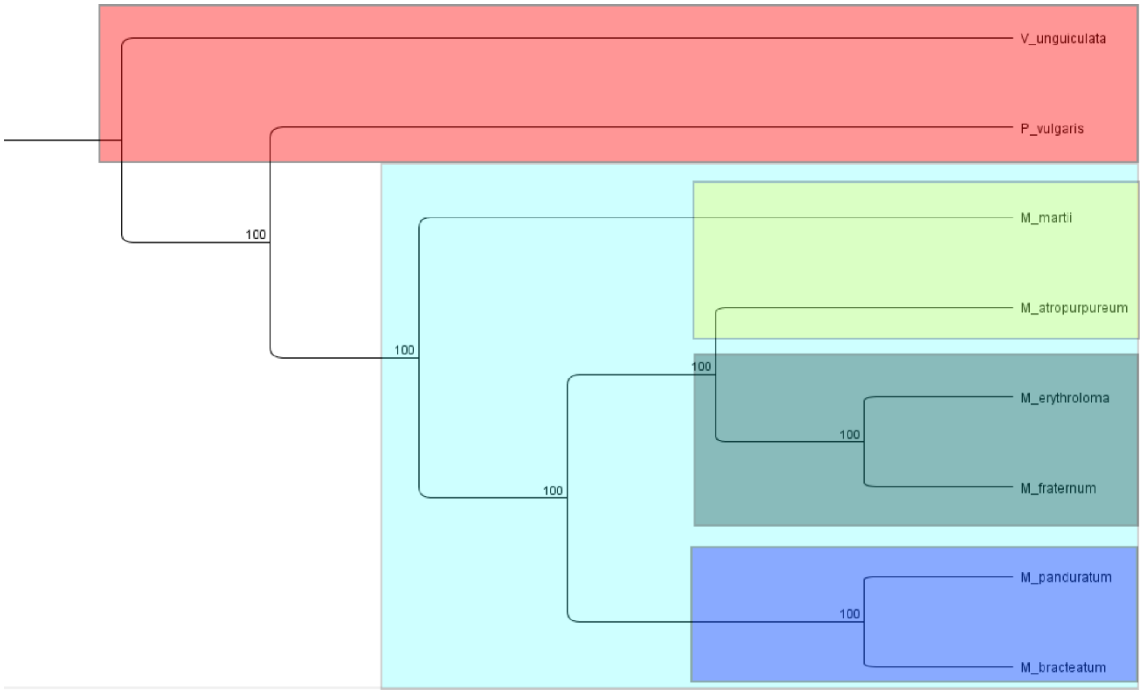

Supplementary Figure 5

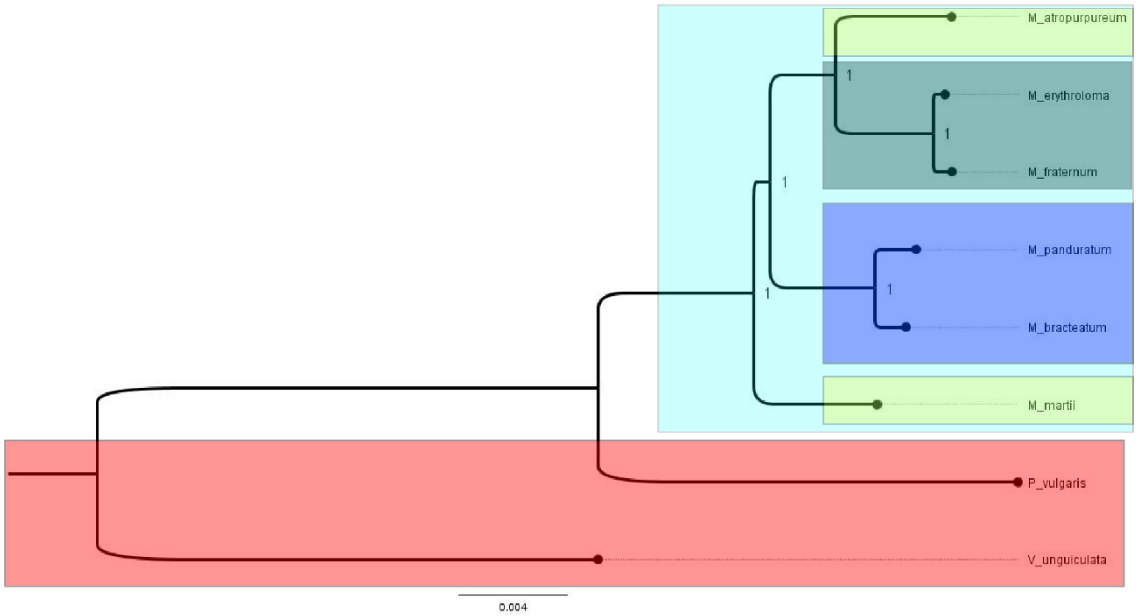

4 CONSIDERAÇÕES FINAIS

A partir da inferência do cariótipo ancestral da tribo Phaseoleae, principais rearranjos cromossômicos envolvido na evolução desse grupo, além de um constante reposicionamento centromérico, mostramos o quanto os genomas dos feijões dessa tribo são dinâmicos mesmo com a manutenção do número cromossômico para maior parte dos representantes. Além disso, demonstramos rearranjos cromossômicos interespecíficos no gênero *Macroptilium*, possibilitando a criação de três grupos citogenéticos para o mesmo, mostrando como a combinação análises genômicas, filogenéticas e citogenômicas são ótimas ferramentas para estudos de evolução cromossômica e para elucidar relações filogenéticas não tão bem resolvidas, mesmo sem um genoma de referência disponível.

5 REFERÊNCIAS

5.1 REFERÊNCIAS DA REVISÃO BIBLIOGRÁFICA

ALBERT, P. S. et al. Whole-chromosome paints in maize reveal rearrangements, nuclear domains, and chromosomal relationships. **Proceedings of the National Academy of Sciences**, v. 116, n. 5, p. 1679–1685, 29 jan. 2019.

ALMEDA, F.; PENNEYS, D. S. Patterns of Chromosome Number Diversity and Evolution in the Melastomataceae. Em: GOLDENBERG, R.; MICHELANGELI, F. A.; ALMEDA, F. (Eds.). **Systematics, Evolution, and Ecology of Melastomataceae**. Cham: Springer International Publishing, 2022. p. 533–561.

ALMEIDA, C.; PEDROSA-HARAND, A. Contrasting rDNA Evolution in Lima Bean (*Phaseolus lunatus* L.) and Common Bean (*P. vulgaris* L., Fabaceae). **Cytogenetic and Genome Research**, v. 132, n. 3, p. 212–217, 2011.

ALSEEKH, S.; SCOSSA, F.; FERNIE, A. R. Mobile Transposable Elements Shape Plant Genome Diversity. **Trends in Plant Science**, v. 25, n. 11, p. 1062–1064, 1 nov. 2020.

AMBORELLA GENOME PROJECT et al. The Amborella Genome and the Evolution of Flowering Plants. **Science**, v. 342, n. 6165, p. 1241089–1241089, 20 dez. 2013.

ANDERSON, J. W. et al. Hypocholesterolemic effects of oat-bran or bean intake for hypercholesterolemic men. **The American Journal of Clinical Nutrition**, v. 40, n. 6, p. 1146–1155, 1 dez. 1984.

ANDERSON, S. N. et al. Subtle Perturbations of the Maize Methylome Reveal Genes and Transposons Silenced by Chromomethylase or RNA-Directed DNA Methylation Pathways. **G3 Genes|Genomes|Genetics**, v. 8, n. 6, p. 1921–1932, 1 jun. 2018.

AZANI, N. et al. A new subfamily classification of the Leguminosae based on a taxonomically comprehensive phylogeny: The Legume Phylogeny Working Group (LPWG). **TAXON**, v. 66, n. 1, p. 44–77, 2017.

BÁEZ, M. et al. Together But Different: The Subgenomes of the Bimodal Eleutherine Karyotypes Are Differentially Organized. **Frontiers in Plant Science**, v. 10, p. 1170, 7 out. 2019.

BANIAGA, A. E. et al. Polyploid plants have faster rates of multivariate niche differentiation than their diploid relatives. **Ecology Letters**, v. 23, n. 1, p. 68–78, 2020.

BARROS E SILVA, A. E. et al. The evolution of CMA bands in Citrus and related genera. **Chromosome Research**, v. 18, n. 4, p. 503–514, jun. 2010.

BARROS FERREIRA, D. D. **ANÁLISE CITOGENÉTICA EM ESPÉCIES DO GÊNERO Macroptilium (BENTH.) URB. E MAPEAMENTO CITOGENÉTICO COMPARATIVO COM ESPÉCIES DO GÊNERO Phaseolus (L.)**. CENTRO DE BIOCIÊNCIAS: UNIVERSIDADE FEDERAL DE PERNAMBUCO, 2019.

BAYAT, S.; LYSAK, M. A.; MANDÁKOVÁ, T. Genome structure and evolution in the cruciferous tribe Thlaspideae (Brassicaceae). **The Plant Journal**, v. 108, n. 6, p. 1768–1785, 2021.

BELYAYEV, A. et al. Transposable elements in a marginal plant population: temporal fluctuations provide new insights into genome evolution of wild diploid wheat. **Mobile DNA**, v. 1, n. 1, p. 6, 2010.

BETEKHTIN, A.; JENKINS, G.; HASTEROK, R. Reconstructing the Evolution of Brachypodium Genomes Using Comparative Chromosome Painting. **PLOS ONE**, v. 9, n. 12, p. e115108, 10 dez. 2014.

BIRCHLER, J. A. Aneuploidy in plants and flies: The origin of studies of genomic imbalance. **Seminars in Cell & Developmental Biology**, v. 24, n. 4, p. 315–319, abr. 2013.

BIRCHLER, J. A.; VEITIA, R. A. The Gene Balance Hypothesis: Dosage Effects in Plants. Em: SPILLANE, C.; MCKEOWN, P. C. (Eds.). **Plant Epigenetics and Epigenomics**. Methods in Molecular Biology. Totowa, NJ: Humana Press, 2014. v. 1112p. 25–32.

BIRCHLER, J. A.; YANG, H. The multiple fates of gene duplications: Deletion, hypofunctionalization, subfunctionalization, neofunctionalization, dosage balance constraints, and neutral variation. **The Plant Cell**, v. 34, n. 7, p. 2466–2474, 1 jul. 2022.

BISCOTTI, M. A.; OLMO, E.; HESLOP-HARRISON, J. S. Repetitive DNA in eukaryotic genomes. **Chromosome Research**, v. 23, n. 3, p. 415–420, set. 2015.

BOMBLIES, K.; MADLUNG, A. Polyploidy in the Arabidopsis genus. **Chromosome Research**, v. 22, n. 2, p. 117–134, jun. 2014.

BONIFÁCIO, E. M. et al. Comparative cytogenetic mapping between the lima bean (Phaseolus lunatus L.) and the common bean (P. vulgaris L.). **Theoretical and Applied Genetics**, v. 124, n. 8, p. 1513–1520, maio 2012.

BOURQUE, G. et al. Ten things you should know about transposable elements. **Genome Biology**, v. 19, n. 1, p. 199, dez. 2018.

BRAZ, G. T. et al. Comparative Oligo-FISH Mapping: An Efficient and Powerful Methodology To Reveal Karyotypic and Chromosomal Evolution. p. 11, 2018a.

BRAZ, G. T. et al. Comparative Oligo-FISH Mapping: An Efficient and Powerful Methodology To Reveal Karyotypic and Chromosomal Evolution. **Genetics**, v. 208, n. 2, p. 513–523, fev. 2018b.

BRAZ, G. T. et al. A universal chromosome identification system for maize and wild Zea species. **Chromosome Research**, v. 28, n. 2, p. 183–194, jun. 2020.

CAFASSO, D.; CHINALI, G. An ancient satellite DNA has maintained repetitive units of the original structure in most species of the living fossil plant genus *Zamia*. **Genome**, v. 57, n. 3, p. 125–135, mar. 2014.

CANNON, S. B. et al. The roles of segmental and tandem gene duplication in the evolution of large gene families in Arabidopsis thaliana. **BMC Plant Biology**, v. 4, n. 1, p. 10, 2004.

CARMAN, J. G. Asynchronous expression of duplicate genes in angiosperms may cause apomixis, bispory, tetraspory, and polyembryony. **Biological Journal of the Linnean Society**, v. 61, n. 1, p. 51–94, maio 1997.

CARVALHO, C. M. B.; LUPSKI, J. R. Mechanisms underlying structural variant formation in genomic disorders. **Nature Reviews Genetics**, v. 17, n. 4, p. 224–238, abr. 2016.

CARVALHO, C. R.; SARAIVA, L. S. An Air Drying Technique for Maize Chromosomes without Enzymatic Maceration. **Biotechnic & Histochemistry**, v. 68, n. 3, p. 142–145, jan. 1993.

CASTIGLIONE, M. R.; CREMONINI, R. A fascinating island: 2n ¼ 4. p. 17, [s.d.].

CHALUP, L. et al. Karyotype characterization and evolution in South American species of Lathyrus (Notolathyrus, Leguminosae) evidenced by heterochromatin and rDNA mapping. **Journal of Plant Research**, v. 128, n. 6, p. 893–908, nov. 2015.

CHANDERBALI, A. S. et al. Buxus and Tetracentron genomes help resolve eudicot genome history. **Nature Communications**, v. 13, n. 1, p. 643, 2 fev. 2022.

CHAOWEN, S. et al. Karyotype analysis of *Psophocarpus tetragonolobus* (L.) DC by chromosome banding and fluorescence in situ hybridization. **Caryologia**, v. 57, n. 4, p. 387–394, jan. 2004.

CHEN, L. et al. Development of a set of chromosome-specific oligonucleotide markers and karyotype analysis in the Japanese morning glory Ipomoea nil. **Scientia Horticulturae**, v. 273, p. 109633, nov. 2020.

CHENG, F.; WU, J.; WANG, X. Genome triplication drove the diversification of Brassica plants. **Horticulture Research**, v. 1, n. 1, p. 1–8, 21 maio 2014.

CHIAVEGATTO, R. B. et al. Heterochromatin Bands and rDNA Sites Evolution in Polyploidization Events in Cynodon Rich. (Poaceae). **Plant Molecular Biology Reporter**, v. 37, n. 5–6, p. 477–487, dez. 2019.

CHOI, H.-W. et al. Molecular cytogenetic analysis of the Vigna species distributed in Korea. **Genes & Genomics**, v. 35, n. 2, p. 257–264, abr. 2013.

CHRISTENHUSZ, M. J. M.; BYNG, J. W. The number of known plants species in the world and its annual increase. **Phytotaxa**, v. 261, n. 3, p. 201, 20 maio 2016.

CHUNDURI, N. K.; STORCHOVÁ, Z. The diverse consequences of aneuploidy. **Nature Cell Biology**, v. 21, n. 1, p. 54–62, jan. 2019.

CHUONG, E. B.; ELDE, N. C.; FESCHOTTE, C. Regulatory activities of transposable elements: from conflicts to benefits. **Nature Reviews Genetics**, v. 18, n. 2, p. 71–86, fev. 2017.

DE OLIVEIRA BUSTAMANTE, F. et al. Oligo-FISH barcode in beans: a new chromosome identification system. **TAG. Theoretical and applied genetics. Theoretische und angewandte Genetik**, v. 134, n. 11, p. 3675–3686, nov. 2021.

DE SMET, R. et al. Convergent gene loss following gene and genome duplications creates single-copy families in flowering plants. **Proceedings of the National Academy of Sciences**, v. 110, n. 8, p. 2898–2903, 19 fev. 2013.

DE STORME, N.; MASON, A. Plant speciation through chromosome instability and ploidy change: Cellular mechanisms, molecular factors and evolutionary relevance. **Current Plant Biology**, v. 1, p. 10–33, ago. 2014.

DO VALE MARTINS, L. et al. BAC- and oligo-FISH mapping reveals chromosome evolution among Vigna angularis, V. unguiculata, and Phaseolus vulgaris. **Chromosoma**, v. 130, n. 2–3, p. 133–147, set. 2021.

DODSWORTH, S. et al. Repetitive DNA Dynamics and Polyploidization in the Genus Nicotiana (Solanaceae). Em: IVANOV, N. V.; SIERRO, N.; PEITSCH, M. C. (Eds.). **The Tobacco Plant Genome**. Compendium of Plant Genomes. Cham: Springer International Publishing, 2020. p. 85–99.

DODSWORTH, S.; CHASE, M. W.; LEITCH, A. R. Is post-polyploidization diploidization the key to the evolutionary success of angiosperms?: Diploidization in Polyploid Angiosperms. **Botanical Journal of the Linnean Society**, v. 180, n. 1, p. 1–5, jan. 2016.

DOMINGUES, D. S. et al. Analysis of plant LTR-retrotransposons at the fine-scale family level reveals individual molecular patterns. **BMC Genomics**, v. 13, n. 1, p. 137, 2012.

DONG, D. et al. Genetic diversity and population structure of vegetable soybean (Glycine max (L.) Merr.) in China as revealed by SSR markers. **Genetic Resources and Crop Evolution**, v. 61, n. 1, p. 173–183, jan. 2014.

DOYLE, J. J.; DOYLE, J. L. Chloroplast DNA Phylogeny of the Papilionoid Legume Tribe Phaseoleae. **Systematic Botany**, v. 18, n. 2, p. 309, abr. 1993a.

DOYLE, J. J.; DOYLE, J. L. Chloroplast DNA Phylogeny of the Papilionoid Legume Tribe Phaseoleae. **Systematic Botany**, v. 18, n. 2, p. 309, abr. 1993b.

EMADZADE, K. et al. Differential amplification of satellite PaB6 in chromosomally hypervariable Prospero autumnale complex (Hyacinthaceae). **Annals of Botany**, v. 114, n. 8, p. 1597–1608, dez. 2014.

ESPERT, S. M. et al. New chromosome reports in the subtribes Diocleinae and Glycininae (Phaseoleae: Papilionoideae: Fabaceae): CHROMOSOME REPORTS IN PHASEOLEAE. **Botanical Journal of the Linnean Society**, v. 158, n. 2, p. 336–341, out. 2008.

ESPERT, S. M.; BURGHARDT, A. D. Biogeography and divergence times of genus Macroptilium (Leguminosae). **AoB PLANTS**, v. 2010, 1 jan. 2010a.

ESPERT, S. M.; BURGHARDT, A. D. Biogeography and divergence times of genus Macroptilium (Leguminosae). **AoB PLANTS**, v. 2010, 1 jan. 2010b.

ESPERT, S. M.; DREWES, S. I.; BURGHARDT, A. D. Phylogeny of Macroptilium (Leguminosae): morphological, biochemical and molecular evidence. **Phylogeny of Macroptilium (Leguminosae): morphological,biochemical and molecular evidence**, v. 23, p. 11, 2007a.

ESPERT, S. M.; DREWES, S. I.; BURGHARDT, A. D. Phylogeny of Macroptilium (Leguminosae): morphological, biochemical and molecular evidence. **Cladistics**, v. 23, n. 2, p. 119–129, abr. 2007b.

FEITOZA, L.; GUERRA, M. Different types of plant chromatin associated with modified histones H3 and H4 and methylated DNA. **Genetica**, v. 139, n. 3, p. 305–314, mar. 2011.

FERRAZ, M. E.; FONSÊCA, A.; PEDROSA-HARAND, A. Multiple and independent rearrangements revealed by comparative cytogenetic mapping in the dysploid Leptostachyus group (Phaseolus L., Leguminosae). **Chromosome Research**, v. 28, n. 3–4, p. 395–405, dez. 2020.

FERREIRA, P. A. A. et al. Isolation, Characterization and Symbiotic Efficiency of Nitrogen-Fixing and Heavy Metal-Tolerant Bacteria from a Coalmine Wasteland. **Revista Brasileira de Ciência do Solo**, v. 42, n. 0, 13 set. 2018.

FILIAULT, D. L. et al. The Aquilegia genome provides insight into adaptive radiation and reveals an extraordinarily polymorphic chromosome with a unique history. **eLife**, v. 7, p. e36426, 16 out. 2018.

FONSÊCA, A. et al. Cytogenetic map of common bean (Phaseolus vulgaris L.). **Chromosome Research**, v. 18, n. 4, p. 487–502, jun. 2010.

FONSÊCA, A.; FERRAZ, M. E.; PEDROSA-HARAND, A. Speeding up chromosome evolution in Phaseolus: multiple rearrangements associated with a one-step descending dysploidy. **Chromosoma**, v. 125, n. 3, p. 413–421, jun. 2016.

FONSÊCA, A.; PEDROSA-HARAND, A. Cytogenetics and Comparative Analysis of Phaseolus Species. Em: PÉREZ DE LA VEGA, M.; SANTALLA, M.; MARSOLAIS, F. (Eds.). **The Common Bean Genome**. Compendium of Plant Genomes. Cham: Springer International Publishing, 2017. p. 57–68.

FRIEBE, B. et al. Standard karyotypes ofAegilops uniaristata, Ae. mutica, Ae. comosa subspeciescomosa andheldreichii (Poaceae). **Plant Systematics and Evolution**, v. 202, n. 3–4, p. 199–210, 1996.

FRIEBE, B. et al. Robertsonian translocations in wheat arise by centric misdivision of univalents at anaphase I and rejoining of broken centromeres during interkinesis of meiosis II. **Cytogenetic and Genome Research**, v. 109, n. 1–3, p. 293–297, 2005.

GABUR, I. et al. Connecting genome structural variation with complex traits in crop plants. **Theoretical and Applied Genetics**, v. 132, n. 3, p. 733–750, 1 mar. 2019.

GARCIA, S. et al. Cytogenetic features of rRNA genes across land plants: analysis of the Plant rDNA database. **The Plant Journal**, v. 89, n. 5, p. 1020–1030, mar. 2017.

GARCIA, T. et al. Comprehensive genomic resources related to domestication and crop improvement traits in Lima bean. **Nature Communications**, v. 12, n. 1, p. 702, 29 jan. 2021.

GARRIDO, M. A. et al. rDNA site number polymorphism and NOR inactivation in natural populations ofAllium schoenoprasum. **Genetica**, v. 94, n. 1, p. 67–71, fev. 1994.

GARRIDO-RAMOS, M. Satellite DNA: An Evolving Topic. **Genes**, v. 8, n. 9, p. 230, 18 set. 2017.

GARRIDO-RAMOS, M. A. Satellite DNA in Plants: More than Just Rubbish. **Cytogenetic and Genome Research**, v. 146, n. 2, p. 153–170, 2015a.

GARRIDO-RAMOS, M. A. Satellite DNA in Plants: More than Just Rubbish. **Cytogenetic and Genome Research**, v. 146, n. 2, p. 153–170, 2015b.

GEARHART, J. D. et al. Developmental consequences of autosomal aneuploidy in mammals. **Developmental Genetics**, v. 8, n. 4, p. 249–265, 1987.

GEIL, P. B.; ANDERSON, J. W. Nutrition and health implications of dry beans: a review. **Journal of the American College of Nutrition**, v. 13, n. 6, p. 549–558, dez. 1994.

GEORGE, C. M.; ALANI, E. Multiple cellular mechanisms prevent chromosomal rearrangements involving repetitive DNA. **Critical Reviews in Biochemistry and Molecular Biology**, v. 47, n. 3, p. 297–313, jun. 2012.

GERLACH, W. L.; BEDBROOK, J. R. Cloning and characterization of ribosomal RNA genes from wheat and barley. **Nucleic Acids Research**, v. 7, n. 7, p. 1869–1885, 11 dez. 1979.

GORDON, D. J.; RESIO, B.; PELLMAN, D. Causes and consequences of aneuploidy in cancer. **Nature Reviews Genetics**, v. 13, n. 3, p. 189–203, mar. 2012.

GRAY, Y. H. M. It takes two transposons to tango:transposable-element-mediated chromosomal rearrangements. **Trends in Genetics**, v. 16, n. 10, p. 461–468, out. 2000.

GREGORY, T. R. Genome Size Evolution in Animals. Em: **The Evolution of the Genome**. [s.l.] Elsevier, 2005. p. 3–87.

GUERRA, M. DOS S. Mitotic and meiotic analysis of a pericentric inversion associated with a tandem duplication in Eleutherine bulbosa. **Chromosoma**, v. 97, n. 1, p. 80–87, set. 1988.

HAN, Y. et al. Chromosome-Specific Painting in *Cucumis* Species Using Bulked Oligonucleotides. **Genetics**, v. 200, n. 3, p. 771–779, jul. 2015a.

HAN, Y. et al. Chromosome-Specific Painting in *Cucumis* Species Using Bulked Oligonucleotides. **Genetics**, v. 200, n. 3, p. 771–779, jul. 2015b.

HARPKE, D.; PETERSON, A. Non-concerted ITS evolution in Mammillaria (Cactaceae). **Molecular Phylogenetics and Evolution**, v. 41, n. 3, p. 579–593, dez. 2006.

HASTEROK, R. et al. The nature and destiny of translocated B-chromosome-speci¢c satellite DNA of rye. p. 4, [s.d.].

HE, L. et al. Chromosome painting in meiosis reveals pairing of specific chromosomes in polyploid Solanum species. **Chromosoma**, v. 127, n. 4, p. 505–513, dez. 2018.

HE, L. et al. Extraordinarily conserved chromosomal synteny of *Citrus* species revealed by chromosome-specific painting. **The Plant Journal**, p. tpj.14894, 16 jul. 2020.

HESLOP-HARRISON, J. S. (PAT); SCHWARZACHER, T. Organisation of the plant genome in chromosomes. **The Plant Journal**, v. 66, n. 1, p. 18–33, 2011.

HOFFMANN, A.; SGRO, C.; WEEKS, A. Chromosomal inversion polymorphisms and adaptation. **Trends in Ecology & Evolution**, v. 19, n. 9, p. 482–488, set. 2004.

HOU, J. et al. Major Chromosomal Rearrangements Distinguish Willow and Poplar After the Ancestral "Salicoid" Genome Duplication. **Genome Biology and Evolution**, v. 8, n. 6, p. 1868–1875, jun. 2016.

HOU, L. et al. Chromosome painting and its applications in cultivated and wild rice. **BMC Plant Biology**, v. 18, n. 1, p. 110, dez. 2018.

HUANG, C. R. L.; BURNS, K. H.; BOEKE, J. D. Active Transposition in Genomes. **Annual Review of Genetics**, v. 46, n. 1, p. 651–675, 15 dez. 2012.

HUANG, C.-H. et al. Multiple Polyploidization Events across Asteraceae with Two Nested Events in the Early History Revealed by Nuclear Phylogenomics. **Molecular Biology and Evolution**, v. 33, n. 11, p. 2820–2835, nov. 2016.

HUFNAGEL, B. et al. High-quality genome sequence of white lupin provides insight into soil exploration and seed quality. **Nature Communications**, v. 11, n. 1, p. 492, dez. 2020.

HUGHES, T. E.; LANGDALE, J. A.; KELLY, S. The impact of widespread regulatory neofunctionalization on homeolog gene evolution following whole-genome duplication in maize. **Genome Research**, v. 24, n. 8, p. 1348–1355, ago. 2014.

IBIAPINO, A. et al. Karyotype asymmetry in Cuscuta L. subgenus Pachystigma reflects its repeat DNA composition. **Chromosome Research**, v. 30, n. 1, p. 91–107, mar. 2022.

IWATA, A. et al. Identification and characterization of functional centromeres of the common bean. **The Plant Journal**, p. n/a-n/a, jul. 2013.

JIANG, J. Fluorescence in situ hybridization in plants: recent developments and future applications. **Chromosome Research**, v. 27, n. 3, p. 153–165, set. 2019a.

JIANG, J. Fluorescence in situ hybridization in plants: recent developments and future applications. **Chromosome Research**, v. 27, n. 3, p. 153–165, set. 2019b.

JIAO, W.-B.; SCHNEEBERGER, K. Chromosome-level assemblies of multiple Arabidopsis genomes reveal hotspots of rearrangements with altered evolutionary dynamics. **Nature Communications**, v. 11, n. 1, p. 989, 20 fev. 2020.

JIAO, Y. et al. Ancestral polyploidy in seed plants and angiosperms. **Nature**, v. 473, n. 7345, p. 97–100, maio 2011.

JO, S.-H. et al. Evolution of ribosomal DNA-derived satellite repeat in tomato genome. **BMC Plant Biology**, v. 9, n. 1, p. 42, 2009.

KAUL, S. et al. Analysis of the genome sequence of the flowering plant Arabidopsis thaliana. **Nature**, v. 408, n. 6814, p. 796–815, 14 dez. 2000.

KELLY, L. J. et al. Analysis of the giant genomes of *Fritillaria* (Liliaceae) indicates that a lack of DNA removal characterizes extreme expansions in genome size. **New Phytologist**, v. 208, n. 2, p. 596–607, out. 2015.

KHANDELWAL, S. Chromosome evolution in the genus Ophioglossum L. **Botanical Journal of the Linnean Society**, v. 102, n. 3, p. 205–217, mar. 1990.

KIROV, I. V. et al. Tandem repeats of Allium fistulosum associated with major chromosomal landmarks. **Molecular Genetics and Genomics**, v. 292, n. 2, p. 453–464, abr. 2017.

KRASILEVA, K. V. The role of transposable elements and DNA damage repair mechanisms in gene duplications and gene fusions in plant genomes. **Current Opinion in Plant Biology**, Genome studies and molecular genetics. v. 48, p. 18–25, 1 abr. 2019.

KREPLAK, J. et al. A reference genome for pea provides insight into legume genome evolution. **Nature Genetics**, v. 51, n. 9, p. 1411–1422, set. 2019.

KUITTINEN, H. et al. Comparing the Linkage Maps of the Close Relatives *Arabidopsis lyrata* and *A. thaliana*. **Genetics**, v. 168, n. 3, p. 1575–1584, nov. 2004.

KUMAR, S. et al. Gamma ray induced chromosomal aberrations and enzyme related defense mechanism in Allium cepa L. p. 11, [s.d.].

LAN, T.; ALBERT, V. A. Dynamic distribution patterns of ribosomal DNA and chromosomal evolution in Paphiopedilum, a lady's slipper orchid. **BMC Plant Biology**, v. 11, n. 1, p. 126, 2011.

LEE, C. et al. Reconstruction of a composite comparative map composed of ten legume genomes. **Genes & Genomics**, v. 39, n. 1, p. 111–119, jan. 2017.

LI, G. et al. An efficient Oligo-FISH painting system for revealing chromosome rearrangements and polyploidization in Triticeae. **The Plant Journal**, v. 105, n. 4, p. 978–993, 2021.

LI, H. et al. Diversification of the phaseoloid legumes: effects of climate change, range expansion and habit shift. **Frontiers in Plant Science**, v. 4, 2013a.

LI, H. et al. Diversification of the phaseoloid legumes: effects of climate change, range expansion and habit shift. **Frontiers in Plant Science**, p. 9, 2013b.

LI, S.-F. et al. Chromosome Evolution in Connection with Repetitive Sequences and Epigenetics in Plants. **Genes**, v. 8, n. 10, p. 290, 24 out. 2017.

LIEHR, T. et al. Recombinant Chromosomes Resulting From Parental Pericentric Inversions—Two New Cases and a Review of the Literature. **Frontiers in Genetics**, v. 10, 2019.

LISCH, D. How important are transposons for plant evolution? **Nature Reviews Genetics**, v. 14, n. 1, p. 49–61, jan. 2013.

LISCH, D.; BENNETZEN, J. L. Transposable element origins of epigenetic gene regulation. **Current Opinion in Plant Biology**, v. 14, n. 2, p. 156–161, abr. 2011.

LIU, C. J. et al. Nonhomoeologous translocations between group 4, 5 and 7 chromosomes within wheat and rye. **Theoretical and Applied Genetics**, v. 83, n. 3, p. 305–312, jan. 1992.

LIU, S. et al. The Brassica oleracea genome reveals the asymmetrical evolution of polyploid genomes. **Nature Communications**, v. 5, n. 1, p. 3930, 23 maio 2014.

LIU, X. et al. Dual-color oligo-FISH can reveal chromosomal variations and evolution in *Oryza* species. **The Plant Journal**, v. 101, n. 1, p. 112–121, jan. 2020a.

LIU, Y. et al. Insights into amphicarpy from the compact genome of the legume *Amphicarpaea edgeworthii*. **Plant Biotechnology Journal**, p. pbi.13520, 11 dez. 2020b.

LONARDI, S. et al. The genome of cowpea (*Vigna unguiculata* [L.] Walp.). **The Plant Journal**, v. 98, n. 5, p. 767–782, jun. 2019a.

LONARDI, S. et al. The genome of cowpea (*Vigna unguiculata* [L.] Walp.). **The Plant Journal**, v. 98, n. 5, p. 767–782, jun. 2019b.

LÓPEZ-FLORES, I.; GARRIDO-RAMOS, M. A. The Repetitive DNA Content of Eukaryotic Genomes. Em: GARRIDO-RAMOS, M. A. (Ed.). **Genome Dynamics**. Basel: S. KARGER AG, 2012a. v. 7p. 1–28.

LÓPEZ-FLORES, I.; GARRIDO-RAMOS, M. A. The Repetitive DNA Content of Eukaryotic Genomes. Em: GARRIDO-RAMOS, M. A. (Ed.). **Genome Dynamics**. Basel: S. KARGER AG, 2012b. v. 7p. 1–28.

LOUZADA, S. et al. Decoding the Role of Satellite DNA in Genome Architecture and Plasticity—An Evolutionary and Clinical Affair. **Genes**, v. 11, n. 1, p. 72, jan. 2020.

LYSAK, M. A.; MANDÁKOVÁ, T.; SCHRANZ, M. E. Comparative paleogenomics of crucifers: ancestral genomic blocks revisited. **Current Opinion in Plant Biology**, v. 30, p. 108–115, abr. 2016.

LYSÁK, M. A.; SCHUBERT, I. Mechanisms of Chromosome Rearrangements. Em: GREILHUBER, J.; DOLEZEL, J.; WENDEL, J. F. (Eds.). **Plant Genome Diversity Volume 2**. Vienna: Springer Vienna, 2013. p. 137–147.

MACAS, J. et al. Hypervariable 3′ UTR region of plant LTR-retrotransposons as a source of novel satellite repeats. **Gene**, v. 448, n. 2, p. 198–206, dez. 2009.

MACAS, J.; NEUMANN, P.; NAVRÁTILOVÁ, A. Repetitive DNA in the pea (Pisum sativum L.) genome: comprehensive characterization using 454 sequencing and comparison to soybean and Medicago truncatula. **BMC Genomics**, v. 8, n. 1, p. 427, 2007.

MANDÁKOVÁ, T. et al. Fast Diploidization in Close Mesopolyploid Relatives of *Arabidopsis*. **The Plant Cell**, v. 22, n. 7, p. 2277–2290, jul. 2010.

MANDÁKOVÁ, T. et al. Diverse genome organization following 13 independent mesopolyploid events in Brassicaceae contrasts with convergent patterns of gene retention. **The Plant Journal**, v. 91, n. 1, p. 3–21, jul. 2017.

MANDÁKOVÁ, T. et al. Genome Evolution in Arabideae Was Marked by Frequent Centromere Repositioning. **The Plant Cell**, v. 32, n. 3, p. 650–665, mar. 2020.

MANDÁKOVÁ, T.; LYSAK, M. A. Post-polyploid diploidization and diversification through dysploid changes. **Current Opinion in Plant Biology**, v. 42, p. 55–65, abr. 2018.

MAPHOSA, Y.; JIDEANI, V. A. The Role of Legumes in Human Nutrition. Em: HUEDA, M. C. (Ed.). **Functional Food - Improve Health through Adequate Food**. [s.l.] InTech, 2017.

MARQUES, A. et al. Holocentromeres in *Rhynchospora* are associated with genome-wide centromere-specific repeat arrays interspersed among euchromatin. **Proceedings of the National Academy of Sciences**, v. 112, n. 44, p. 13633–13638, 3 nov. 2015.

MARTINS, L. DO V. et al. BAC- and oligo-FISH mapping reveals chromosome evolution among Vigna angularis, V. unguiculata, and Phaseolus vulgaris. **Chromosoma**, 28 abr. 2021.

MAYER, K. F. X. et al. Unlocking the Barley Genome by Chromosomal and Comparative Genomics. **The Plant Cell**, v. 23, n. 4, p. 1249–1263, abr. 2011.

MCCLEAN, P. E. et al. Synteny mapping between common bean and soybean reveals extensive blocks of shared loci. **BMC Genomics**, v. 11, n. 1, p. 184, 2010.

MCCLINTOCK, B. Controlling Elements and the Gene. **Cold Spring Harbor Symposia on Quantitative Biology**, v. 21, n. 0, p. 197–216, 1 jan. 1956.

MOGHE, G. D.; SHIU, S.-H. The causes and molecular consequences of polyploidy in flowering plants: Plant polyploidy. **Annals of the New York Academy of Sciences**, v. 1320, n. 1, p. 16–34, jul. 2014.

MOUSAVI-DERAZMAHALLEH, M. et al. Adapting legume crops to climate change using genomic approaches. **Plant, Cell & Environment**, v. 42, n. 1, p. 6–19, 2019.

MUN, J.-H. et al. Genome-wide comparative analysis of the Brassica rapa gene space reveals genome shrinkage and differential loss of duplicated genes after whole genome triplication. **Genome Biology**, v. 10, n. 10, p. R111, 12 out. 2009.

MURAT, F. et al. Ancestral grass karyotype reconstruction unravels new mechanisms of genome shuffling as a source of plant evolution. **Genome Research**, v. 20, n. 11, p. 1545–1557, 1 nov. 2010.

NEUMANN, P. et al. Systematic survey of plant LTR-retrotransposons elucidates phylogenetic relationships of their polyprotein domains and provides a reference for element classification. **Mobile DNA**, v. 10, n. 1, p. 1, dez. 2019.

NOVAK, P. et al. RepeatExplorer: a Galaxy-based web server for genome-wide characterization of eukaryotic repetitive elements from next-generation sequence reads. **Bioinformatics**, v. 29, n. 6, p. 792–793, 15 mar. 2013.

NOVÁK, P. et al. TAREAN: a computational tool for identification and characterization of satellite DNA from unassembled short reads. **Nucleic Acids Research**, v. 45, n. 12, p. e111–e111, 7 jul. 2017.

OLIVEIRA, A. R. DA S. et al. Breaks of macrosynteny and collinearity among moth bean (Vigna aconitifolia), cowpea (V. unguiculata), and common bean (Phaseolus vulgaris). **Chromosome Research**, 11 jul. 2020a.

OLIVEIRA, A. R. DA S. et al. Breaks of macrosynteny and collinearity among moth bean (Vigna aconitifolia), cowpea (V. unguiculata), and common bean (Phaseolus vulgaris). **Chromosome Research**, 11 jul. 2020b.

ORDON, J. et al. Generation of chromosomal deletions in dicotyledonous plants employing a user-friendly genome editing toolkit. **The Plant Journal**, v. 89, n. 1, p. 155–168, jan. 2017.

PARISOD, C.; HOLDEREGGER, R.; BROCHMANN, C. Evolutionary consequences of autopolyploidy: Research review. **New Phytologist**, v. 186, n. 1, p. 5–17, abr. 2010.

PARK, S. T.; KIM, J. Trends in Next-Generation Sequencing and a New Era for Whole Genome Sequencing. **International Neurourology Journal**, v. 20, n. Suppl 2, p. S76-83, nov. 2016.

PEDROSA, A. et al. Chromosomal map of the model legume Lotus japonicus. **Genetics**, v. 161, n. 4, p. 1661–1672, ago. 2002.

PEDROSA-HARAND, A. et al. Extensive ribosomal DNA amplification during Andean common bean (Phaseolus vulgaris L.) evolution. **Theoretical and Applied Genetics**, v. 112, n. 5, p. 924–933, mar. 2006.

PELLICER, J. et al. Genome Size Diversity and Its Impact on the Evolution of Land Plants. **Genes**, v. 9, n. 2, p. 88, fev. 2018.

PELLICER, J.; LEITCH, I. J. The Plant DNA C-values database (release 7.1): an updated online repository of plant genome size data for comparative studies. **New Phytologist**, v. 226, n. 2, p. 301–305, abr. 2020.

PETTERSSON, M. et al. Cytogenetically visible inversions are formed by multiple molecular mechanisms. **Human Mutation**, v. 41, n. 11, p. 1979–1998, 2020.

PEZER, Ž. et al. Satellite DNA-Mediated Effects on Genome Regulation. Em: GARRIDO-RAMOS, M. A. (Ed.). **Genome Dynamics**. Basel: S. KARGER AG, 2012. v. 7p. 153–169.

PLOHL, M. et al. Satellite DNAs between selfishness and functionality: Structure, genomics and evolution of tandem repeats in centromeric (hetero)chromatin. **Gene**, v. 409, n. 1–2, p. 72–82, fev. 2008.

PLOHL, M.; MEŠTROVIC, N.; MRAVINAC, B. Satellite DNA Evolution. Em: GARRIDO-RAMOS, M. A. (Ed.). **Genome Dynamics**. Basel: S. KARGER AG, 2012. v. 7p. 126–152.

PLOHL, M.; MEŠTROVIĆ, N.; MRAVINAC, B. Centromere identity from the DNA point of view. **Chromosoma**, v. 123, n. 4, p. 313–325, ago. 2014.

PONT, C. et al. Paleogenomics: reconstruction of plant evolutionary trajectories from modern and ancient DNA. **Genome Biology**, v. 20, n. 1, p. 29, 11 fev. 2019.

POWO. "Plants of the World Online. Facilitated by the **Royal Botanic Gardens**, Kew. Published on the Internet; http://www.plantsoftheworldonline.org/
Retrieved 30 September 2022."

PURUGGANAN, M. D. Evolutionary Insights into the Nature of Plant Domestication. **Current Biology**, v. 29, n. 14, p. R705–R714, 22 jul. 2019.

QI, K. et al. Development and characterization of novel Triticum aestivum-Agropyron cristatum 6P Robertsonian translocation lines. **Molecular Breeding**, v. 41, n. 10, p. 59, 16 set. 2021.

QIN, S. et al. A draft genome for Spatholobus suberectus. **Scientific Data**, v. 6, n. 1, p. 113, dez. 2019.

QU, M. et al. Integrated Karyotyping of Woodland Strawberry (***Fragaria vesca***) with Oligopaint FISH Probes. **Cytogenetic and Genome Research**, v. 153, n. 3, p. 158–164, 2017a.

QU, M. et al. Integrated Karyotyping of Woodland Strawberry (Fragaria vesca) with Oligopaint FISH Probes. **Cytogenetic and Genome Research**, v. 153, n. 3, p. 158–164, 2017b.

RAMÍREZ-JIMÉNEZ, A. K. et al. Functional properties and sensory value of snack bars added with common bean flour as a source of bioactive compounds. **LWT**, v. 89, p. 674–680, 1 mar. 2018.

RASKINA, O. et al. Repetitive DNA and chromosomal rearrangements: speciation-related events in plant genomes. **Cytogenetic and Genome Research**, v. 120, n. 3–4, p. 351–357, 2008.

RASKINA, O.; BELYAYEV, A.; NEVO, E. Repetitive DNAs of wild emmer wheat (*Triticum dicoccoides*) and their relation to S-genome species: molecular cytogenetic analysis. **Genome**, v. 45, n. 2, p. 391–401, 1 abr. 2002.

REDDY, A. S. N. et al. Decoding co-/post-transcriptional complexities of plant transcriptomes and epitranscriptome using next-generation sequencing technologies. **Biochemical Society Transactions**, v. 48, n. 6, p. 2399–2414, 16 nov. 2020.

REIS, L. K. et al. Reproductive strategies of the Macroptilium lathyroides (Papilionoideae: Phaseoleae) explain the success of ruderal species in anthropized environments. **Rodriguésia**, v. 72, p. e01782020, 2021.

REN, L.; HUANG, W.; CANNON, S. B. Reconstruction of ancestral genome reveals chromosome evolution history for selected legume species. **New Phytologist**, v. 223, n. 4, p. 2090–2103, set. 2019.

RIBEIRO, T. et al. Centromeric and non-centromeric satellite DNA organisation differs in holocentric Rhynchospora species. **Chromosoma**, v. 126, n. 2, p. 325–335, mar. 2017a.

RIBEIRO, T. et al. Evolutionary dynamics of satellite DNA repeats from Phaseolus beans. **Protoplasma**, v. 254, n. 2, p. 791–801, mar. 2017b.

RIBEIRO, T. et al. Evolutionary dynamics of satellite DNA repeats from Phaseolus beans. **Protoplasma**, v. 254, n. 2, p. 791–801, mar. 2017c.

RIBEIRO, T. et al. Diversity of repetitive sequences within compact genomes of Phaseolus L. beans and allied genera Cajanus L. and Vigna Savi. **Chromosome Research**, v. 28, n. 2, p. 139–153, jun. 2020a.

RIBEIRO, T. et al. Diversity of repetitive sequences within compact genomes of Phaseolus L. beans and allied genera Cajanus L. and Vigna Savi. **Chromosome Research**, v. 28, n. 2, p. 139–153, jun. 2020b.

RICE, A. et al. The Chromosome Counts Database (CCDB) - a community resource of plant chromosome numbers. **New Phytologist**, v. 206, n. 1, p. 19–26, abr. 2015a.

RICE, A. et al. The Chromosome Counts Database (CCDB) – a community resource of plant chromosome numbers. **New Phytologist**, v. 206, n. 1, p. 19–26, abr. 2015b.

ROBBERECHT, C. et al. Nonallelic homologous recombination between retrotransposable elements is a driver of de novo unbalanced translocations. **Genome Research**, v. 23, n. 3, p. 411–418, 3 jan. 2013.

RODIN, S. N.; RIGGS, A. D. Epigenetic Silencing May Aid Evolution by Gene Duplication. **Journal of Molecular Evolution**, v. 56, n. 6, p. 718–729, 1 jun. 2003.

ROSIN, L. F. et al. Oligopaint DNA FISH reveals telomere-based meiotic pairing dynamics in the silkworm, Bombyx mori. **PLOS Genetics**, v. 17, n. 7, p. e1009700, 28 jul. 2021.

RUIZ-RUANO, F. J. et al. High-throughput analysis of the satellitome illuminates satellite DNA evolution. **Scientific Reports**, v. 6, n. 1, p. 28333, set. 2016.

SALINA, E. A. et al. The impact of Ty3-gypsy group LTR retrotransposons Fatima on B-genome specificity of polyploid wheats. **BMC Plant Biology**, v. 11, n. 1, p. 99, 2011.

SANTOS, F. C. et al. Chromosomal distribution and evolution of abundant retrotransposons in plants: gypsy elements in diploid and polyploid Brachiaria forage grasses. **Chromosome Research**, v. 23, n. 3, p. 571–582, set. 2015.

SAX, K. TYPES AND FREQUENCIES OF CHROMOSOMAL ABERRATIONS INDUCED BY X-RAYS. **Cold Spring Harbor Symposia on Quantitative Biology**, v. 9, n. 0, p. 93–103, 1 jan. 1941.

SCHLUETER, J. A. et al. Gene duplication and paleopolyploidy in soybean and the implications for whole genome sequencing. **BMC Genomics**, v. 8, n. 1, p. 330, 2007.

SCHMUTZ, J. et al. Genome sequence of the palaeopolyploid soybean. **Nature**, v. 463, n. 7278, p. 178–183, jan. 2010a.

SCHMUTZ, J. et al. Genome sequence of the palaeopolyploid soybean. **Nature**, v. 463, n. 7278, p. 178–183, jan. 2010b.

SCHMUTZ, J. et al. A reference genome for common bean and genome-wide analysis of dual domestications. **Nature Genetics**, v. 46, n. 7, p. 707–713, jul. 2014a.

SCHMUTZ, J. et al. A reference genome for common bean and genome-wide analysis of dual domestications. **Nature Genetics**, v. 46, n. 7, p. 707–713, jul. 2014b.

SCHNABLE, P. S. et al. The B73 Maize Genome: Complexity, Diversity, and Dynamics. **Science**, v. 326, n. 5956, p. 1112–1115, 20 nov. 2009.

SCHRANZ, M.; LYSAK, M.; MITCHELLOLDS, T. The ABC's of comparative genomics in the Brassicaceae: building blocks of crucifer genomes. **Trends in Plant Science**, v. 11, n. 11, p. 535–542, nov. 2006.

SCHUBERT, I. et al. An efficient screening for terminal deletions and translocations of barley chromosomes added to common wheat: *Deletion screening in barley chromosomes*. **The Plant Journal**, v. 14, n. 4, p. 489–495, maio 1998.

SCHUBERT, I. et al. Chromosome painting in plants. Em: SHARMA, A. K.; SHARMA, A. (Eds.). **Chromosome Painting**. Dordrecht: Springer Netherlands, 2001. p. 57–69.

SCHUBERT, I. Chromosome evolution. **Current Opinion in Plant Biology**, v. 10, n. 2, p. 109–115, abr. 2007.

SCHUBERT, I.; LYSAK, M. A. Interpretation of karyotype evolution should consider chromosome structural constraints. **Trends in Genetics**, v. 27, n. 6, p. 207–216, jun. 2011.

SCHUBERT, I.; WOBUS, U. In situ hybridization confirms jumping nucleolus organizing regions in Allium. **Chromosoma**, v. 92, n. 2, p. 143–148, jun. 1985.

SCOLES, G. J. et al. Frequent duplication and deletion events in the 5S RNA genes and the associated spacer regions of theTriticeae. **Plant Systematics and Evolution**, v. 160, n. 1–2, p. 105–122, 1988.

SCOTT, D.; FOX, M.; FOX, B. W. The relationship between chromosomal aberrations, survival and DNA repair in tumour cell lines of differential sensitivity to X-rays and sulphur mustard. **Mutation Research/Fundamental and Molecular Mechanisms of Mutagenesis**, v. 22, n. 2, p. 207–221, fev. 1974.

SENDEROWICZ, M. et al. Descending Dysploidy and Bidirectional Changes in Genome Size Accompanied Crepis (Asteraceae) Evolution. **Genes**, v. 12, n. 9, p. 1436, set. 2021.

SHAKOORI, A. R.; AFTAB, S.; SHAKOORI, F. R. Numerical Changes in Chromosomes. Em: BHAT, T. A.; WANI, A. A. (Eds.). **Chromosome Structure and Aberrations**. New Delhi: Springer India, 2017. p. 275–306.

SHI, P. et al. Chromosome painting reveals inter-chromosomal rearrangements and evolution of subgenome D of wheat. **The Plant Journal**, v. 112, n. 1, p. 55–67, 2022.

SHIRASAWA, K. et al. Integrated Consensus Map of Cultivated Peanut and Wild Relatives Reveals Structures of the A and B Genomes of Arachis and Divergence of the Legume Genomes. **DNA Research**, v. 20, n. 2, p. 173–184, 1 abr. 2013.

SHIRASAWA, K. et al. A chromosome-scale draft genome sequence of horsegram (Macrotyloma uniflorum). **Gigabyte**, v. 2021, p. 1–23, 8 out. 2021.

SILVA, S. DA C. et al. Chromosome homologies between Citrus and Poncirus—the comparative cytogenetic map of mandarin (Citrus reticulata). **Tree Genetics & Genomes**, v. 11, n. 1, p. 811, fev. 2015.

SILVA, S. DA C. et al. Cytogenetic Map of Pummelo and Chromosome Evolution of True Citrus Species and the Hybrid Sweet Orange. **Journal of Agricultural Science**, v. 11, n. 14, p. 148, 31 ago. 2019.

SINGHI, D. et al. Rhodoccoccus erythropolis Is Different from Other Members of Actinobacteria: Monoploidy, Overlapping Replication Cycle, and Unique Segregation Pattern. **Journal of Bacteriology**, v. 201, n. 24, p. e00320-19, 20 nov. 2019.

SNAK, C.; MIOTTO, S. T. S.; GOLDENBERG, R. Phaseolinae (Leguminosae, Papilionoideae, Phaseoleae) no estado do Paraná, Brasil. **Rodriguésia**, v. 62, n. 3, p. 695–716, set. 2011.

SONG, X. et al. Development and application of oligonucleotide-based chromosome painting for chromosome 4D of Triticum aestivum L. **Chromosome Research**, v. 28, n. 2, p. 171–182, jun. 2020.

SONNHAMMER, E. L. L.; DURBIN, R. A dot-matrix program with dynamic threshold control suited for genomic DNA and protein sequence analysis. **Gene**, v. 167, n. 1–2, p. GC1–GC10, dez. 1995.

SOUZA, R. B. DE L. et al. Dereplication-guided isolation of a new flavonoid triglycoside from Macroptilium martii and its cytotoxicity evaluation. **Phytochemistry Letters**, v. 39, p. 144–150, out. 2020.

STEFANOVIĆ, S. et al. Relationships Among Phaseoloid Legumes Based on Sequences from Eight Chloroplast Regions. **Systematic Botany**, v. 34, n. 1, p. 115–128, 1 mar. 2009.

STORCHOVA, Z.; KUFFER, C. The consequences of tetraploidy and aneuploidy. **Journal of Cell Science**, v. 121, n. 23, p. 3859–3866, 1 dez. 2008.

SZINAY, D. et al. Chromosome evolution in Solanum traced by cross-species BAC-FISH. **New Phytologist**, v. 195, n. 3, p. 688–698, ago. 2012.

TALUKDAR, D. Reciprocal Translocations in Grass Pea (Lathyrus sativus L.): Pattern of Transmission, Detection of Multiple Interchanges and their Independence. **Journal of Heredity**, v. 101, n. 2, p. 169–176, 1 mar. 2010.

TANG, L. et al. Phylogeny and biogeography of the rice tribe (Oryzeae): evidence from combined analysis of 20 chloroplast fragments. **Molecular Phylogenetics and Evolution**, v. 54, n. 1, p. 266–277, jan. 2010.

TESHIMA, K. M.; INNAN, H. Neofunctionalization of Duplicated Genes Under the Pressure of Gene Conversion. **Genetics**, v. 178, n. 3, p. 1385–1398, mar. 2008.

THE BRASSICA RAPA GENOME SEQUENCING PROJECT CONSORTIUM et al. The genome of the mesopolyploid crop species Brassica rapa. **Nature Genetics**, v. 43, n. 10, p. 1035–1039, out. 2011.

THE FRENCH–ITALIAN PUBLIC CONSORTIUM FOR GRAPEVINE GENOME CHARACTERIZATION. The grapevine genome sequence suggests ancestral hexaploidization in major angiosperm phyla. **Nature**, v. 449, n. 7161, p. 463–467, set. 2007.

THE POTATO GENOME SEQUENCING CONSORTIUM. Genome sequence and analysis of the tuber crop potato. **Nature**, v. 475, n. 7355, p. 189–195, jul. 2011.

TOWN, C. D. et al. Comparative Genomics of *Brassica oleracea* and *Arabidopsis thaliana* Reveal Gene Loss, Fragmentation, and Dispersal after Polyploidy. **The Plant Cell**, v. 18, n. 6, p. 1348–1359, jun. 2006.

VAN-LUME, B. et al. Evolutionary convergence or homology? Comparative cytogenomics of Caesalpinia group species (Leguminosae) reveals diversification in the pericentromeric heterochromatic composition. **Planta**, v. 250, n. 6, p. 2173–2186, dez. 2019.

VANNESTE, K. et al. Analysis of 41 plant genomes supports a wave of successful genome duplications in association with the Cretaceous–Paleogene boundary. **Genome Research**, v. 24, n. 8, p. 1334–1347, 8 jan. 2014.

VANZELA, A. L. L.; LUCEÑO, M.; GUERRA, M. Karyotype evolution and cytotaxonomy in Brazilian species of Rhynchospora Vahl (Cyperaceae). **Botanical Journal of the Linnean Society**, v. 134, n. 4, p. 557–566, dez. 2000.

VARSHNEY, R. K. et al. Draft genome sequence of pigeonpea (Cajanus cajan), an orphan legume crop of resource-poor farmers. **Nature Biotechnology**, v. 30, n. 1, p. 83–89, jan. 2012.

VASCONCELOS, E. V. et al. Intra- and interchromosomal rearrangements between cowpea [Vigna unguiculata (L.) Walp.] and common bean (Phaseolus vulgaris L.) revealed by BAC-FISH. **Chromosome Research**, v. 23, n. 2, p. 253–266, jun. 2015.

VERDCOURT, B. Studies in the Leguminosae-Papilionoideae for the "Flora of Tropical East Africa": II. **Kew Bulletin**, v. 24, n. 2, p. 235, 1970.

VERMA, R. C.; PURBIYA, R.; KHAH, M. A. Gamma Irradiation Induced Reciprocal Translocation in Pea (*Pisum sativum* L.). **Chromosome Botany**, v. 13, n. 2, p. 71–74, 2019.

VITALES, D. et al. Third release of the plant rDNA database with updated content and information on telomere composition and sequenced plant genomes. **Plant Systematics and Evolution**, v. 303, n. 8, p. 1115–1121, out. 2017.

VITALES, D.; GARCIA, S.; DODSWORTH, S. Reconstructing phylogenetic relationships based on repeat sequence similarities. **Molecular Phylogenetics and Evolution**, v. 147, p. 106766, jun. 2020.

WALDEN, N. et al. Genomic Blocks in Aethionema arabicum Support Arabideae as Next Diverging Clade in Brassicaceae. **Frontiers in Plant Science**, v. 11, p. 719, 3 jun. 2020.

WANG, J. et al. Hierarchically Aligning 10 Legume Genomes Establishes a Family-Level Genomics Platform. **Plant Physiology**, v. 174, n. 1, p. 284–300, maio 2017.

WANG, W. et al. A transposon-mediated reciprocal translocation promotes environmental adaptation but compromises domesticability of wild soybeans. **New Phytologist**, v. 232, n. 4, p. 1765–1777, 2021.

WANG, Z.-H. et al. Reshuffling of the ancestral core-eudicot genome shaped chromatin topology and epigenetic modification in Panax. **Nature Communications**, v. 13, n. 1, p. 1902, dez. 2022.

WATANABE, K. et al. Chromosomal Evolution in the Genus Brachyscome (Asteraceae, Astereae): Statistical Tests Regarding Correlation Between Changes in Karyotype and Habit Using Phylogenetic Information. **Journal of Plant Research**, v. 112, n. 2, p. 145–161, jun. 1999.

WELLENREUTHER, M.; BERNATCHEZ, L. Eco-Evolutionary Genomics of Chromosomal Inversions. **Trends in Ecology & Evolution**, v. 33, n. 6, p. 427–440, 1 jun. 2018.

WICKER, T. et al. A unified classification system for eukaryotic transposable elements. **Nature Reviews Genetics**, v. 8, n. 12, p. 973–982, dez. 2007.

WOLF, J. B. W.; LINDELL, J.; BACKSTRÖM, N. Speciation genetics: current status and evolving approaches. **Philosophical Transactions of the Royal Society B: Biological Sciences**, v. 365, n. 1547, p. 1717–1733, 12 jun. 2010.

WU, S.; HAN, B.; JIAO, Y. Genetic Contribution of Paleopolyploidy to Adaptive Evolution in Angiosperms. **Molecular Plant**, v. 13, n. 1, p. 59–71, 6 jan. 2020.

YANG, K. et al. Genome sequencing of adzuki bean (*Vigna angularis*) provides insight into high starch and low fat accumulation and domestication. **Proceedings of the National Academy of Sciences**, v. 112, n. 43, p. 13213–13218, 27 out. 2015.

YOGEESWARAN, K. et al. Comparative genome analyses of Arabidopsis spp.: inferring chromosomal rearrangement events in the evolutionary history of A. thaliana. **Genome research**, v. 15, n. 4, p. 505–515, 2005.

ZHANG, K.; WANG, X.; CHENG, F. Plant Polyploidy: Origin, Evolution, and Its Influence on Crop Domestication. **Horticultural Plant Journal**, Advance of Horticultural Plant Genomes. v. 5, n. 6, p. 231–239, 1 nov. 2019.

ZHANG, P. et al. Simultaneous painting of three genomes in hexaploid wheat by BAC-FISH. **Genome**, v. 47, n. 5, p. 979–987, 1 out. 2004.

ZHANG, T. et al. Chorus2: design of genome-scale oligonucleotide-based probes for fluorescence in situ hybridization. **Plant Biotechnology Journal**, v. 19, n. 10, p. 1967–1978, 2021.

ZHAO, W. et al. Development and characterization of two new Triticum aestivum–Dasypyrum villosum Robertsonian translocation lines T1DS·1V#3L and T1DL·1V#3S and their effect on grain quality. **Euphytica**, v. 175, n. 3, p. 343–350, out. 2010.

ZUO (左胜), S. et al. Genome diploidization associates with cladogenesis, trait disparity, and plastid gene evolution. **Plant Physiology**, v. 190, n. 1, p. 403–420, 1 set. 2022.

5.2 REFERÊNCIAS DO ARTIGO 1

Bertioli DJ, Moretzsohn MC, Madsen LH, et al (2009) An analysis of synteny of *Arachis* with *Lotus* and *Medicago* sheds new light on the structure, stability and evolution of legume genomes. BMC Genomics 10:45. https://doi.org/10.1186/1471-2164-10-45

Bonifácio EM, Fonsêca A, Almeida C, et al (2012) Comparative cytogenetic mapping between the lima bean (*Phaseolus lunatus* L.) and the common bean (*P. vulgaris* L.). Theor Appl Genet 124:1513–1520. https://doi.org/10.1007/s00122-012-1806-x

Carvalho CR, Saraiva LS (1993) An Air Drying Technique for Maize Chromosomes without Enzymatic Maceration. Biotechnic & Histochemistry 68:142–145. https://doi.org/10.3109/10520299309104684

Chen F, Dong W, Zhang J, et al (2018) The Sequenced Angiosperm Genomes and Genome Databases. Front Plant Sci 9:418. https://doi.org/10.3389/fpls.2018.00418

Cheng C, Chen J (2022) Cyto-Molecular Genetics of the Interspecific Hybridization in Cucumber. In: Pandey S, Weng Y, Behera TK, Bo K (eds) The Cucumber Genome. Springer International Publishing, Cham, pp 121–144. https://doi.org/10.1007/978-3-030-88647-9_10

Cheng F, Wu J, Wang X (2014) Genome triplication drove the diversification of *Brassica* plants. Horticulture Research 1:1–8. https://doi.org/10.1038/hortres.2014.24

de Oliveira Bustamante F, do Nascimento TH, Montenegro C, et al (2021) Oligo-FISH barcode in beans: a new chromosome identification system. Theor Appl Genet 134:3675–3686. https://doi.org/10.1007/s00122-021-03921-z

Ferraz ME, Fonsêca A, Pedrosa-Harand A (2020) Multiple and independent rearrangements revealed by comparative cytogenetic mapping in the dysploid Leptostachyus group (*Phaseolus* L., Leguminosae). Chromosome Res. https://doi.org/10.1007/s10577-020-09644-z

Fonsêca A, Ferraz ME, Pedrosa-Harand A (2016) Speeding up chromosome evolution in *Phaseolus*: multiple rearrangements associated with a one-step descending dysploidy. Chromosoma 125:413–421. https://doi.org/10.1007/s00412-015-0548-3

Fonsêca A, Pedrosa-Harand A (2013) Karyotype stability in the genus *Phaseolus* evidenced by the comparative mapping of the wild species *Phaseolus microcarpus*. 56:9. https://doi.org/10.1139/gen-2013-0025

Garcia T, Duitama J, Zullo SS, et al (2021) Comprehensive genomic resources related to domestication and crop improvement traits in Lima bean. Nature Communications 12:702. https://doi.org/10.1038/s41467-021-20921-1

Geiser C, Mandáková T, Arrigo N, et al (2016) Repeated Whole-Genome Duplication, Karyotype Reshuffling, and Biased Retention of Stress-Responding Genes in Buckler Mustard. The Plant Cell 28:17–27. https://doi.org/10.1105/tpc.15.00791

Gong Z, Wu Y, Koblízková A, et al (2012) Repeatless and repeat-based centromeres in potato: implications for centromere evolution. Plant Cell 24:3559–3574. https://doi.org/10.1105/tpc.112.100511

Han Y, Zhang T, Thammapichai P, et al (2015) Chromosome-Specific Painting in *Cucumis* Species Using Bulked Oligonucleotides. Genetics 200:771–779. https://doi.org/10.1534/genetics.115.177642

Ho WK, Chai HH, Kendabie P, et al (2017) Integrating genetic maps in bambara groundnut [*Vigna subterranea* (L) Verdc.] and their syntenic relationships among closely related legumes. BMC Genomics 18:192. https://doi.org/10.1186/s12864-016-3393-8

Hu Q, Ma Y, Mandáková T, et al (2021a) Genome evolution of the psammophyte *Pugionium* for desert adaptation and further speciation. Proc Natl Acad Sci USA 118:e2025711118. https://doi.org/10.1073/pnas.2025711118

Hu T, Chitnis N, Monos D, Dinh A (2021b) Next-generation sequencing technologies: An overview. Human Immunology 82:801–811. https://doi.org/10.1016/j.humimm.2021.02.012

Hufnagel B, Marques A, Soriano A, et al (2020) High-quality genome sequence of white lupin provides insight into soil exploration and seed quality. Nat Commun 11:492. https://doi.org/10.1038/s41467-019-14197-9

Iwata A, Tek AL, Richard MMS, et al (2013) Identification and characterization of functional centromeres of the common bean. Plant J 76:47-60. https://doi.org/10.1111/tpj.12269

Iwata-Otsubo A, Lin J-Y, Gill N, Jackson SA (2016) Highly distinct chromosomal structures in cowpea (*Vigna unguiculata*), as revealed by molecular cytogenetic analysis. Chromosome Res 24:197–216. https://doi.org/10.1007/s10577-015-9515-3

Jiao Y, Wickett NJ, Ayyampalayam S, et al (2011) Ancestral polyploidy in seed plants and angiosperms. Nature 473:97–100. https://doi.org/10.1038/nature09916

Kamphuis LG, Williams AH, D'Souza NK, et al (2007) The *Medicago truncatula* reference accession A17 has an aberrant chromosomal configuration. New Phytologist 174:299–303. https://doi.org/10.1111/j.1469-8137.2007.02039.x

Kreplak J, Madoui M-A, Cápal P, et al (2019) A reference genome for pea provides insight into legume genome evolution. Nature Genetics 51:1411–1422. https://doi.org/10.1038/s41588-019-0480-1

Li C, Lin F, An D, et al (2018) Genome Sequencing and Assembly by Long Reads in Plants. Genes 9:6. https://doi.org/10.3390/genes9010006

Li H, Wang W, Lin L, et al (2013) Diversification of the phaseoloid legumes: effects of climate change, range expansion and habit shift. Frontiers in Plant Science 4:386. https://doi.org/10.3389/fpls.2013.00386

Liao Y, Zhang X, Li B, et al (2018) Comparison of *Oryza sativa* and *Oryza brachyantha* Genomes Reveals Selection-Driven Gene Escape from the Centromeric Regions. Plant Cell 30:1729–1744. https://doi.org/10.1105/tpc.18.00163

Liu Y, Su H, Pang J, et al (2015) Sequential de novo centromere formation and inactivation on a chromosomal fragment in maize. Proc Natl Acad Sci USA 112:. https://doi.org/10.1073/pnas.1418248112

Liu Y, Su H, Zhang J, et al (2020a) Rapid Birth or Death of Centromeres on Fragmented Chromosomes in Maize. Plant Cell 32:3113–3123. https://doi.org/10.1105/tpc.20.00389

Liu Y, Zhang X, Han K, et al (2020a) Insights into amphicarpy from the compact genome of the legume *Amphicarpaea edgeworthii*. Plant Biotechnol J pbi.13520. https://doi.org/10.1111/pbi.13520

Liu Y, Zhang X, Han K, et al (2020b) Insights into amphicarpy from the compact genome of the legume *Amphicarpaea edgeworthii*. Plant Biotechnol J pbi.13520. https://doi.org/10.1111/pbi.13520

Lonardi S, Muñoz-Amatriaín M, Liang Q, et al (2019) The genome of cowpea (*Vigna unguiculata* [L.] Walp.). Plant J 98:767–782. https://doi.org/10.1111/tpj.14349

Lyons E, Pedersen B, Kane J, et al (2008) Finding and Comparing Syntenic Regions among *Arabidopsis* and the Outgroups Papaya, Poplar, and Grape: CoGe with Rosids. Plant Physiol 148:1772–1781. https://doi.org/10.1104/pp.108.124867

Lysak MA (2014) Live and let die: centromere loss during evolution of plant chromosomes. New Phytol 203:1082–1089. https://doi.org/10.1111/nph.12885

Lysak MA, Berr A, Pecinka A, et al (2006) Mechanisms of chromosome number reduction in *Arabidopsis thaliana* and related Brassicaceae species. Proceedings of the National Academy of Sciences 103:5224–5229. https://doi.org/10.1073/pnas.0510791103

Lysak MA, Fransz PF, Ali HBM, Schubert I (2002) Chromosome painting in *Arabidopsis thaliana*: Chromosome painting in Arabidopsis. The Plant Journal 28:689–697. https://doi.org/10.1046/j.1365-313x.2001.01194.x

Lysak MA, Mandáková T, Schranz ME (2016) Comparative paleogenomics of crucifers: ancestral genomic blocks revisited. Current Opinion in Plant Biology 30:108–115. https://doi.org/10.1016/j.pbi.2016.02.001

Mandáková T, Hloušková P, Koch MA, Lysak MA (2020) Genome Evolution in Arabideae Was Marked by Frequent Centromere Repositioning. Plant Cell 32:650–665. https://doi.org/10.1105/tpc.19.00557

Mandáková T, Lysak MA (2018) Post-polyploid diploidization and diversification through dysploid changes. Current Opinion in Plant Biology 42:55–65. https://doi.org/10.1016/j.pbi.2018.03.001

Mandáková T, Pouch M, Brock JR, et al (2019) Origin and Evolution of Diploid and Allopolyploid *Camelina* Genomes was Accompanied by Chromosome Shattering. Plant Cell tpc.00366.2019. https://doi.org/10.1105/tpc.19.00366

Martins L do V, de Oliveira Bustamante F, da Silva Oliveira AR, et al (2021) BAC- and oligo-FISH mapping reveals chromosome evolution among *Vigna angularis*, *V. unguiculata*, and *Phaseolus vulgaris*. Chromosoma. https://doi.org/10.1007/s00412-021-00758-9

McConnell M, Mamidi S, Lee R, et al (2010) Syntenic relationships among legumes revealed using a gene-based genetic linkage map of common bean (*Phaseolus vulgaris* L.). Theor Appl Genet 121:1103–1116. https://doi.org/10.1007/s00122-010-1375-9

Murat F, Armero A, Pont C, et al (2017) Reconstructing the genome of the most recent common ancestor of flowering plants. Nature Genetics 49:490–496. https://doi.org/10.1038/ng.3813

Murat F, Xu J-H, Tannier E, et al (2010) Ancestral grass karyotype reconstruction unravels new mechanisms of genome shuffling as a source of plant evolution. Genome Res 20:1545–1557. https://doi.org/10.1101/gr.109744.110

Oliveira AR da S, Martins L do V, Bustamante F de O, et al (2020) Breaks of macrosynteny and collinearity among moth bean (*Vigna aconitifolia*), cowpea (*V. unguiculata*), and common bean (*Phaseolus vulgaris*). Chromosome Res. https://doi.org/10.1007/s10577-020-09635-0

Parkin IA, Koh C, Tang H, et al (2014) Transcriptome and methylome profiling reveals relics of genome dominance in the mesopolyploid Brassica oleracea. Genome Biol 15:R77. https://doi.org/10.1186/gb-2014-15-6-r77

Pavy N, Pelgas B, Laroche J, et al (2012) A spruce gene map infers ancient plant genome reshuffling and subsequent slow evolution in the gymnosperm lineage leading to extant conifers. BMC Biology 10:84. https://doi.org/10.1186/1741-7007-10-84

Pecrix Y, Staton SE, Sallet E, et al (2018) Whole-genome landscape of *Medicago truncatula* symbiotic genes. Nature Plants 4:1017–1025. https://doi.org/10.1038/s41477-018-0286-7

Pellicer J, Hidalgo O, Dodsworth S, Leitch IJ (2018) Genome Size Diversity and Its Impact on the Evolution of Land Plants. Genes 9:88. https://doi.org/10.3390/genes9020088

Qin S, Wu L, Wei K, et al (2019) A draft genome for *Spatholobus suberectus*. Sci Data 6:113. https://doi.org/10.1038/s41597-019-0110-x

Ren L, Huang W, Cannon SB (2019) Reconstruction of ancestral genome reveals chromosome evolution history for selected legume species. New Phytol 223:2090–2103. https://doi.org/10.1111/nph.15770

Ribeiro T, Dos Santos KGB, Richard MMS, et al (2017) Evolutionary dynamics of satellite DNA repeats from *Phaseolus* beans. Protoplasma 254:791–801. https://doi.org/10.1007/s00709-016-0993-8

Ribeiro T, Vasconcelos E, dos Santos KGB, et al (2020) Diversity of repetitive sequences within compact genomes of *Phaseolus* L. beans and allied genera *Cajanus* L. and *Vigna* Savi. Chromosome Res 28:139–153. https://doi.org/10.1007/s10577-019-09618-w

Rice A, Glick L, Abadi S, et al (2015) The Chromosome Counts Database (CCDB) – a community resource of plant chromosome numbers. New Phytol 206:19–26. https://doi.org/10.1111/nph.13191

Ruprecht C, Lohaus R, Vanneste K, et al (2017) Revisiting ancestral polyploidy in plants. Science Advances 3:e1603195. https://doi.org/10.1126/sciadv.1603195

Schmutz J, Cannon SB, Schlueter J, et al (2010) Genome sequence of the palaeopolyploid soybean. Nature 463:178–183. https://doi.org/10.1038/nature08670

Schmutz J, McClean PE, Mamidi S, et al (2014a) A reference genome for common bean and genome-wide analysis of dual domestications. Nat Genet 46:707–713. https://doi.org/10.1038/ng.3008

Schmutz J, McClean PE, Mamidi S, et al (2014b) A reference genome for common bean and genome-wide analysis of dual domestications. Nat Genet 46:707–713. https://doi.org/10.1038/ng.3008

Schneider KL, Xie Z, Wolfgruber TK, Presting GG (2016) Inbreeding drives maize centromere evolution. Proc Natl Acad Sci USA 113:E987–E996. https://doi.org/10.1073/pnas.1522008113

Schranz M, Lysak M, Mitchellolds T (2006) The ABC's of comparative genomics in the Brassicaceae: building blocks of crucifer genomes. Trends in Plant Science 11:535–542. https://doi.org/10.1016/j.tplants.2006.09.002

Schubert I, Lysak MA (2011). Interpretation of karyotype evolution should consider chromosome structural constraints. Trends in Genetics 27: 207-216. https://doi.org/10.1016/j.tig.2011.03.004

Schubert I (2018) What is behind "centromere repositioning"? Chromosoma 127:229–234. https://doi.org/10.1007/s00412-018-0672-y

Soltis PS, Marchant DB, Van de Peer Y, Soltis DE (2015) Polyploidy and genome evolution in plants. Current Opinion in Genetics & Development 35:119–125. https://doi.org/10.1016/j.gde.2015.11.003

Song X, Sun P, Yuan J, et al (2021) The celery genome sequence reveals sequential paleo-polyploidizations, karyotype evolution and resistance gene reduction in apiales. Plant Biotechnology Journal 19:731–744. https://doi.org/10.1111/pbi.13499

Talbert PB, Henikoff S (2020) What makes a centromere? Experimental Cell Research 389:111895. https://doi.org/10.1016/j.yexcr.2020.111895

The Arabidopsis Genome Initiative (2000) Analysis of the genome sequence of the flowering plant *Arabidopsis thaliana*. Nature 408:796–815. https://doi.org/10.1038/35048692

Vasconcelos EV, de Andrade Fonsêca AF, Pedrosa-Harand A, et al (2015a) Intra- and interchromosomal rearrangements between cowpea [*Vigna unguiculata* (L.) Walp.] and common bean (*Phaseolus vulgaris* L.) revealed by BAC-FISH. Chromosome Res 23:253–266. https://doi.org/10.1007/s10577-014-9464-2

Walden N, Nguyen T-P, Mandáková T, et al (2020) Genomic Blocks in *Aethionema arabicum* Support Arabideae as Next Diverging Clade in Brassicaceae. Front Plant Sci 11:719. https://doi.org/10.3389/fpls.2020.00719

Wang J, Sun P, Li Y, et al (2017) Hierarchically Aligning 10 Legume Genomes Establishes a Family-Level Genomics Platform. Plant Physiol 174:284–300. https://doi.org/10.1104/pp.16.01981

Wang J, Zi H, Wang R, et al (2021a) A high-quality chromosome-scale assembly of the centipedegrass [*Eremochloa ophiuroides* (Munro) Hack.] genome provides insights into chromosomal structural evolution and prostrate growth habit. Hortic Res 8:1–13. https://doi.org/10.1038/s41438-021-00636-6

Wang S, Xiao Y, Zhou Z-W, et al (2021b) High-quality reference genome sequences of two coconut cultivars provide insights into evolution of monocot chromosomes and differentiation of fiber content and plant height. Genome Biol 22:304. https://doi.org/10.1186/s13059-021-02522-9

Wang X, Jin D, Wang Z, et al (2015) Telomere-centric genome repatterning determines recurring chromosome number reductions during the evolution of eukaryotes. New Phytol 205:378–389. https://doi.org/10.1111/nph.12985

Wendel JF, Jackson SA, Meyers BC, Wing RA (2016) Evolution of plant genome architecture. Genome Biology 17:37. https://doi.org/10.1186/s13059-016-0908-1

Willing E-M, Rawat V, Mandáková T, et al (2015) Genome expansion of *Arabis alpina* linked with retrotransposition and reduced symmetric DNA methylation. Nature Plants 1:14023. https://doi.org/10.1038/nplants.2014.23

Wu S, Han B, Jiao Y (2020) Genetic Contribution of Paleopolyploidy to Adaptive Evolution in Angiosperms. Molecular Plant 13:59–71. https://doi.org/10.1016/j.molp.2019.10.012

Xie D, Xu Y, Wang J, et al (2019) The wax gourd genomes offer insights into the genetic diversity and ancestral cucurbit karyotype. Nature Communications 10:5158. https://doi.org/10.1038/s41467-019-13185-3

Yang L, Koo D-H, Li D, et al (2014) Next-generation sequencing, FISH mapping and synteny-based modeling reveal mechanisms of decreasing dysploidy in *Cucumis*. Plant J 77:16–30. https://doi.org/10.1111/tpj.12355

Yang L, Sagar V (2022) Genome Evaluation of Cucumber in Relation to Cucurbit Family. In: Pandey S, Weng Y, Behera TK, Bo K (eds) The Cucumber Genome. Springer International Publishing, Cham, pp 105–119. https://doi.org/10.1007/978-3-030-88647-9_9

Zhang H, Koblížková A, Wang K, et al (2014) Boom-Bust Turnovers of Megabase-Sized Centromeric DNA in *Solanum* Species: Rapid Evolution of DNA Sequences Associated with Centromeres. The Plant Cell 26:1436–1447. https://doi.org/10.1105/tpc.114.123877

Zhang H, Zhang Y, Xu W, et al (2022) Development and performance evaluation of whole-genome sequencing with paired-end and mate-pair strategies in molecular characterization of GM crops: One GM rice 114-7-2 line as an example. Food Chemistry: Molecular Sciences 4:100061. https://doi.org/10.1016/j.fochms.2021.100061

Zhang S-J, Liu L, Yang R, Wang X (2020) Genome Size Evolution Mediated by Gypsy Retrotransposons in Brassicaceae. Genomics, Proteomics & Bioinformatics 18:321–332. https://doi.org/10.1016/j.gpb.2018.07.009

Zhao H, Zeng Z, Koo D-H, et al (2017) Recurrent establishment of de novo centromeres in the pericentromeric region of maize chromosome 3. Chromosome Res 25:299–311. https://doi.org/10.1007/s10577-017-9564-x

Zhao Q, Meng Y, Wang P, et al (2021a) Reconstruction of ancestral karyotype illuminates chromosome evolution in the genus *Cucumis*. The Plant Journal. https://doi.org/10.1111/tpj.15381

Zhao Y, Zhang R, Jiang K W, et al (2021b). Nuclear phylotranscriptomics and phylogenomics support numerous polyploidization events and hypotheses for the evolution of rhizobial nitrogen-fixing symbiosis in Fabaceae. Molecular plant, 14(5): 748-773. https://doi.org/10.1016/j.molp.2021.02.006

Zhuang W, Chen H, Yang M, et al (2019) The genome of cultivated peanut provides insight into legume karyotypes, polyploid evolution and crop domestication. Nat Genet 51:865–876. https://doi.org/10.1038/s41588-019-0402-2

APÊNDICE

APÊNDICE A – Comparative cytogenomics reveals genome reshuffling and centromere repositioning in the legume tribe Phaseoleae

Claudio Montenegro[1], Lívia do Vale Martins[2,3], Fernanda de Oliveira Bustamante[4], Ana Christina Brasileiro-Vidal[2], Andrea Pedrosa-Harand[1]✉

Publicado na Chromosome Res. 2022 Jun 18. doi: 10.1007/s10577-022-09702-8

[1]Laboratory of Plant Cytogenetics and Evolution, Department of Botany, Federal University of Pernambuco, Recife, PE, Brazil.

[2]Laboratory of Plant Genetics and Biotechnology, Department of Genetics, Federal University of Pernambuco, Recife, PE, Brazil.

[3]Department of Biology, Federal University of Piauí, Teresina, PI, Brazil

[4]Minas Gerais State University, Divinópolis Unity, Divinópolis, MG, Brazil.

Claudio Montenegro - ORCID: 0000-0003-2089-1608

Lívia do Vale Martins - ORCID: 0000-0003-4645-9055

Fernanda de Oliveira Bustamante - ORCID: 0000-0002-2826-5217

Ana Christina Brasileiro-Vidal - ORCID: 0000-0002-9704-5509

Andrea Pedrosa-Harand - ORCID: 0000-0001-5213-4770

✉ For correspondence (e-mail: andrea.harand@ufpe.br)

Andrea Pedrosa-Harand

Laboratório de Citogenética e Evolução Vegetal, Departamento de Botânica, Universidade Federal de Pernambuco – UFPE

R. Prof. Moraes Rego, s/n, CDU, 50670-420, Recife, PE, Brazil

Tel. number: + 55 81 2126 8846

Fax number: + 55 81 2126 8358

E-mail: andrea.harand@ufpe.br

ABSTRACT

The tribe Phaseoleae includes several legume crops with assembled genomes. Comparative genomic studies have evidenced the preservation of large genomic blocks among legumes, although chromosome dynamics during Phaseoleae evolution has not been investigated. We conducted a comparative genomic analysis to define an informative genomic block (GB) system and to reconstruct the ancestral Phaseoleae karyotype (APK). We identified GBs based on the orthologous genes between *Phaseolus vulgaris* and *Vigna unguiculata*, and searched for GBs in different genomes of the Phaseolinae (*P. lunatus*) and Glycininae (*Amphicarpaea edgeworthii*) subtribes, and *Spatholobus suberectus* (sister to Phaseolinae and Glycininae), using *Medicago truncaluta* as the outgroup. We also used oligo-FISH probes of two *P. vulgaris* chromosomes to paint the orthologous chromosomes of two non-sequenced Phaseolinae species. We inferred the APK as having $n = 11$ and 19 GBs (A to S), hypothesizing five chromosome fusions that reduced the ancestral legume karyotype to $n = 11$. We identified the rearrangements among the APK and the subtribes and species, with extensive centromere repositioning in *Phaseolus*. We also reconstructed the chromosome number reduction in *S. suberectus*. The development of the GB system and the proposed APK provide useful approaches for future comparative genomic analyses of legume species.

Keywords: Ancestral Karyotype; Centromere repositioning; Comparative genomics; Dysploidy; Genomic Blocks; Phaseoleae; Oligo-FISH.

DECLARATIONS

Funding

This work was supported by CAPES (Coordenação de Pessoal de Nível Superior, Finance Code 001), CNPq (Conselho Nacional de Desenvolvimento Científico e Tecnológico, grants no. 310804/2017-5 and no. 313944/2020-2), and FACEPE (Fundação de Amparo à Ciência e Tecnologia do Estado de Pernambuco, grants no. IBPG-1520-2.03/18 and APQ-0409-2.02/16).

Conflicts of interest/Competing interest

The authors declare no conflicts of interest.

Availability of data and material

All data generated or analyzed during this study are included as supplementary materials.

Code Availability

Not applicable

Author's contributions

C.M.: conducted the genome comparisons, defined the blocks, performed the oligo-FISH painting experiments with *M. atropurpureum* and *L. purpureus*, constructed the images, and wrote the original draft of the manuscript. L.V.M: synthesized the oligo painting probes, performed the oligo-FISH in *P. vulgaris* and *V. unguiculata,* constructed the oligo-FISH images and helped write the manuscript. F.O.B: provided the resources for this research and discussed the data. A.C.B.V: co-supervised the experiments and contributed to the data analyses and discussion. A.P.H: conceptualized and supervised the experiments and provided resources for this research. All authors reviewed the manuscript.

Ethical approval

Not applicable

Consent to participate

Not applicable

Consented for publication

Not applicable

Key message

We developed a useful genomic block system and proposed the Ancestral Phaseoleae Karyotype based on available genome assemblies of legume crops. These tools enabled the reconstruction of the main chromosomal rearrangements responsible for genome reshuffling among the diploid taxa investigated. The analyses revealed centromere repositioning in all chromosomes within the tribe, despite the chromosome number conservation.

Acknowledgments

We thank Embrapa Meio-Norte (Teresina, Piauí, Brazil), Embrapa Cenargen (Brasília, Distrito Federal, Brazil), CIAT (International Center for Tropical Agriculture), and Prof. Marcelo Guerra (UFPE) for providing the *V. unguiculata*, *P. vulgaris*, *M. atropurpureum* and *L. purpureus* seeds respectively. We thank Ingo Schubert (IPK) and André Marques (MPIPZ) for the early critical review of the manuscript. We also thank CAPES (Coordenação de Pessoal de Nível Superior, Finance Code 001), CNPq (Conselho Nacional de Desenvolvimento Científico e Tecnológico), and FACEPE (Fundação de Amparo à Ciência e Tecnologia do Estado de Pernambuco) for their financial support.

Abbreviations:

8HQ: 8-hydroxyquinoline

ACK: Ancestral Crucifer Karyotype

Ae: *Amphicarpaea edgeworthii* chromosome

ALK: Ancestral Legume Karyotype

APhsK: Ancestral *Phaseolus* Karyotype

APK: Ancestral Phaseoleae Karyotype

APnK: Ancestral Phaseolinae Karyotype

BACs: Bacterial Artificial Chromosomes

DAPI: 4,6-Diamidino-2-phenylindole

DSB: Double Strand Break

FISH: Fluorescence *in situ* Hybridization

GB: Genomic Blocks

LCT: Legume-Common Tetraploidization

Lp: *Lablab purpureus* chromosome

LTR: Long Terminal Repeats

Ma: *Macroptilium atropurpureum* chromosome

Mt: *Medicago truncatula* chromosome

Mya: Million Years Ago

Oligo: Oligonucleotide

Pl: *Phaseolus lunatus* chromosome

Pv: *Phaseolus vulgaris* chromosome

satDNA: Satellite DNA

Ss: *Spatholobus suberectus* chromosome

Vu: *Vigna unguiculata* chromosome

WGD: Whole Genome Duplication

WGT: Whole Genome Triplication

INTRODUCTION

Genome sequencing technologies have greatly improved, and have became more accessible since the first plant genome sequencing and assembly efforts (The Arabidopsis Genome Initiative 2000), increasing the genomic data available for economically and evolutionarily important plant species (Li et al. 2018; Chen et al. 2018; Hu et al. 2021b; Zhang et al. 2022). Genome sequencing is essential for functional and comparative genomics, and plays a fundamental role in understanding plant biology and chromosomal evolutionary dynamics, such as genome reshuffling (Pavy et al. 2012; Cheng et al. 2014; Wang et al. 2021a), genome size variations (Wendel et al. 2016; Pellicer et al. 2018; Kreplak et al. 2019; Zhang et al. 2020), polyploidy (Jiao et al. 2011; Soltis et al. 2015; Geiser et al. 2016; Ruprecht et al. 2017; Wu et al. 2020; Hu et al. 2021a), dysploidy (Lysak et al. 2006; Yang et al. 2014; Mandáková and Lysak 2018; Zhao et al. 2021a), hybridization (Cheng and Chen 2022), and other mechanisms of genome and species diversification.

Cytogenomic comparisons of related species provide important evolutionary insights. In Brassicaceae, for instance, chromosome painting based on *A. thaliana* BACs (Bacterial Artificial Chromosomes) as FISH (Fluorescent *in situ* Hybridization) probes (Lysak et al. 2001), together with a genomic block system (Schranz et al. 2006), were used to elucidate karyotype evolution within the family. Those studies allowed the inference of the ancestral crucifer karyotype (ACK), revealing chromosomal rearrangements related to the decreasing dysploidy seen in *A. thaliana* (Lysak et al. 2006), chromosomal reshuffling after whole genome triplication (WGT) as seen in *Brassica* species (Cheng et al. 2014), and centromere repositioning (i.e., centromere position changes without collinearity breaks) across the family (Willing et al. 2015; Lysak et al. 2016; Mandáková et al. 2020). In *Cucumis* L., genomic blocks, combined with FISH maps, have revealed genome reshuffling mechanisms, centromere repositioning, and decreasing dysploidy in cucumbers (*C. sativus* L.) using the ancestral karyotype as a reference (Yang et al. 2014; Zhao et al. 2021a; Yang and Sagar 2022). Similar ancestral karyotype reconstructions and phylogenomic studies were performed in *Apium* L.(Song et al. 2021), *Camelina* Crantz (Mandáková et al. 2019), and *Cocos* L. (Wang et al. 2021b). Those efforts, however, required genome assemblies at the chromosomal level and/or chromosome painting probes designed to detect unique sequences and specific chromosome pairs that are still not available for most plant groups.

Leguminosae L. (Fabaceae Lindl.) is one of the largest families of flowering plants. The Papilionoideae subfamily has many economically important members with assembled genomes, as seen in the polyploids peanut ($2n = 4x = 40$, *Arachis hypogaea* L.), soybean ($2n = 4x = 40$, *Glycine max* L.), and white lupin ($2n = 6x = 50$, *Lupinus albus* L.), and the diploids common bean ($2n = 2x = 22$, *Phaseolus vulgaris* L.), cowpea [$2n = 2x = 22$, *Vigna unguiculata* (L.) Walp.], and barrel medic ($2n = 2x = 16$, *Medicago*

truncatula Gaertn) (Schmutz et al. 2010, 2014; Pecrix et al. 2018; Zhuang et al. 2019; Lonardi et al. 2019; Hufnagel et al. 2020). Comparative genomics revealed a legume-common tetraploidization (LCT) approximately 60 million years ago (Mya), with independent polyploidization events in the *Arachis* (~0.4 Mya), *Glycine* (~ 12 Mya), and *Lupinus* clades (~ 20 Mya) (Schmutz et al. 2010; Wang et al. 2017; Kreplak et al. 2019; Hufnagel et al. 2020). Additionally, high levels of synteny with large conserved genomic blocks were identified among those genomes (Wang et al. 2017), enabling the reconstruction of ancestral legume karyotypes (ALK), ranging from n = 9 (Ren et al. 2019) to n = 25 (Kreplak et al. 2019), although n = 16 appears more consistent for the ALK (Zhuang et al. 2019; Hufnagel et al. 2020). Most of these analyses used orthologous genes from *P. vulgaris* to detect shared genomic blocks (GBs) among those legumes, suggesting conservation of synteny between the *P. vulgaris* genome and at least five chromosomes from the ALK.

BAC-FISH, based on *P. vulgaris* probes, demonstrated conserved synteny among three species (*P. vulgaris*, *P. lunatus* L., and *P. microcarpus* Mart.) belonging to different clades within the genus *Phaseolus* L. (Bonifácio et al. 2012; Fonsêca and Pedrosa-Harand 2013). Similar comparative cytogenetic mappings of *P. leptostachyus* Benth. and *P. macvaughii* Delgado (Leptostachyus clade), on the other hand, evidenced extensive genome reshuffling associated with descending dysploidy involving a nested chromosome fusion between chromosomes 10 and 11 (Fonsêca et al. 2016; Ferraz et al. 2020). Furthermore, even though comparative cytogenetics and sequence alignments between *Vigna* Savi species and *P. vulgaris* revealed a high degree of macrosynteny between the genera, at least five chromosomes were found to be involved in synteny breaks (Vasconcelos et al. 2015; Lonardi et al. 2019; Oliveira et al. 2020; do Vale Martins et al. 2021). A detailed analysis of chromosomes 2 and 3 of *V. angularis*, *V. unguiculata*

and *P. vulgaris*, based on integrative sequence alignment and oligo-FISH painting approaches, identified additional macro- and micro-inversions, translocations, and intergeneric centromere repositioning among the species analysed (do Vale Martins et al. 2021). Centromere repositioning was also detected in chromosomes 5, 7, and 9 of *V. unguiculata* and *P. vulgaris* by oligo-FISH barcode combined with genome sequence data (de Oliveira Bustamante et al. 2021). Those authors also identified the participation of chromosome 5 in a translocation involving chromosomes 1 and 8, a paracentric inversion on chromosome 10, and a pericentric inversion on chromosome 4. The directions of those rearrangements were not, however, elucidated.

The Phaseoleae tribe (Leguminosae; Papilionoideae), now phylogenetically recircumscribed as the phaseoloid clade, includes several crops, mainly in the subtribes Phaseolinae and Glycininae (Li et al. 2013; Zhao et al. 2021b, Figure 1A), which were targets of genomic sequencing (Schmutz et al. 2010, 2014a; Lonardi et al. 2019; Garcia et al. 2021). Although many putative ancestral karyotypes have been proposed for legumes, there is no current proposal for the Phaseoleae tribe, nor an applicable GB system that could provide a phylogenetic direction for the chromosome rearrangements that occurred during Phaseoleae evolution. Thus, we constructed a GB system based on comparative cytogenomic data to better understand the dynamics of genome reshuffling among the diploid species of Phaseoleae. To that end, we selected the genome of *P. vulgaris* as a reference due to its high synteny to ALK (Hufnagel et al. 2020). We first compared *P. vulgaris* and *V. unguiculata* genomes to define the GB system, as the rearrangements between those genomes had previously been validated (de Oliveira Bustamante et al. 2021). We then applied the system to four species with assembled genomes: *Phaseolus lunatus* L. ($2n = 2x = 22$) from Phaseolinae; *Amphicarpaea edgeworthii* Benth. ($2n = 2x = 22$) from Glycininae, *Spatholobus suberectus* Dunn ($2n =$

2*x* = 18), sister to Phaseolineae and Glycininae (Zhao et al. 2021b); using *Medicago truncatula* Gaertn (2*n* = 2*x* = 16, tribe Trifolieae) as an outgroup. We also conducted oligo-painting experiments using available probes for *P. vulgaris* chromosomes 2 and 3 to visualize the orthologous chromosomes in two non-sequenced Phaseolinae species: *Macroptilium atropurpureum* DC. Urb. (2*n* = 2*x* = 22) and *Lablab purpureus* L. (2*n* = 2*x* = 22). Altogether, our results enabled us to hypothesize the ancestral Phaseoleae karyotype (APK) and to infer the main chromosomal rearrangements related to the evolution and diversification of those legumes. Our results indicated extensive genome reshuffling in particular lineages as well as centromere repositioning, especially in *Phaseolus*. Our GB system and the proposed APK are promising tools for future comparative genomic analyses when further legumes genome assemblies become available.

MATERIALS AND METHODS

Genomic data sets

We selected and analysed the reference genomes of *P. vulgaris* 'G19833' (GenBank ID: 8715468, Schmutz et al. 2014), *P. lunatus* 'G27455' (GenBank ID: 20288068, Garcia et al. 2021), *V. unguiculata* 'IT97K-499-35' (GenBank ID: 8372728, Lonardi et al. 2019), *S. suberectus* 'SS-2018' (GenBank ID: 8715468, Qin et al. 2019) and *A. edgeworthii* 'Qianfo Mountain' (GenBank ID: 22470258, Liu et al. 2020). The *M. truncatula* 'Jemalong A17' (GenBank ID: 7445598, Pecrix et al. 2018) genome was used as the outgroup.

Genomic block definitions and APK reconstruction

The CoGe SynMap platform was used to identify the syntenic blocks between the *P. vulgaris* and *V. unguiculata* genomes (https://genomevolution.org/coge/SynMap.pl) (Lyons et al. 2008). The orthologs were identified following the steps and parameters described by Walden et al. (2020): 1) using the BlastZ tool; 2) synteny analysis was performed by using DAGChainer, with 25 genes as the maximum distance between two matches (-D), and 20 genes as the minimum number of aligned pairs (-A); 3) Quota Align Merge was used to merge the syntenic blocks, with 50 genes as the maximum distance between them; and 4) the ortholog and paralog blocks were differentiated based on the synonymous substitution rate (Ks) by CodeML (where 2 was the maximum value of log10), and they were represented by different colours in the dot plot.

The syntenic blocks were defined using the 'Final syntenic gene-set output with GEvo link' (Table S1), with the starts and ends of the blocks being represented by the gene IDs of each species. Each generated genomic block (GB) contained at least 20 genes. The main criterion for defining a GB was the presence of translocation break points along its borders.

Based on the gene orthology between *P. vulgaris* and *V. unguiculata* and the defined GBs, we compared the *P. vulgaris* genome with those of *P. lunatus, S. suberectus, A. edgeworthii,* and *M. truncatula,* following the parameters described above. The comparisons generated sub-genomic blocks (sub-GBs) based on the following criteria: 1) breaks of collinearity inside the GBs (inversions); and, 2) breaks of collinearity or synteny involving associations with other GBs via inter- and intrachromosomal translocations (i.e., transference of chromosomal segments to the same or to other chromosomes, Schubert and Lysak, 2011). Each species had specific sub-GBs, indicating lineage-specific chromosomal rearrangements.

We analysed all of the dotplot patterns to infer the APK, and selected the most frequent GB associations, especially those shared with the outgroup (*M. truncatula*), considering the phylogenetic relationships among species, as described by Li et al. (2013) and Zhao et al. (2021b), checking the same or similar breaks points, and comparing the GBs to ALK (Hufnagel et al. 2020). Altogether, we selected the most conserved GBs and placed them into 11 chromosomes, following the pseudomolecules of the *P. vulgaris* genome. Once we defined the APK, we named the GBs in all species using the APK as the reference. Chromosome regions that did not correspond to GBs were conservatively assigned to the APK considering the neighbouring GBs, but are indicated using fainter colours. Those mostly correspond to gene-poor pericentromeric regions.

The centromeric regions were defined based on centromeric data available in the genome assemblies (Schmutz et al. 2014; Pecrix et al. 2018; Lonardi et al. 2019; Liu et al. 2020; Garcia et al. 2021). As the centromere positions for *S. suberecuts* were not indicated in the genome assembly, we hypothesized the centromere regions according to peaks of TE accumulation along the chromosomes (Qin et al. 2019). Finally, we standardized the centromere regions using the mid-point of each of them, considering that each centromere represents ~2 Mb.

Plant material and chromosome preparation

For the cytogenetic analyses, we used *P. vulgaris* 'BAT 93' (Embrapa Recursos Genéticos e Biotecnologia - Cenargen, Brasília, Distrito Federal, Brazil), *V. unguiculata* 'BR14 Mulato' (Embrapa Meio-Norte, Teresina, Piauí, Brazil), *M. atropurpureum* (International Center for Tropical Agriculture, CIAT 4413), and *L. purpureus* (UFP87699). Root tips from germinated seeds were collected and pre-treated with 2 mM

8-hydroxyquinoline (8HQ) for 5 h at 18 ºC, fixed in methanol or ethanol:acetic acid (3:1 v/v) for 2-24 h at room temperature, and stored at -20 ºC until used. For the chromosome preparations, the roots were washed twice with distilled water, digested with an enzymatic solution containing 2% pectolyase (Sigma-Aldrich), 4% cellulase (Onozuka or Sigma-Aldrich), and 20% pectinase (Sigma-Aldrich) for 1-2 h at 37 ºC (in a humid chamber). The slides were prepared following the air dry protocol (CARVALHO; SARAIVA, 1993), with minor modifications.

Oligo-FISH, image acquisition, and data processing

The design, synthesis, and labelling of the *Pv*2 and *Pv*3 oligo probes were described by do Vale Martins et al. (2021). Oligo-FISH was carried out according to (Han et al. 2015), with minor modifications. The hybridization mixture consisted of 50% formamide, 10% dextran sulphate, 2× saline sodium citrate (SSC), 350 ng of the biotin-labelled probe (*Pv*2, green), and 300 ng of the digoxigenin-labelled probe (*Pv*3, red), in a total volume of 10 µL per slide. The hybridization mixture was applied to the slides for 5 min at 75 °C and hybridized for 2-3 days at 37 °C. *Pv*2 and *Pv*3 oligo probes were detected with anti-biotin fluorescein (Vector Laboratories) and anti-digoxigenin rhodamine (Roche), respectively, both diluted in 1× TNB (1M Tris HCl pH 7.5, 3 M NaCl-blocking reagent, Sigma-Aldrich) with posterior incubation for 1 h at 37 ºC. The chromosomes were then counterstained with 2 µg/mL DAPI in Vectashield antifade solution (Vector Laboratories). Oligo-FISH images were captured using a Hamamatsu CCD camera coupled to an Olympus BX51 epifluorescence microscope or Leica DM5500B fluorescence microscope. The images were adjusted and optimized for brightness and contrast using Adobe Photoshop CC (2019). *Phaseolus vulgaris* and *V. unguiculata* idiograms were assembled based on Vasconcelos et al. (2015).

RESULTS

Genomic blocks and the inferred Ancestral Phaseoleae Karyotype

To infer the ancestral karyotype of the Phaseoleae tribe, we aligned the *P. vulgaris* (*Pv*) and *V. unguiculata* (*Vu*) genomes based on the collinear arrangement of orthologous genes in dot plots (Table S1), following Walden et al. (2020). We then compared the *Pv* genome to those of *P. lunatus* (*Pl*), *S. suberectus* (*Ss*), *A. edgeworthii* (*Ae*), and *M. truncatula* (*Mt*) to define the GBs (Table S2-5). We selected the most frequent GB associations (cases in which different GBs were present in adjacent positions in some taxa, e.g.: A+B, C+D, etc.), particularly those shared with *M. truncatula* (outgroup). We confirmed those GBs associations by determining if they were flanked by similar break points, using dot plot analysis (Supplementary Figure 1-5). After comparing the 19 proposed GBs (A-S) to ALK (Hufnagel et al. 2020), we proposed the APK (Figure 1A; Table S6) as $n = 11$ (the most common chromosome number within the tribe; Rice et al. 2015). Due to inversions within a block, or transpositions involving parts of blocks, some blocks were divided into sub-blocks (Table S7-12). Different numbers of sub-blocks were defined for each species, due to independent rearrangements among them. The centromere positions in APK chromosomes were hypothesized based on the frequency of associations between GBs and centromeres in the analysed species (although some of them may not represent the ancestral state).

Chromosomal rearrangements and centromere repositioning in the Phaseolinae subtribe in relation to the APK

Eight APK chromosomes displayed full synteny with at least one chromosome of the three analysed Phaseolinae subtribe species: APK2 (*Vu*2), APK3 (*Vu*3), APK4 (*Pv*4, *Pl*4, *Vu*4), APK5 (*Pv*5, *Pl*5), APK7 (*Vu*7, *Pv*7, *Pl*7), APK8 (*Vu*8), APK10 (*Pv*10, *Pl*10, *Vu*10), and APK11 (*Pv*11, *Pl*11, *Vu*11). We proposed the main chromosomal rearrangements, common to all Phaseolinae species, using APK as the reference, to infer the ancestral Phaseolinae karyotype (APnK). The APnK was very similar to the APK, although it had experienced reciprocal translocations among chromosomes 1, 6 and 9 (Figure 1.B1). We also confirmed exclusive rearrangements for *V. unguiculata* and *Phaseolus* species (Figure 1.B2 and 1.B3 respectively). We observed a reciprocal translocation between APnK1 and APK5 in *V. unguiculata* (*Vu*), resulting in chromosomes *Vu*1 (I+B+K2) and *Vu*5 (A+J), as well as a large pericentric inversion comprising most of APK4 (H), corresponding to *Vu*4 (Figure 1.B2). We subsequently applied the same approach to infer the ancestral *Phaseolus* karyotype (APhsK), with shared rearrangements between *P. vulgaris* and *P. lunatus*. The APhsK resulted from two reciprocal translocations [between APnK1 and APK8, resulting in APhsK1 (N+B+K2) and 8 (A+O); and between APK2 and 3], generating APhsK2 (E+G) and 3 (D+F), followed by inversions and intrachromosomal translocations on APhsK2 (E and G) and 3 (F) (Figure 1.B3). We also detected previously described inversions between *P. vulgaris* and *P. lunatus* (Bonifácio et al. 2012; Garcia et al. 2021) in Chr1 (in B); Chr2 (E and G); Chr3 (within F2); Chr7 (M); Chr9 (in L); and Chr10 (in R). The complex multiple inversions in chromosomes 2 and 7, also involving intrachromosomal translocations, occurred independently in *P. vulgaris* and *P. lunatus*. Intrachromosomal translocations occurred on chromosome 1, and inversions on chromosomes 1, 3, 9 and 10 occurred in the *P. lunatus* (*Pl*1) and *P. vulgaris* (*Pv*1, 3, 9 and 10) lineages respectively (Figure 1.B4 and 1.B5).

Based on the positions of the centromeres relative to the GBs or sub-GBs, we inferred centromere repositioning events in Phaseolinae species (Figure 2). The most evident repositioning events were those in which the centromere was present in a different GB as compared to the ancestral karyotype, as in APK2 (D): *Pl*/*Pv*2 (E); APK3 (F): *Vu*3 (G); and APK5 (I): *Pl*/*Pv*5 (J). New centromeres originated in GBs B (*Pl*/*Pv*1) and K (*Vu*/*Pl*/*Pv*6), while the putative ancestral centromeres in GBs N (APK8) and P (APK9) were lost (Figure 2). Other centromeres were preserved on the same GB; some sub-GBs, however, evidenced that their positions had changed, such as in APK3: *Pl*/*Pv*3, APK4: *Vu*4, APK7: *Pl*/*Pv*/*Vu*7 and APK10: *Pv*10, which could indicate further centromere repositioning events (Figure 2). To confirm those additional putative centromere repositioning events, we compared the dot plots with centromere positions (dashed lines in Figure S1 and S2) and the orthologous genes flanking the centromere regions in *Phaseolus* and *Vigna* (gene borders in Table S7-9). The results evidenced that all centromeres were surrounded by different gene blocks in *P. vulgaris* and *V. unguiculata*, which suggests that all centromeres were repositioned in one or another lineage, except for the APK1 centromere, which was maintained in *Vu*5 or *Pv*/*Pl*8 due to independent translocations involving chromosomes 1 and 5 in *Vigna* or 1 and 8 in *Phaseolus* (see in Figure 2).

To place these events in a phylogenetic context for Phaseolineae, we compared centromere locations in different species with the APK, and suggest the following events: a new centromere was established for Chr6 in K within the subtribe, after the translocations involving APK 1, 6 and 9 (Figure 1.A1); centromeres from Chr3, 4, 7 and 11 were repositioned in the *V. unguiculata* lineage (Figure 1.A2); new centromeres were established for Chr1 (in B), 2 (in E), 3 (in F) and 5 (in J) in the *Phaseolus* lineage (Figure 1.A4), with further changes in *Pl*6 and 7, as well as in *Pv*2, 6, 7, 9 and 10. In the *P. lunatus*

lineage, however, the imprecise centromere locations in the genome assembly may be hindering the identification of additional events.

The main rearrangements among Phaseolinae, *A. edgeworthii*, *S. suberectus*, and *M. truncatula* inferred from comparisons with the APK

All of the GBs generated were conserved in *A. edgeworthii* (Glycininae), *S. suberectus*, and *M. truncatula* (Figure 1A). Two APK associations were shared between *S. suberectus* and *M. truncatula*: B+C (APK1: *Ss*4, *Mt*7) and Q+P (APK9: *Ss*1, *Mt*2). However, those associations were not evidenced within Phaseolinae species. The GBs M (APK7: *Pv*7, *Pl*7, *Vu*7, *Ss*7, *Mt*1) and O (APK8: *Pv*8, *Pl*8, *Vu*8, *Ss*6, *Ae*3, *Mt*5) were highly syntenic between the subtribes, with an exclusive inversion in O2 in *Phaseolus* (Figure 1A). The GB M was also maintained in a single chromosome among the species, except for *A. edgeworthii* (M8: *Ae*1 and M1-M7: *Ae*8; Figure 1A).

Based on the APK, we propose the following main chromosomal rearrangements that lead to the descending dysploidy in *S. suberectus* ($n = 11$ to $n = 9$). This chromosome number reduction involved seven APK chromosomes (APK2, APK4, APK5, APK6, APK9, APK10 and APK11), resulting in four *S. suberectus* chromosomes (*Ss*1, *Ss*2, *Ss*8 and *Ss*9; Figure 1.B6). APK 4, 5, 6 and 9 were involved in a complex translocation that originated *Ss*1, *Ss*8 and *Ss*9. The whole APK2, and part of APK10 and APK11, were combined by a translocation with terminal breakpoints, resulting in *Ss*2, followed by centromere loss in the D block. Additional reciprocal translocations occurred between APK1 and both APK10 and APK11, generating *Ss*3 and *Ss*4, and between APK3 and APK8, resulting in *Ss*5 and *Ss*6. APK7 was conserved in *S. suberectus*. Comparisons among those species evidenced that almost all chromosomes were involved in breaks of

synteny and/or collinearity, which led to a higher number of sub-GBs, especially in *A. edgeworthii*. Although this species maintained the ancestral chromosome number *n* = 11, several rearrangements lead to complex GB associations (Figure 1.A7). We were nonetheless able to identify the APK associations, which helped reveal the main translocations in this genome (Supplementary Figure 6). Despite its descending dysploidy, the *S. suberectus* genome showed fewer rearrangements, when compared to the APK, than did Phaseolinae species (Figure 1.A6). All 19 GBs were detected in the *M. truncatula* genome (which diverged from *P. vulgaris* ~50 Mya), with *Mt*1 (M) and *Mt*6 (H) being highly syntenic to Phaseolinae chromosomes 7 and 4 respectively (Figure 1A).

Reconstructing the chromosomal rearrangements in APK based on the Ancestral Legume Karyotype

Using data from the ALK, and the rearrangements in *P. vulgaris* detected by Hufnagel et al. (2020), we identified the corresponding blocks from three ancestral karyotypes of legumes in our proposed APK (Table S3). We hypothesize that the formation of the APK involved five chromosomal fusions between 10 chromosomes of the ALK, which reduced the chromosome number from *n* = 16 to *n* = 11 (Figure 3). Considering ALK's from Hufnagel et al. (2020), Kreplak et al. (2019), and Zhuang et al. (2019), we observed that at least six APK chromosomes were well-preserved during the diversification of legumes (APK4, 5, 7, 9, 10 and 11), which explains the preservation of these chromosomes in many analysed species (Figure 1; Table S3). The APK patterns for *P. vulgaris* and *M. truncatula* are similar to the ALK pattern (Hufnagel et al. 2020), corroborating our APK reconstruction. Moreover, the APK pattern for *M. truncatula* confirms the translocation between *Mt*4-*Mt*8 (Kamphuis et al. 2007), which involved APK3, 10 and 11.

Oligopainting of chromosomes 2 and 3 in the two non-sequenced species *M. atropurpureum* and *L. purpureus*

To further investigate chromosomal evolution within the Phaseolinae subtribe, we expanded our comparative cytogenomic analysis to two species with no assembled genome, namely *M. atropurpureum* (*Ma*) and *L. purpureus* (*Lp*). We hybridized two oligopainting probes from *P. vulgaris* chromosomes (Figure 4a) [*Pv*2 (green) and *Pv*3 (red)] to *M. atropurpureum* and *L. purpureus* metaphase cells. The oligo-FISH painting did not reflect the patterns expected for the APK as the probes were generated from *Pv* chromosomes, which experienced rearrangements between chromosomes 2 and 3 (Figure 4). *Macroptillium atropurpureum* (Figure 4c) and *L. purpureus* (Figure 4d) showed similar oligo-FISH signals to *V. unguiculata* (Figure 4b). *Macroptillium atropurpureum* orthologous chromosome 2 (*Ma*2) evidenced the short arm in red (*Pv*3) and almost the entire long arm in green (*Pv*2), except for an interstitial pericentromeric red region on the long chromosome arm. The *Ma*3 chromosome had the short arm and approximately half of the long arm in red (*Pv*3), with the distal region painted green (*Pv*2) (Figure 4c). We observed a more complex oligo-painting pattern in *L. purpureus* (Figure 4d) chromosomes: the short arm of chromosome 2 (*Lp*2) had small terminal and pericentromeric green (*Pv*2) signals intermingled with a large red (*Pv*3) signal, while the opposite arm, similar to the *Vu*2 long arm, was painted green (*Pv*2), with a red pericentromeric region (*Pv*3). The *Lp*3 short arm, similar to the short arm of *Vu*3, was painted green (*Pv*2), with a small intermingled red signal (*Pv*3). The long arm of *Lp*3 was painted red (*Pv*3), with an intermingled green signal (*Pv*2) in its proximal region (Figure 4d).

Our data support the exclusivity of the translocation event between APK2 and APK3 for the genus *Phaseolus*, as *L. purpureus* and *M. atropurpureum* chromosomes 2 and 3 resemble *V. unguiculata* ortholog chromosomes and are closer to the APK. Gaps in the pericentromeric regions of *M. atropurpureum* and *L. purpureus* chromosomes 2 and 3 (Figure 4c, 4d), different chromosome arm sizes in *Ma*3 (Figure 4c), and intermingled oligo-FISH signals in *L. purpureus* (represented by green and red arrows in Figure 4d) may, however, indicate independent rearrangements and small collinearity breaks related to inversions.

DISCUSSION

We established here a GB/sub-GB system for comparative chromosome analyses of Phaseoleae legumes. Our system identified several chromosomal rearrangements and frequent centromere repositioning events, especially in the *Phaseolus* lineage. The sub-GBs revealed further rearrangements inside the GBs as independent events during their evolution. In Brassicaceae, the identification of independent rearrangements inside the GBs was essential for understanding the phylogenetic relationships in taxa such as *Aethionema arabicum* (L.) Andrz. ex DC. (Walden et al. 2020), *Arabis alpina* L. (Willing et al. 2015), and *Brassica oleracea* L. (Parkin et al. 2014).

Recent comparative genomic studies were able to reconstruct the ALKs, with proposed chromosome numbers ranging from $n = 9$ to $n = 25$ (Zhuang et al. 2019; Kreplak et al. 2019; Ren et al. 2019; Hufnagel et al. 2020). Nevertheless, comparisons among grape (*Vitis vinifera* L.) and legumes revealed independent chromosome fusions before and after the LCT event, resulting in $n = 16$ as the putative ancestral chromosome number for legumes (Zhuang et al. 2019). The ALK revealed detailed chromosome rearrangement

events that shaped the chromosome numbers in specific lineages, mainly marked by polyploidization and chromosome fusions and fissions (Zhuang et al. 2019; Kreplak et al. 2019; Hufnagel et al. 2020). Additional analyses, however, such as centromere repositioning and inversions, were not discussed, and *V. unguiculata*, *P. lunatus*, *S. suberectus*, and *A. edgeworthii* were not investigated (Zhuang et al. 2019; Kreplak et al. 2019; Hufnagel et al. 2020).

We reconstructed an ancestral Phaseoleae karyotype (APK) with $n = 11$ chromosomes and 19 GBs. Despite chromosome number variations within the tribe ($2n = 18$ to $2n = 84$; Rice et al. 2015), genomic, cytogenetic, and phylogenetic evidences suggest the ancestral chromosome number as $n = 11$ (Li et al. 2013; Rice et al. 2015; Wang et al. 2017). Comparing the ALK (Hufnagel et al. 2020) with our APK, we were able to identify a chromosome number reduction of $n = 16$ to $n = 11$ that involved the fusion of five chromosomes. Reconstructions of ancestral karyotypes have been essential for comparative genomic analyses in other groups, such as grasses, cucurbits, crucifers, and other flowering plants, contributing to our comprehension of fractionation processes after whole genome duplication (WGD) events, genome reshuffling, and recombination hotspots (Murat et al. 2010, 2017; Wang et al. 2015; Lysak et al. 2016; Xie et al. 2019). More recently, an ancestral karyotype of *Cucumis* was inferred by comparative oligo-painting (COP) in different species of African and Asian clades that indicated constant genome reshuffling caused by large-scale inversions, centromere repositioning, and other rearrangements (Zhao et al. 2021a). Similarly, our analyses showed highly conserved macrosynteny in the Phaseoleae tribe, revealing particular rearrangements within each clade.

Five APK chromosomes (APK4, APK5, APK7, APK10, APK11) showed high conservation of synteny within the tribe and with the ALK (Hufnagel et al. 2020), as had

been observed in previous studies (Schmutz et al. 2010; McConnell et al. 2010; Wang et al. 2017; Ho et al. 2017; Lonardi et al. 2019). Overall, APK7 is the most conserved chromosome, with the GB "M" only involved in intrachromosomal rearrangements, except in *A. edgeworthii*, which displayed a higher number of rearrangements. Chromosome 7 showed high conservation of synteny when compared to non-Phaseoleae species such as *Mt*1, *Ah*9 (*Arachis hypogaea* L. chromosome 9) and *Lj*5 [*Lotus japonicus* (Regel) K.Larsen chromosome 5] (Bertioli et al. 2009), as well as to soybean *Gm*10 and *Gm*20 chromosomes (Schmutz et al. 2014; Wang et al. 2017). Gene family analyses in *Pisum sativum* L. and *M. truncatula* indicated the expression of important genes for the seed storage (Legumin, Vicilin, Convicilin) in the *Ps*6 and *Mt*1, orthologous to APK7 (Kreplak et al. 2019). This could indicate that the high synteny of this chromosome is important for seed development. Additional analyses will be necessary to test this hypothesis.

Few translocations and many inversions were identified within Phaseolinae. Some of those rearrangements were previously identified by BAC-FISH, oligo-FISH, and comparative genomics in *P. vulgaris*, *P. lunatus,* and *V. unguiculata* (Bonifácio et al. 2012; Vasconcelos et al. 2015; Lonardi et al. 2019; Oliveira et al. 2020; do Vale Martins et al. 2021; Garcia et al. 2021; de Oliveira Bustamante et al. 2021). Based on our APK and oligo-FISH approaches, we are now able to propose the direction of those rearrangements within a phylogenetic context. The reciprocal translocation between chromosomes 1 and 8, between 2 and 3, and inversions on chromosomes 2 and 3 were exclusive events in the *Phaseolus* genus, while the translocation between chromosomes 1 and 5, and the inversions on chromosome 4 were exclusive to *Vigna*. Independent intrachromosomal translocations and inversions in *P. vulgaris* (*Pv*1, 2, 3, 7, 9 and 10) and

P. lunatus (*Pl*1, 2 and 7) were also detected, which corroborate previous results of comparative genomic analyses between *P. lunatus* and *P. vulgaris* (Garcia et al. 2021).

Several translocations and inversions were detected in the *A. edgeworthii* genome. Although the ancestral chromosome number was conserved, its karyotype was the most rearranged among all of the species analysed. Whole genome analysis indicated large-scale ectopic recombinations and reductions of Long Terminal Repeat (LTR) retrotransposons during evolution, compacting the genome but preserving important genes (Liu et al. 2020). That genomic analysis also indicated that the remarkable genome reshuffling observed was not a consequence of polyploidy (Liu et al. 2020). The dysploid *S. suberectus*, on the other hand, evidenced the most conserved karyotype in comparison to the APK, which supports its phylogenetic position (Zhao et al. 2021b). We propose two major translocations events combining APK6 and 9 into *Ss*1, and APK2, APK10 and APK11 into *Ss*2, leading to descending dysploidy in *S. suberectus* (from $n = 11$ to $n = 9$). Descending dysploidy events were also revealed by ancestral karyotype analysis in Brassicaceae (Lysak et al. 2006, 2016; Schranz et al. 2006) and in the Cucurbitaceae family, with variation from $n = 12$ to $n = 7$ (Yang et al. 2014; Yang and Sagar 2022).

Despite the uncertain centromere positions of *S. suberectus* pseudomolecules in the genome assembly, we hypothesize that many GB-centromeric associations may have been conserved among Phaseoleae, as well as in other legumes. Our GBs system nonetheless revealed that changes in centromere positions were not a direct result of major structural rearrangements, changes in collinearity, or chromosome number reductions, but rather reflect centromere repositioning, especially in Phaseolinae. We confirmed previously inferred centromere repositioning events in five chromosome pairs of *P. vulgaris* and *V. unguiculata*: chromosomes 2, 3, 5, 7 and 9 (do Vale Martins et al. 2021; de Oliveira Bustamante et al. 2021). Additionally, we identified centromere repositioning

in five additional chromosomes of *P. vulgaris* or *V. unguiculata* when compared to the APK. Apart from one putative event in the ancestral karyotype of both genera (K in Chr. 6), four events occurred in the *V. unguiculata* lineage, while the remaining occurred in the genus *Phaseolus*, mainly in the *P. vulgaris* lineage. Thus, our results indicate repositioning for all except one APK centromere (APK1), mostly in the last 6 -10 Mya (Li et al. 2013; Garcia et al., 2021).

Phaseolus vulgaris and *V. unguiculata* have different centromeric satellite DNA (satDNA) families, and there is more than one centromeric tandem repeat sequence in each species (Iwata et al. 2013; Iwata-Otsubo et al. 2016). Repetitive sequences showed different amplification dynamics within *Phaseolus* and among *Phaseolus, Vigna,* and *Cajanus* – indicating the fast evolution of centromeric repeats in Phaseoleae (Iwata et al. 2013; Iwata-Otsubo et al. 2016; Ribeiro et al. 2017, 2020). This fast evolution of centromeric repeats may have occurred via the invasion of retroelements and tandem repeats, associated recruitment of the centromeric protein CENH3 to a new position, forming a functional *de novo* centromere (Lysak 2014; Schubert 2018; Talbert and Henikoff 2020), as evidenced in *Solanum* L. (Gong et al. 2012; Zhang et al. 2014), *Oryza* L. (Liao et al. 2018), *Aubrieta* Adans., and *Draba* L. (Mandáková et al. 2020). In maize (*Zea mays* L.), for example, centromere repositioning occurred after double strand breaks (DSBs) in centromeric satellite sequences that led to the loss of *CentC*, and resulted in *de novo* centromere formation at linked genes (selected during domestication), which facilitated the emergence of *de novo* centromeres (Schneider et al. 2016; Zhao et al. 2017).

Centromere repositioning events seem to have occurred frequently in Phaseoleae (especially in Phaseolinae), which would explain the observed variations between centromere-GB and sub-GB. Chromosome rearrangements may have contributed to centromere changes in other groups (Schubert 2018; Talbert and Henikoff 2020), as

observed for *S. suberectus*, in which a dysploidy event was involved in centromere inactivation and the subsequent formation of new centromeres (Figure 1). Our GB analysis, however, revealed that most of the changes in centromere positions in this tribe were not the result of changes in the collinearity of the GBs, thus suggesting that emergence of *de novo* centromeres, or transpositions/inversions involving just the centromeres, may have occurred in this group. Similar evidences were found in maize, indicating that *de novo* centromere events are common and rapidly established (Liu et al. 2015, 2020a). However, further analyses, such as the assembly of whole centromeres after long-read sequencing, will be necessary to confirm the mechanisms involved in those centromere repositioning events.

Our GBs system enabled us to reconstruct the ancestral karyotype of the Phaseoleae tribe and to determine the directions of the main chromosomal evolutionary events related to diversification and speciation of both closely and distantly related legume species. We correlated our APK with a previously proposed ALK, showing that the chromosome reduction in the tribe was caused by five chromosome fusions. At least five legume chromosomes were highly conserved during diversification of the group. We also observed frequent centromere repositioning in this tribe, especially in *P. vulgaris*, despite its karyotype stability. Our findings offer bright perspectives for future genomic analysis within Phaseoleae and other legumes. With increasing numbers of legume genome sequencing projects underway, this genomic tool will provide new opportunities for understanding the events that have shaped legume genomes, as well as the role of centromere repositioning in plant evolution within a phylogenetic context.

FIGURE CAPTIONS

Figure 1. Genomic block system and the hypothetical Ancestral Phaseoleae Karyotype (APK). Arrows in **A** indicate changes in block orientation, with fainter colours along the chromosomes indicating putative assignments to APK without GB support. Stars in A indicate centromere repositioning, with the colours of the stars indicating their respective ancestral chromosomes (dark blue: APK1; light green: APK2; red: APK3; brass: APK4; brown: APK5; purple: APK6; dark green: APK7; pink: APK8; yellow: APK9; light blue: APK10; orange: APK11), and the letter inside indicating the respective GB. Some entire chromosome orientations were inverted (underlined chromosomes) to better demonstrate the orthology between the APK and other karyotypes. **A**) Species are grouped according to the phylogenetic relationships proposed by Li *et al*. (2013). **1** to **5**) Phaseolinae subtribe species: *Vigna unguiculata*, *Phaseolus lunatus*, and *P. vulgaris*; **6)** *Amphicarpaea edgeworthii* (Glycininae subtribe specie)*;* and **7**) *Spatholobus suberectus* (sister to Phaseolinae and Glycininae). **B**) Main chromosomal rearrangements: **1**) Translocations and pericentric inversions resulting in the Ancestral Phaseolinae Karyotype (APnK); **2**) Reciprocal translocation and pericentric inversion resulting in *V. unguiculata* (*Vu*) chromosomes 1, 4 and 5; **3**) Reciprocal translocation and inversions resulting in the Ancestral *Phaseolus* Karyotype (APhsK); **4**) Inversions and intrachromosomal translocations resulting in *P. lunatus* (*Pl*) chromosomes 1 and 7; **5**) Inversions and intrachromosomal translocations resulting in *P. vulgaris* (*Pv*) chromosomes 1, 2, 7, 9 and 10; **6**) Descending dysploidy and genome rearrangements in the *S. suberectus* (*Ss*) karyotype.

Figure 2. Centromere repositioning in the Phaseoleae tribe and in *M. truncatula*, based on the established Ancestral Phaseoleae Karyotype (APK). Stars indicate centromere repositioning, with the colours of the stars indicating their respective ancestral

chromosomes (dark blue: APK1; light green: APK2; red: APK3; brass: APK4; brown: APK5; purple: APK6; dark green: APK7; pink: APK8; yellow: APK9; light blue: APK10; orange: APK11), and the letter inside indicating the respective GB. Dashed lines indicate regions orthologous to putative APK centromeres. Sub-GBs are indicated in some *Pl/Pv* chromosomes to demonstrate the altered position of the centromere independent of structural rearrangements.

Figure 3. The Ancient Legume Karyotype (ALK, *n* = 16) by Hufnagel et al. (2020) compared to the APK (*n* = 11). Ten ALKs were involved in five end-to-end chromosome fusions, reducing from *n* = 16 to *n* = 11.

Figure 4. Oligo-FISH using *Phaseolus vulgaris* chromosomes-specific 2 (green) and 3 (red) probes hybridized to other Phaseolinae species. (**a**) *P. vulgaris*, (**b**) *Vigna unguiculata*, (**c**) *Macroptilium atropurpureum*, and (**d**) *Lablab purpureus*. Green and red arrows indicate small differences in the painting patterns, corresponding to specific regions of *Pv*2 (green) or *Pv*3 (red) probes respectively. For each species, orthologous chromosomes of *P. vulgaris* chromosomes 2 and 3 are detailed in the insets (right) of each metaphase cell and represented to the right of each inset. Differences between the APK and oligo-FISH painting signals of chromosomes 2 and 3 are indicated for *P. vulgaris* and *V. unguiculata*. Vertical bar = 5 µm.

SUPPLEMENTARY INFORMATION CAPTIONS

Supplementary Figure 1. Dot plot of genome comparison between *P. vulgaris* and *V. unguiculata*, with each GB colour based on the APK. Corresponding chromosomes are

distributed according to the dot plot order. Dashed lines indicate the centromere positions in the respective GBs.

Supplementary Figure 2. Dot plot of genome comparisons between *P. vulgaris* and *P. lunatus,* with each GB colour based on the APK. Corresponding chromosomes are distributed according to the dot plot order. Dashed lines indicate the centromere positions in the respective GBs.

Supplementary Figure 3. Dot plot of genome comparison between *P. vulgaris* and *A. edgeworthii* with each GB colour based on the APK. Corresponding chromosomes are distributed according to the dot plot order.

Supplementary Figure 4. Dot plot of genome comparison between *P. vulgaris* and *S. suberectus* with each GB colour based on the APK. Corresponding chromosomes are distributed according to the dot plot order.

Supplementary Figure 5. Dot plot of genome comparison between *P. vulgaris* and *M. truncatula* with each GB colour based on the APK. Corresponding chromosomes are distributed according to the dot plot order.

Supplementary Figure 6. Schematic representation of the most conserved GB associations of the *A. edgeworthii* (*Ae*) karyotype as inferred from comparison with the APK. Despite extensive genome reshuffling, the main GB associations involved in the formation of each *Ae* chromosome are indicated by dotted lines in the corresponding APK chromosome colours.

Supplementary Table 1. Output of final syntenic gene set for *P. vulgaris* x *V. unguiculata* genomic comparisons.

Supplementary Table 2. Output of final syntenic gene set for *P. vulgaris* x *P. lunatus* genomic comparisons.

Supplementary Table 3. Output of final syntenic gene set for *P. vulgaris* x *A. edgeworthii* genomic comparisons.

Supplementary Table 4. Output of final syntenic gene set for *P. vulgaris* x *S. suberectus* genomic comparisons.

Supplementary Table 5. Output of final syntenic gene set for *P. vulgaris* x *M. truncatula* genomic comparisons.

Supplementary Table 6. Genomic blocks in APK.

Supplementary Table 7. Genomic blocks in *P. vulgaris.*

Supplementary Table 8. Genomic blocks in *P. lunatus*.

Supplementary Table 9. Genomic blocks in *V. unguiculata*.

Supplementary Table 10. Genomic blocks in *S. suberectus*.

Supplementary Table 11. Genomic blocks in *A. edgeworthii*.

Supplementary Table 12. Genomic blocks in *M. truncatula*.

Supplementary Table 13. ALKs compared to APK and *P. vulgaris.*

FIGURES

Figure 1

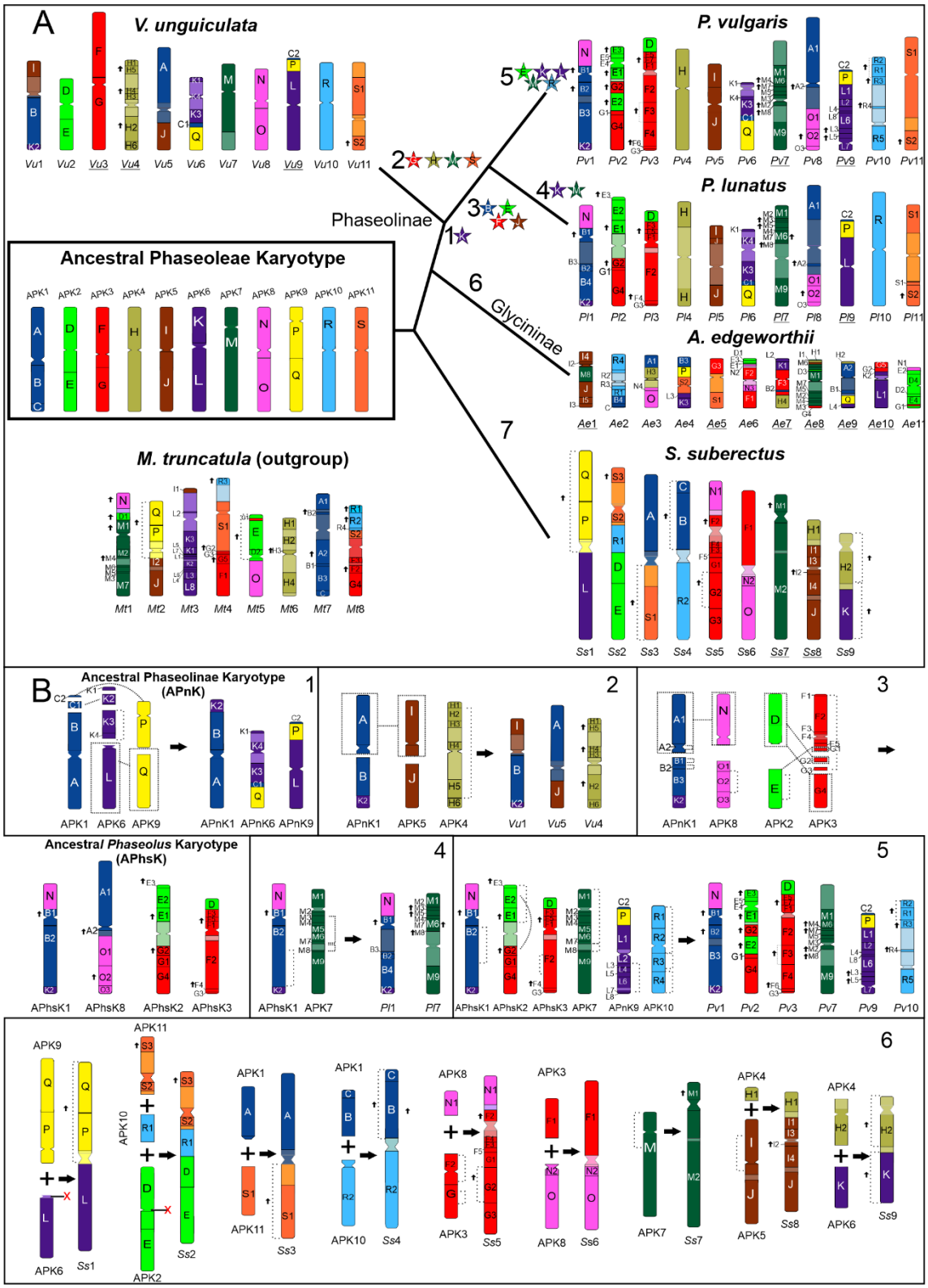

Figure 2

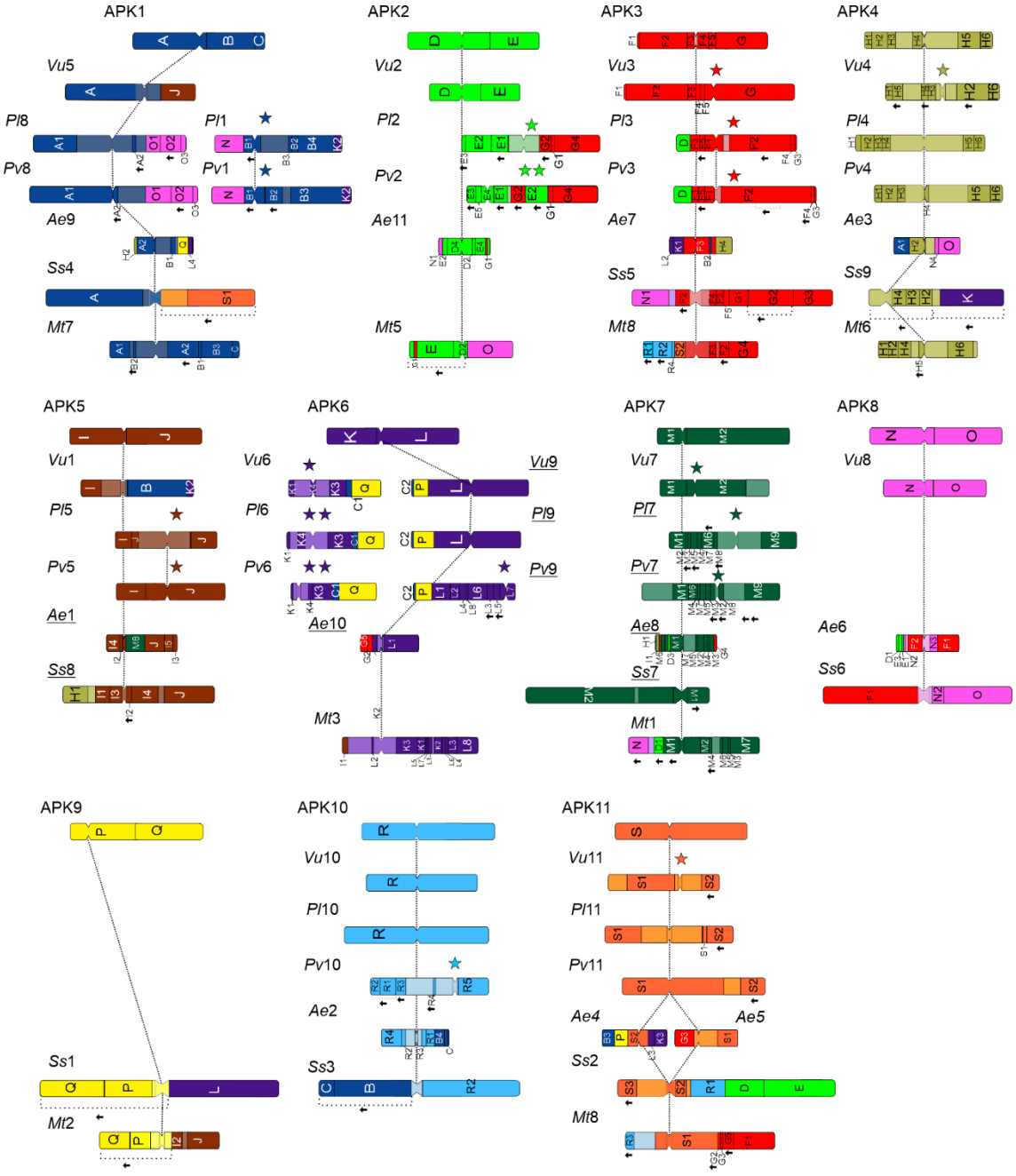

Figure 3

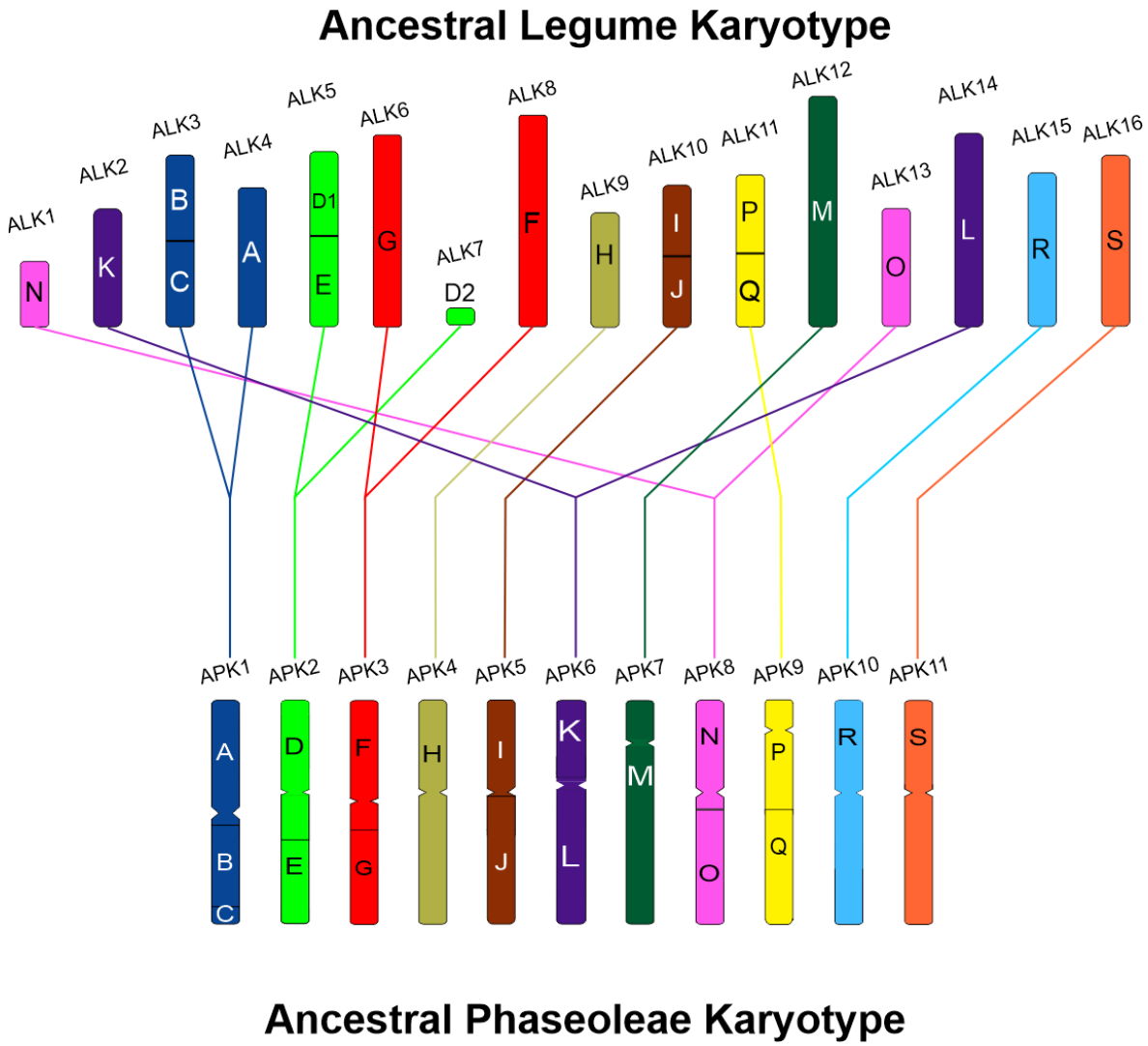
Ancestral Legume Karyotype
ALK1
ALK2
ALK3
ALK4
ALK5
ALK6
ALK7
ALK8
ALK9
ALK10
ALK11
ALK12
ALK13
ALK14
ALK15
ALK16
N
K
B
C
A
D1
E
G
D2
F
H
I
J
P
Q
M
O
L
R
S
APK1
APK2
APK3
APK4
APK5
APK6
APK7
APK8
APK9
APK10
APK11
A
B
C
D
E
F
G
H
I
J
K
L
M
N
O
P
Q
R
S
Ancestral Phaseoleae Karyotype

Figure 4

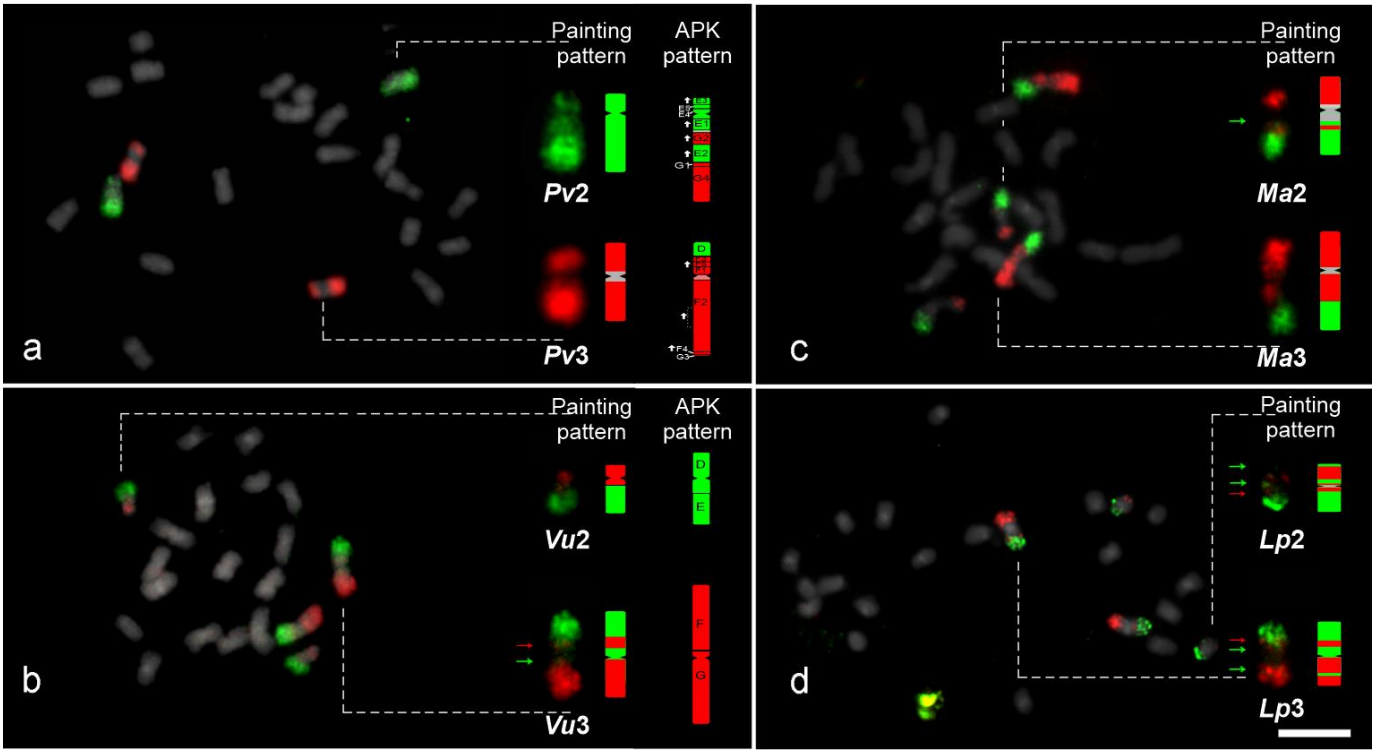
Painting pattern
APK pattern
Pv2
Pv3
a
Painting pattern
Ma2
Ma3
c
Painting pattern
APK pattern
Vu2
Vu3
b
Painting pattern
Lp2
Lp3
d

Supplementary Figure 1

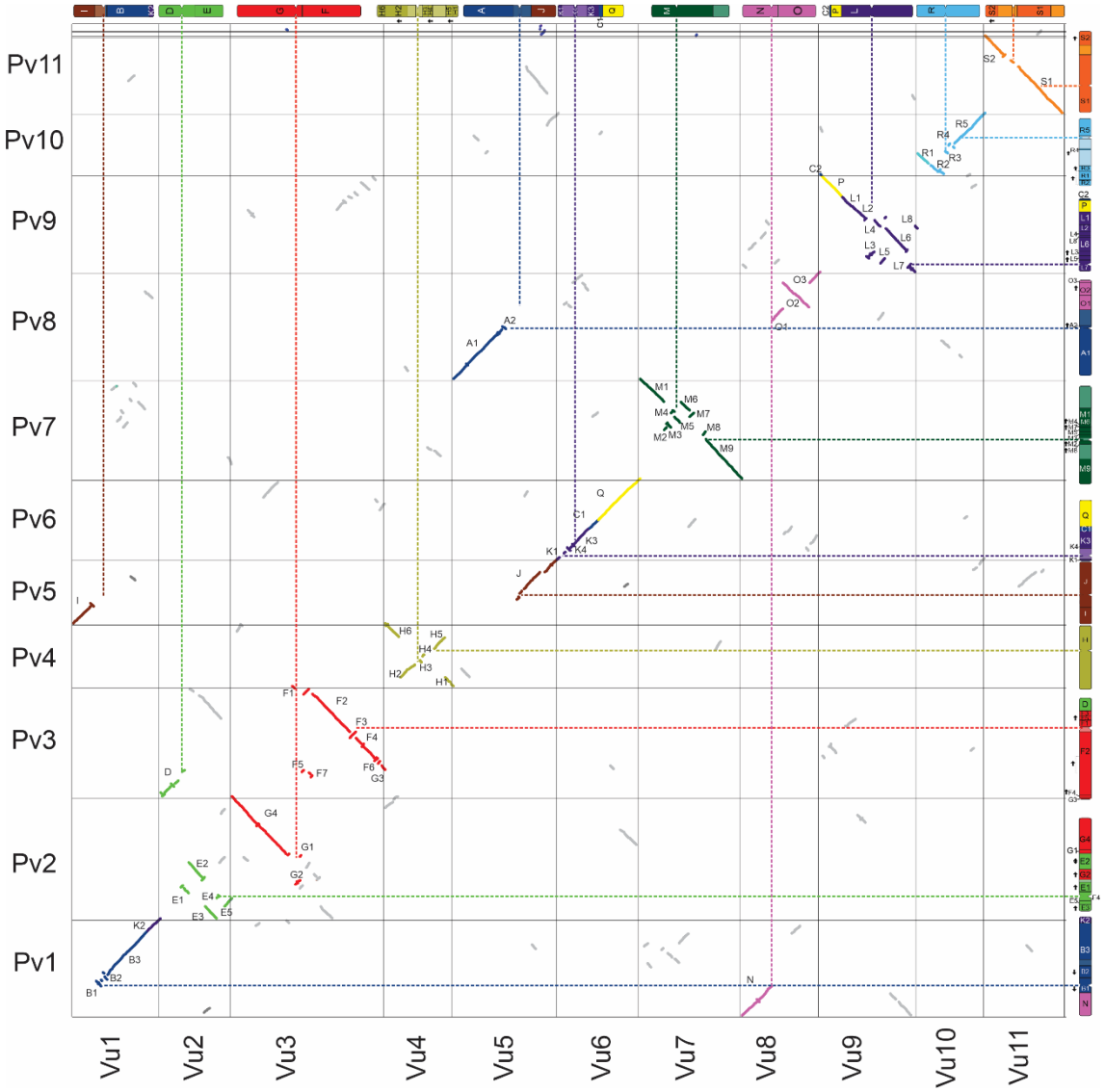

Supplementary Figure 2

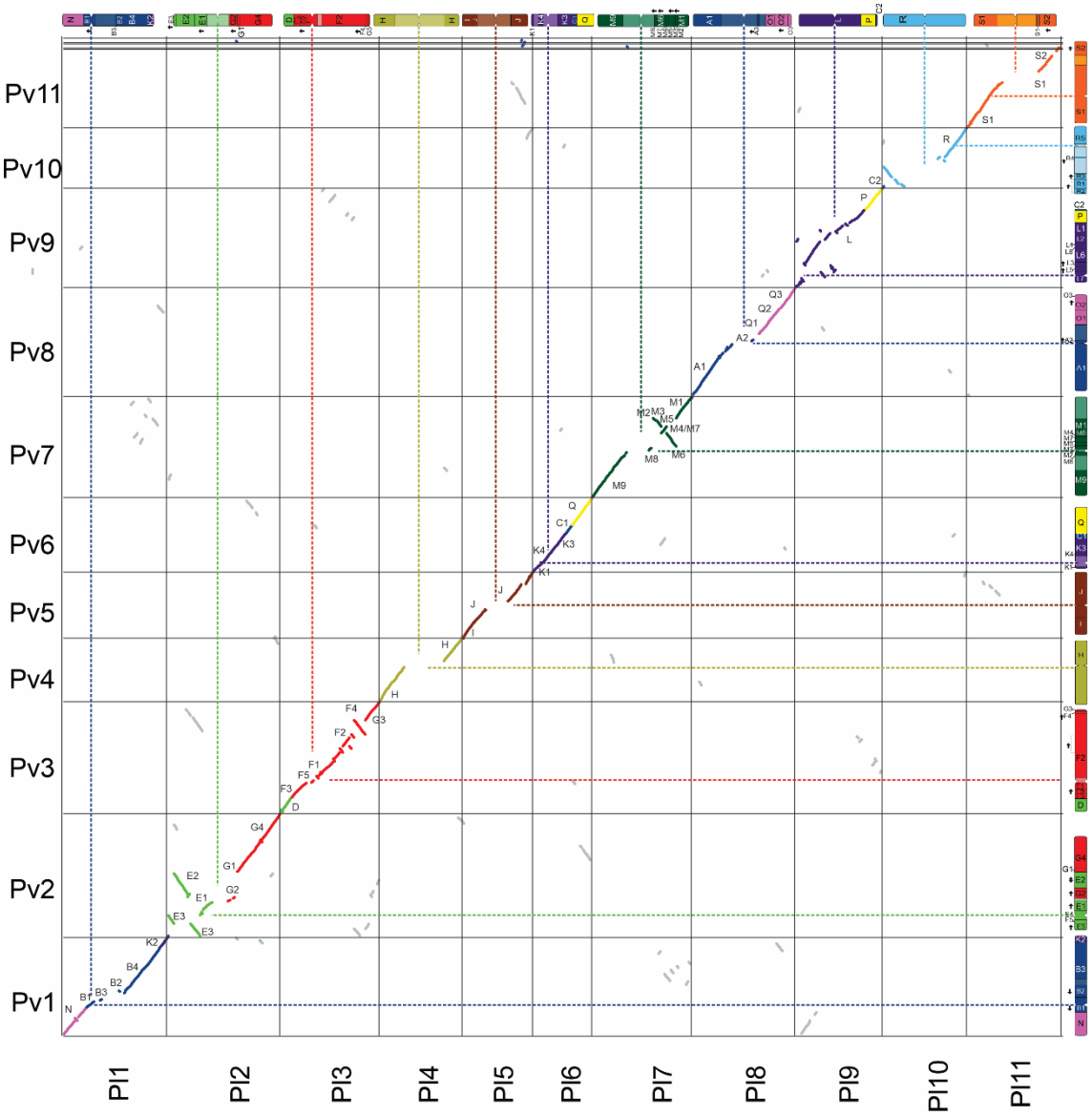

Supplementary Figure 3

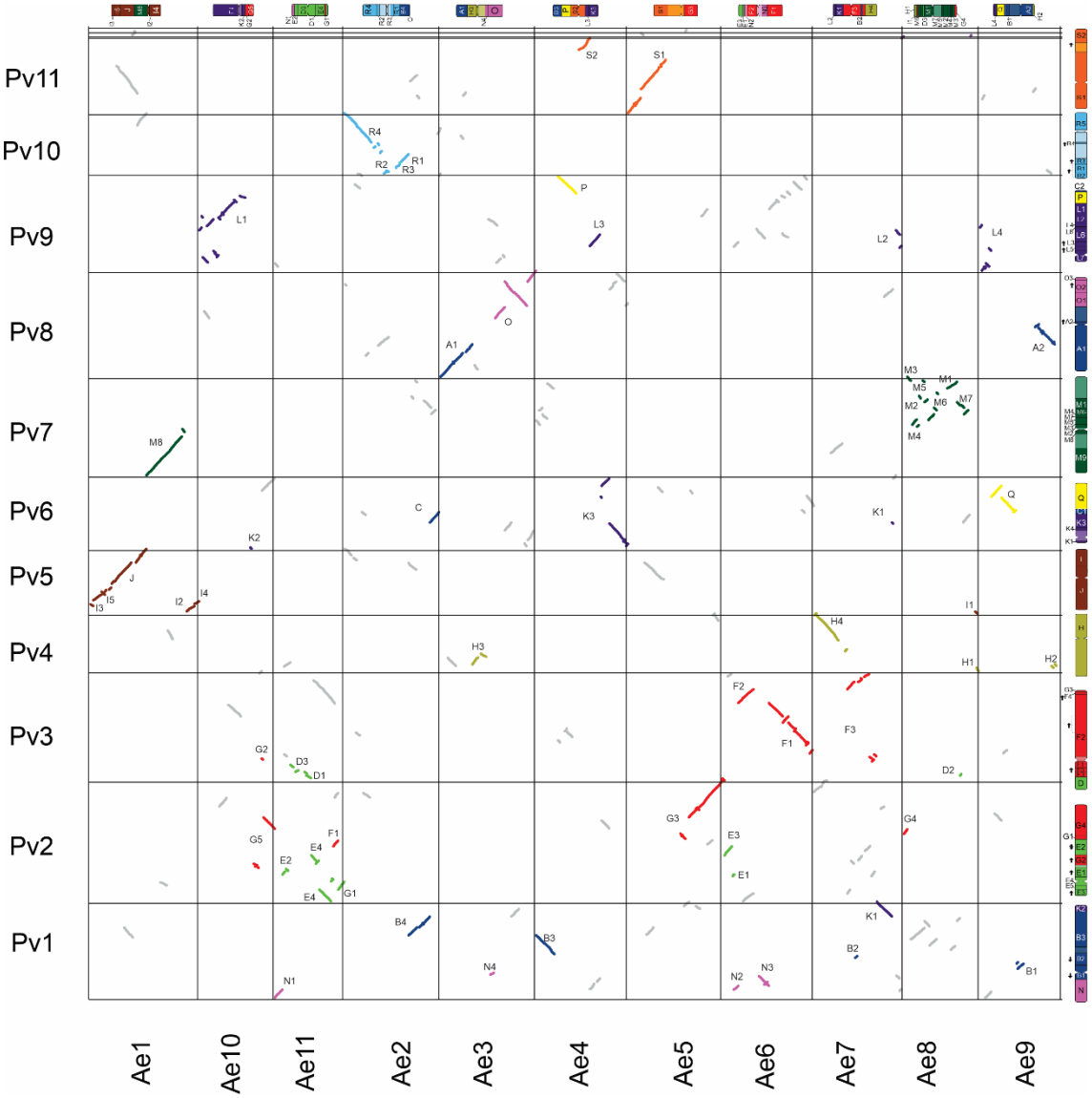

Supplementary Figure 4

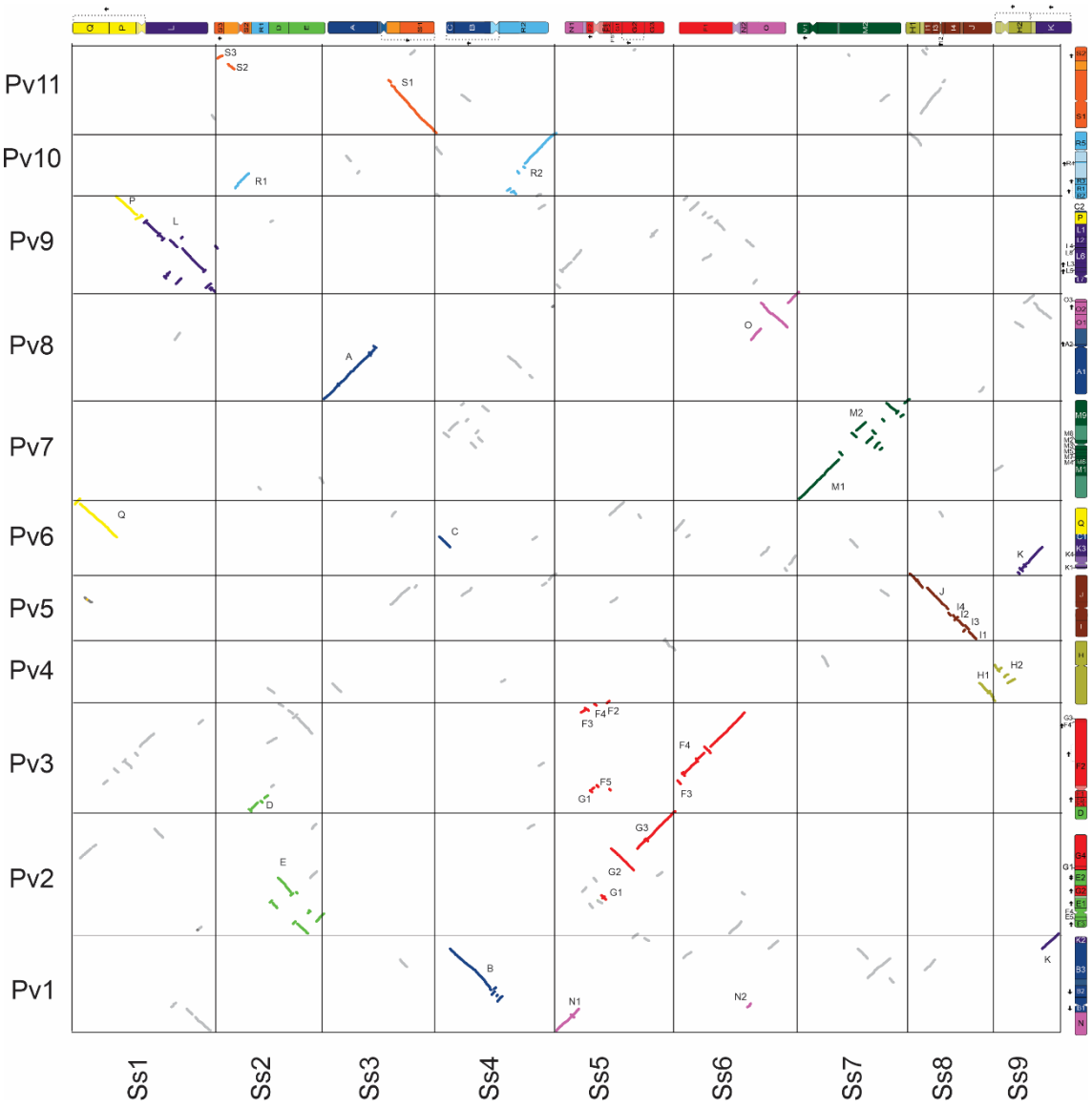

Supplementary Figure 5

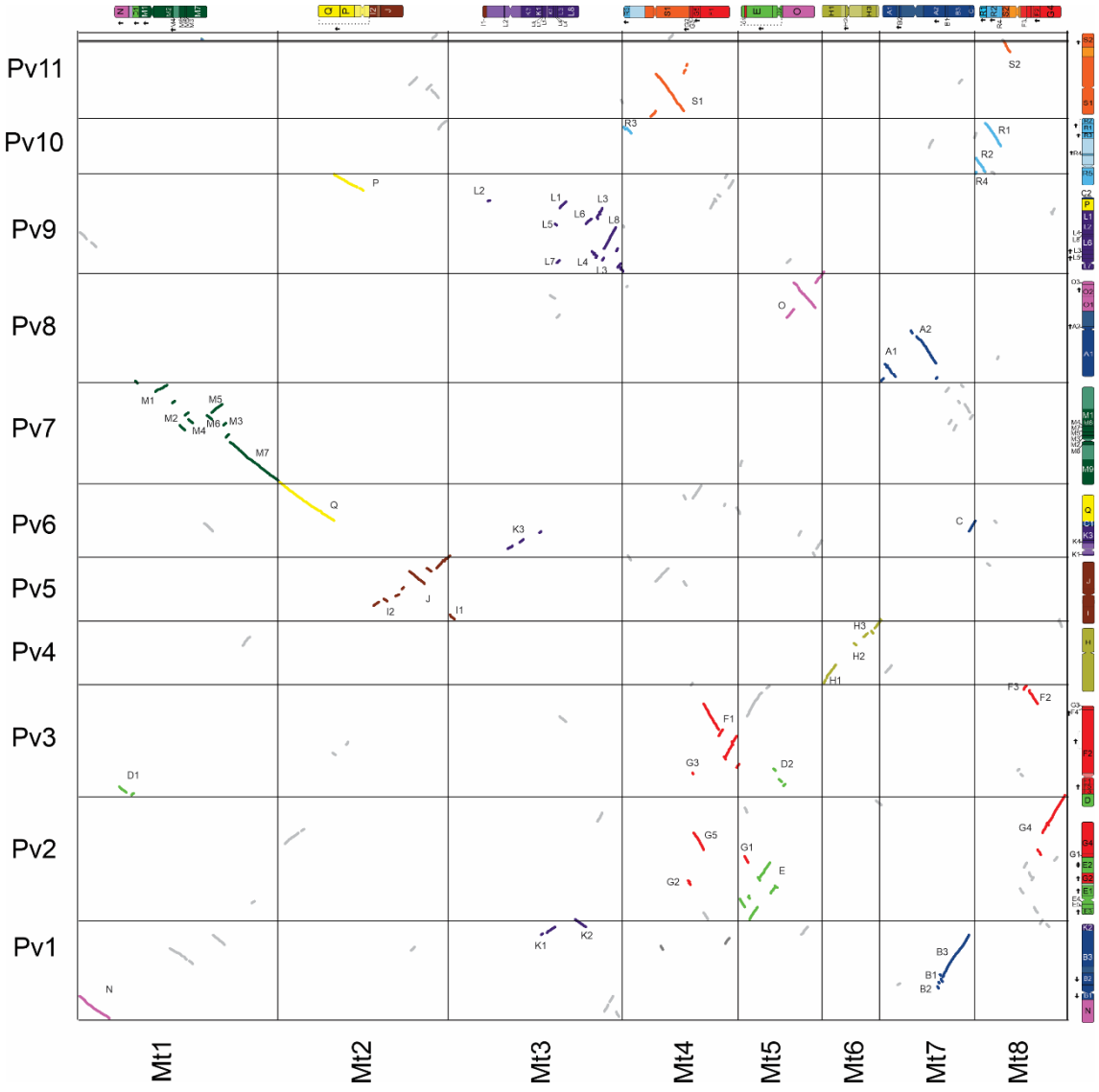

Supplementary Figure 6

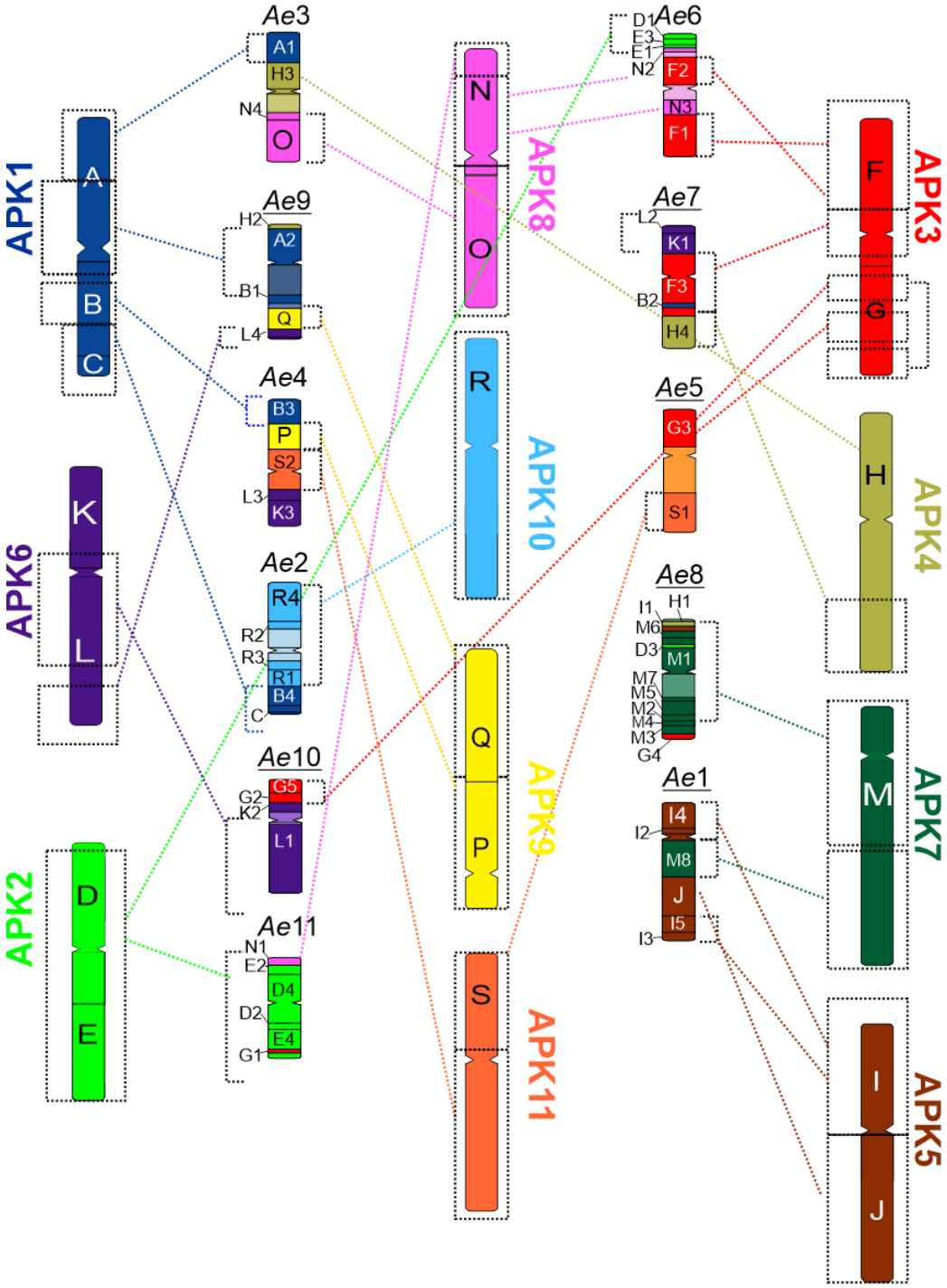

Supplementary Table 1:

https://static-content.springer.com/esm/art%3A10.1007%2Fs10577-022-09702-8/MediaObjects/10577_2022_9702_MOESM1_ESM.xlsx

Supplementary Table 2:

https://static-content.springer.com/esm/art%3A10.1007%2Fs10577-022-09702-8/MediaObjects/10577_2022_9702_MOESM2_ESM.xlsx

Supplementary Table 3

https://static-content.springer.com/esm/art%3A10.1007%2Fs10577-022-09702-8/MediaObjects/10577_2022_9702_MOESM3_ESM.xlsx

Supplementary Table 4

https://static-content.springer.com/esm/art%3A10.1007%2Fs10577-022-09702-8/MediaObjects/10577_2022_9702_MOESM4_ESM.xlsx

Supplementary Table 5

https://static-content.springer.com/esm/art%3A10.1007%2Fs10577-022-09702-8/MediaObjects/10577_2022_9702_MOESM5_ESM.xlsx

Supplementary Table 6

https://static-content.springer.com/esm/art%3A10.1007%2Fs10577-022-09702-8/MediaObjects/10577_2022_9702_MOESM6_ESM.xlsx

Supplementary Table 7

https://static-content.springer.com/esm/art%3A10.1007%2Fs10577-022-09702-8/MediaObjects/10577_2022_9702_MOESM7_ESM.xlsx

Supplementary Table 8

https://static-content.springer.com/esm/art%3A10.1007%2Fs10577-022-09702-8/MediaObjects/10577_2022_9702_MOESM8_ESM.xlsx

Supplementary Table 9

https://static-content.springer.com/esm/art%3A10.1007%2Fs10577-022-09702-8/MediaObjects/10577_2022_9702_MOESM9_ESM.xlsx

Supplementary Table 10

https://static-content.springer.com/esm/art%3A10.1007%2Fs10577-022-09702-8/MediaObjects/10577_2022_9702_MOESM10_ESM.xlsx

Supplementary Table 11

https://static-content.springer.com/esm/art%3A10.1007%2Fs10577-022-09702-8/MediaObjects/10577_2022_9702_MOESM11_ESM.xlsx

Supplementary Table 12

https://static-content.springer.com/esm/art%3A10.1007%2Fs10577-022-09702-8/MediaObjects/10577_2022_9702_MOESM12_ESM.xlsx

Supplementary Table 13

https://static-content.springer.com/esm/art%3A10.1007%2Fs10577-022-09702-8/MediaObjects/10577_2022_9702_MOESM13_ESM.xlsx